Environmental Security Technology Certification Program
Final Report - Revision 1

Project Number UX-0534
High Density Lidar and Orthophotography in UXO Wide Area Assessment

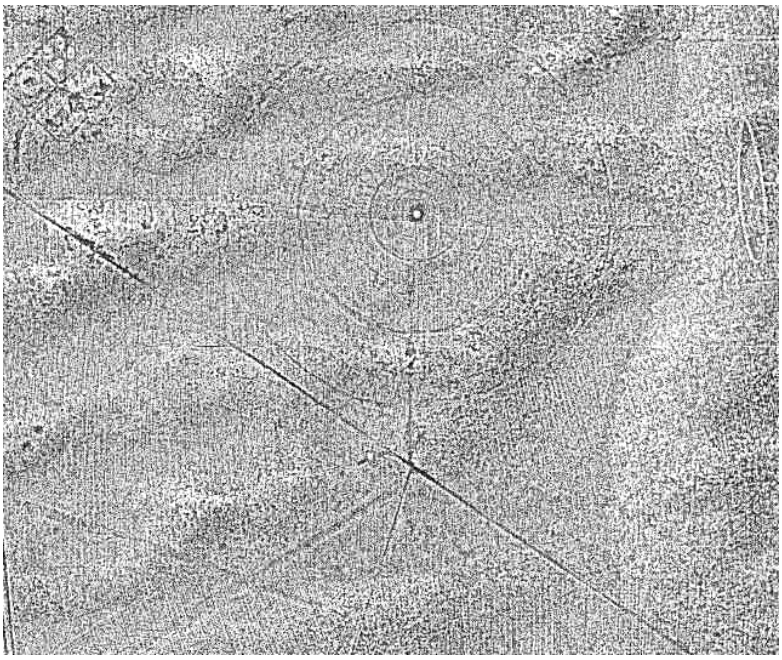

August 2007

Report Documentation Page

Form Approved
OMB No. 0704-0188

1. REPORT DATE	2. REPORT TYPE	3. DATES COVERED
AUG 2007		**00-00-2007 to 00-00-2007**

4. TITLE AND SUBTITLE	5a. CONTRACT NUMBER
High Density Lidar and Orthophotography in UXO Wide Area Assessment	5b. GRANT NUMBER
	5c. PROGRAM ELEMENT NUMBER
6. AUTHOR(S)	5d. PROJECT NUMBER
	5e. TASK NUMBER
	5f. WORK UNIT NUMBER
7. PERFORMING ORGANIZATION NAME(S) AND ADDRESS(ES) **Environmental Security Technology Certification Program (ESTCP),4800 Mark Center Drive, Suite 17D08,Alexandria,VA,22350-3605**	8. PERFORMING ORGANIZATION REPORT NUMBER
9. SPONSORING/MONITORING AGENCY NAME(S) AND ADDRESS(ES)	10. SPONSOR/MONITOR'S ACRONYM(S)
	11. SPONSOR/MONITOR'S REPORT NUMBER(S)

12. DISTRIBUTION/AVAILABILITY STATEMENT
Approved for public release; distribution unlimited

13. SUPPLEMENTARY NOTES

14. ABSTRACT

URS Corporation and Terra Remote Sensing, Inc. were awarded ESTCP funding to demonstrate the utility of high-density lidar and orthophotography as one component of a multi-technology approach to UXO/munitions and explosives of concern (MEC) Wide Area Assessment (WAA). Lidar and orthophotography were collected at two former military sites: the 5,000-acre Kirtland Precision Bombing Range site near Albuquerque, New Mexico, and the 5,640 Victorville Demonstration Bombing Target (DBT) Y site near Victorville, California. Data was collected at the Kirtland site over three days in August 2005 and at the Victorville site over two three-day periods in January and February 2006. Performance objectives of the demonstration were to ? Identify munitions response sites (MRS) such as bombing targets, open burn/open detonation areas, and burial pits that are the result of sanctioned military activities (whether documented or undocumented) that could reasonably be expected to result in the release of MEC to the environment ? Provide information about the site and the MRS to support future investigation prioritization, and cost estimation ? For areas outside of the MRS, provide information to support regulatory decisions regarding the portions of the munitions response areas outside of the MRS, including decisions as to requirements for further investigation, institutional controls, or no further action ? Describe the certainty associated with the initial conceptual site model (CSM), and examine the incremental contributions of each technology to improvements in that certainty These objectives were met. The MRS and munitions-related features were successfully identified, and findings were used to verify and correct the initial CSM. Information from the demonstration was successfully used by subsequent demonstrators and ESTCP in subsequent phases of the WAA Pilot Program. All data accuracy specifications were met. The demonstration provided important insights regarding the appropriate uses and confidence levels for both lidar and orthophoto technologies. At the Kirtland site, all four of the known targets from the CSM were identified using lidar data. Additionally, three sub-target areas and 16 additional areas of interest were identified, including a potential bull?s-eye target ring not documented in the CSM. The areas of interest consisted of

15. SUBJECT TERMS

16. SECURITY CLASSIFICATION OF:			17. LIMITATION OF ABSTRACT	18. NUMBER OF PAGES	19a. NAME OF RESPONSIBLE PERSON
a. REPORT	b. ABSTRACT	c. THIS PAGE			
unclassified	**unclassified**	**unclassified**	**Same as Report (SAR)**	**199**	

CONTENTS

CONTENTS (Continued)

CONTENTS (Continued)

APPENDICES

CONTENTS (Continued)

FIGURES

CONTENTS (Continued)

CONTENTS (Continued)

TABLES

ABBREVIATIONS AND ACRONYMS

AOI	area of interest
CERCLA	Comprehensive Environmental Response, Compensation, and Liability Act
CSM	conceptual site model
DBT	Demolition Bombing Target
DEM	digital elevation model
DoD	Department of Defense
EM	electromagnetic
EMI	electromagnetic induction
ESTCP	Environmental Security Technology Certification Program
GIS	Geographical Information System
GPS	Global Positioning System
HE	high explosive
IMU	Inertial Measurement Unit
lidar	light detection and ranging
MEC	munitions and explosives of concern
MRS	munitions response site
NDIA	New Demolitions Impact Area
PBR	Precision Bombing Range
QA	quality assurance
QC	quality control
SAR	synthetic aperture radar
SORT	Simulated Oil Refinery Target
TIN	Triangulated Irregular Network
TRSI	Terra Remote Sensing, Inc.
UXO	unexploded ordnance
WAA	wide area assessment

ACKNOWLEDGEMENTS

This project was made possible through funding provided by the Environmental Security Technology Certification Program (ESTCP). We express our sincere appreciation to Dr. Jeffrey Marqusee, ESTCP Program Director, and Dr. Anne Andrews, Unexploded Ordnance (UXO) Program Manager, as well as Dr. Herb Nelson of the Naval Research Lab, the project manager for the Wide Area Assessment Pilot Program, for their support and guidance to URS for this project. We would also like to express our thanks to ESTCP's support staff at Versar, Inc. and HGL Inc., and to the contract staff at the US Army Corps of Engineers Humphreys Engineering Center.

Grateful acknowledgement is also made to our demonstration partner Terra Remote Sensing, Inc. of Sydney, British Columbia, who performed lidar and orthophoto data acquisition and contributed significantly to development of data analysis and quality assurance/quality control methods.

ABSTRACT

URS Corporation and Terra Remote Sensing, Inc. were awarded ESTCP funding to demonstrate the utility of high-density lidar and orthophotography as one component of a multi-technology approach to UXO/munitions and explosives of concern (MEC) Wide Area Assessment (WAA). Lidar and orthophotography were collected at two former military sites: the 5,000-acre Kirtland Precision Bombing Range site near Albuquerque, New Mexico, and the 5,640 Victorville Demonstration Bombing Target (DBT) Y site near Victorville, California. Data was collected at the Kirtland site over three days in August 2005 and at the Victorville site over two three-day periods in January and February 2006.

Performance objectives of the demonstration were to:

- Identify munitions response sites (MRS) such as bombing targets, open burn/open detonation areas, and burial pits that are the result of sanctioned military activities (whether documented or undocumented) that could reasonably be expected to result in the release of MEC to the environment

- Provide information about the site and the MRS to support future investigation, prioritization, and cost estimation

- For areas outside of the MRS, provide information to support regulatory decisions regarding the portions of the munitions response areas outside of the MRS, including

decisions as to requirements for further investigation, institutional controls, or no further action

- Describe the certainty associated with the initial conceptual site model (CSM), and examine the incremental contributions of each technology to improvements in that certainty

These objectives were met. The MRS and munitions-related features were successfully identified, and findings were used to verify and correct the initial CSM. Information from the demonstration was successfully used by subsequent demonstrators and ESTCP in subsequent phases of the WAA Pilot Program. All data accuracy specifications were met. The demonstration provided important insights regarding the appropriate uses and confidence levels for both lidar and orthophoto technologies.

At the Kirtland site, all four of the known targets from the CSM were identified using lidar data. Additionally, three sub-target areas and 16 additional areas of interest were identified, including a potential bull's-eye target ring not documented in the CSM. The areas of interest consisted of isolated groups of potential craters.

Bombing targets at the Kirtland site were constructed from berms; these had weathered to between 5 cm and 15 cm (2 and 7 inches) in height, and most were not visible to ground crews on the site. These targets were clearly visible in the lidar data but generally not in the orthophotos. However, the orthophotos did show some target elements, such as target cross-hairs, that were not visible in the lidar data.

Subsequent validation activities using magnetometry and intrusive investigation verified the bombing targets and the three ancillary target areas, and indicated that the 16 additional areas of interest likely were not munitions-related. Validation activities also showed the presence of two areas of concentrated munitions-related scrap near one of the targets that were not revealed by either the lidar or orthophoto data.

At the Victorville site, both targets identified in the initial CSM were visible in both the lidar and orthophoto data. Large craters were visible in and near DBT Y, the Means Dry Lake bed. Potential craters ranged from 5 to 8 m in diameter and up to 1 m deep. Potential crater locations were used to modify the boundary of the MRS presented in the CSM. Target PBR 15, a bull's-eye target used for precision bombing practice, consisted of a series of rings constructed from asphalt. The target area was clearly visible in the orthophoto and lidar intensity data, and showed no evidence of craters.

Increasing the lidar data density increased the rate of detection of craters in the 1 m to 3 m size range substantially, but had only a weak effect on detection of larger craters, additional areas of interest, and bombing targets. Lidar density effects were most pronounced between the

1.5 pts./m^2 data and the 4.5 pts./m^2 data sets, and diminished thereafter. Detection of faint linear features was affected by flight line orientation. Common lidar surface artifacts were encountered, consisting of faint lines approximately 0.5 m in height.

The probability of detection for the bombing targets at both sites was 100%, with all of the known targets from the CSM being detected at both sites. Nevertheless, MRS at the Kirtland site were missed: validation activities revealed two sites with concentrated ordnance-related scrap that were not identified using either lidar or orthophotos, presumably because they left little or no surface disturbance. No clear false alarms were encountered for bombing targets. There was no attempt to measure false alarm rates for individual potential craters.

Overall costs for acquisition and processing of lidar and orthophotos were approximately $48/acre for Kirtland and $27/acre for Victorville. Per-acre costs at Kirtland were higher due to acquisition of four lidar flights and two orthophoto sets, compared to two lidar flights and one orthophoto set at Victorville. Costs are projected to be approximately $20/acre for an 18,000-acre site, based on preliminary results from the Former Camp Beale site acquired in late 2006. Costs are projected at between $12 and $14/acre for sites in the 50,000 – 110,000 acre range. Costs for competing technologies are discussed in the Final Report for the WAA Pilot Program.

The results of the demonstration support the use of lidar and orthophotos as an integral part of the WAA Process. These technologies proved to be a cost-effective and reliable means to characterize the sites, validate and correct the initial CSMs, and provide data to focus the application of subsequent methods of investigation. Lidar and orthophotos will not detect sites where there are no surface indications. Consequently, use of lidar and orthophotos should be followed by technologies that detect munitions components directly.

1.0 INTRODUCTION

1.1 BACKGROUND

Many millions of acres of Department of Defense (DoD) lands are potentially contaminated with military munitions or their components. On the majority of these sites, munitions are concentrated in specific ranges and training areas, while the remainder of the site is ordnance-free. Contaminated sites traditionally have been very expensive to investigate and remediate because of the nature of the contamination and the relatively few innovative approaches available to date.

The current demonstration was conducted as part of the Environmental Security Technology Certification Program (ESTCP) Wide Area Assessment (WAA) Pilot Program, which explored the use of an integrated suite of airborne and ground-based technologies as a means to identify and validate pilot WAA technologies and approaches. Light detection and ranging (lidar) and orthophotography, the subjects of this demonstration, were used in conjunction with synthetic aperture radar (SAR), hyperspectral sensing, helicopter-based magnetometry, and towed-array magnetometry and electromagnetic induction (EMI), along with statistical modeling, in an integrated Geographical Information System (GIS)-based analytical environment.

This report discusses the results of lidar and orthophoto data collection and analysis at two demonstration sites. The results from the WAA Pilot Program as a whole, and the relationship of these two technologies to the entire suite of technologies tested, are discussed in the final report for the WAA Pilot Program as a whole.

1.2 OBJECTIVES OF THE DEMONSTRATION

The objective of the demonstration was to demonstrate and validate the ability of lidar and orthophotos to contribute to the WAA process by:

- Identifying munitions response sites (MRS) such as bombing targets, open burn/open detonation areas, and burial pits that are the result of sanctioned military activities (whether documented or undocumented) that could reasonably be expected to result in the release of munitions and explosives of concern (MEC) to the environment

- Providing information about the site and the MRS to support future investigation, prioritization, and cost estimation

- For areas outside of the MRS, providing information to support regulatory decisions, including decisions as to requirements for further investigation, institutional controls, or no further action

- Describing the certainty associated with the initial conceptual site model (CSM), and examining the incremental contributions of each technology to improvements in that certainty

An additional objective was to develop information about the factors that would affect the cost and performance of both technologies, including the relationship between levels of effort and confidence in conclusions. Data density was the primary performance factor tested.

1.3 REGULATORY DRIVERS

MEC remediation is generally conducted under authority of the Comprehensive Environmental Response, Compensation, and Liability Act (CERCLA). With many millions of acres of land potentially contaminated with MEC, estimates of the cost of elimination of environmental liability under this statute at known and former DoD sites range as high as several hundred billion dollars. These potentially high costs have led to interest in the development of innovative investigative or screening methods, in order to reduce the costs of conducting WAA and associated remediation activities.

1.4 STAKEHOLDER/END-USER ISSUES

The demonstration showed that both lidar and orthophotos can contribute to the WAA process through cost-effective delineation of MRS- and MEC-related features. The demonstration results indicate that lidar and orthophotos are most appropriately used during the early phases of the WAA process, in order to focus and prioritize the subsequent application of more expensive low-altitude and ground-based technologies.

2.0 TECHNOLOGY DESCRIPTION

2.1 TECHNOLOGY DEVELOPMENT AND APPLICATION

2.1.1 Technology Background

Lidar is a well-established airborne technology for modeling ground surfaces. Topographic lidar was first developed in the late 1960s and early 1970s, and has been used for terrain profiling since the mid-1980s. Lidar has been in wide commercial use since around 1993, and the accuracies and limitations of lidar for surface modeling are well documented.

Lidar uses the time of return for a laser pulse to be reflected back to the sensor to measure the elevation of the point of reflection. Use of Global Positioning System (GPS) and Inertial Measurement Unit (IMU) technology to locate the sensor precisely in the air allows for the accurate calculation of the point of reflection of the laser signal from the ground, buildings or vegetation. Multiple returns from a single laser pulse can be detected, increasing the chance of sampling the ground surface through gaps in vegetation. Once elevation data is collected in the form of lidar points, surface models are created and analyzed. The surface modeling process is typically conducted using standard GIS software and methods, and much of the process can be successfully automated. Lidar vendors typically guarantee a vertical accuracy of 0.15 m and a horizontal accuracy of 0.3–0.75 m.

Figure 2-1
Helicopter-Mounted Lidar and Orthophoto Sensor Equipment

Figure 2-2
Lidar System Operations

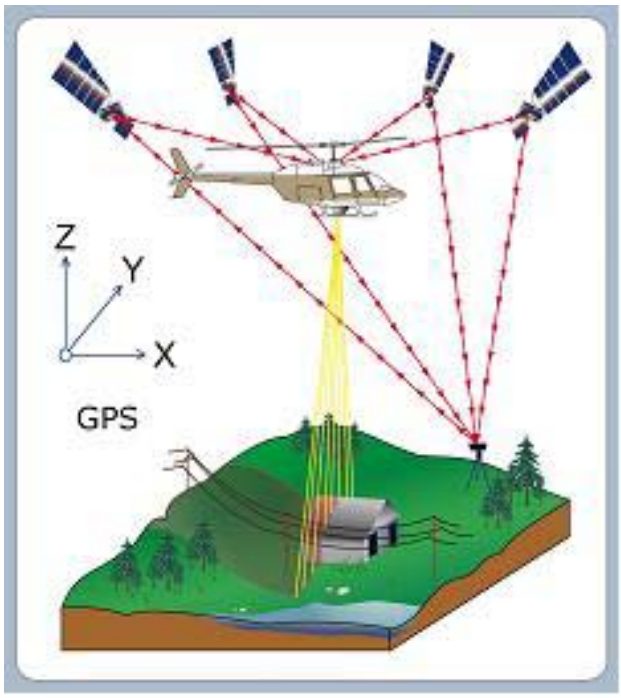

The development of higher-speed (50–100 kHz) laser scanners beginning around 2002 has significantly improved the ability of lidar to locate small features. Currently, high-speed lidar systems are being used to characterize objects in the sub-meter range, such as power line insulators. The accuracy and data density of current lidar systems suggest that the technology could be used to detect ground features indicative of ordnance use, including targets and craters, and that the presence of these features could in turn be used to develop more accurate locations of MEC.

Digital orthophotography has been commercially available since the early 1980s, with steady improvement in the resolution (i.e., pixel size) and precision (i.e., pixel placement) of the images as the technology of digital cameras, GPS, and IMU systems has advanced. Since the mid 1990s, image size has advanced from 1,500 pixels across an image to 4,500 pixels. This has allowed for increased flying heights and a reduced number of images for a given area, with consequent cost savings. Commensurate with this improvement has been a twofold increase in the accuracy of the IMU, allowing for accurate positioning of image pixels at a higher flying height.

Airborne digital cameras have been successfully integrated with lidar sensors. Cameras with an image density of roughly 4,000 x 4,000 pixels are generally favored, because the width of the images collected is very similar to that of the typical lidar point swath. Once collected, individual digital images are mosaiced and color balanced, and the resulting composite image is orthorectified using the lidar data. Orthorectification allows for the accurate location of each photo pixel, eliminating distortion caused by camera angle and topography. Vendors generally guarantee a horizontal accuracy of 3 pixel widths compared to ground control for orthophotography.

Digital images are collected concurrently with lidar and, because the two sensors use the same GPS and IMU, the two data sets can be integrated very accurately. Vendors generally guarantee spatial integration of orthophotos and lidar within 2 pixel widths. Final orthophoto pixel size depends on the flight altitude and the camera specifications; helicopter-based cameras flying at altitudes of 400–450 meters are capable of pixel sizes of approximately 10 cm. Smaller pixel sizes than this are generally impractical due to the low flight elevations and slow flight speeds required to collect properly overlapping images, and the very large numbers of images that would need to be mosaiced.

The ability to produce spatially accurate orthophotos with relatively small pixel sizes suggests that this technology could be used to identify ordnance-related features, and to cross-validate technologies such as lidar.

2.2 PREVIOUS TESTING OF THE TECHNOLOGY

URS and Terra Remote Sensing, Inc. (TRSI) conducted a successful demonstration of lidar and high-resolution digital imagery at an operational US Navy range near Boardman, Oregon during November 2004. Both the lidar data and the orthophotos were successful in detecting patterns of surface disturbance indicative of unexploded ordnance (UXO)/MEC activities. Moreover, the two data sets were found to complement each other well, each revealing features that the other did not. Orthophotos collected during the November 2004 test flight showed color variations that could not be detected by lidar (for example, painted truck tires used to outline bombing targets). Very subtle ground features, such as vehicle tracks, which were beyond the resolution of the lidar data at that resolution, were visible in the photos.

Even though the lidar data was collected at relatively low density, lidar revealed depressions such as craters better than the orthophotos, where it was difficult to distinguish depressions from shadows or mounds. Lidar was very successful at locating target features such as bull's-eye rings. Disposal craters could be distinguished from bombing practice craters by their patterns on the ground. Surface models created from lidar data could be analyzed in ways that orthophoto data could not be, such as measuring the depth of craters.

2.3 FACTORS AFFECTING COST AND PERFORMANCE

Factors affecting cost and performance of lidar and orthophotos are detailed in Table 2-1.

Table 2-1
Cost and Performance Factors

Item	Cost and Performance Factors
Lidar data density	Higher lidar data density is generally more expensive, due to the need to acquire and process additional flight lines.
Orthophoto data density	Orthophotos with smaller pixels are more expensive, because of the additional flight lines required and the larger number of individual digital images that must be processed and mosaiced.
Accuracy and precision requirements	Accuracy and precision are largely determined by the equipment used and the care of the operators. Projects with extremely high accuracy requirements, such as creation of contour lines under 1-foot intervals, can only be accomplished by vendors with extremely new equipment, at higher cost.
Site location and logistics	Sites with longer flying times to an airport will be more expensive, as they will require either longer flight times or placing fuel on the test site.
Accuracy verification requirements	Verification of accuracy and precision is accomplished through placement of survey control points and comparison of lidar and orthophoto data to those points. Projects with higher verification requirements will be more costly, although this factor is small compared to other factors.
Site size	Larger sites can achieve substantial cost savings through amortization of fixed costs, such as mobilization and project planning, as well as through increased efficiency in data acquisition and processing.
Vegetation conditions	More densely vegetated sites will have higher costs due to the requirement for additional lidar passes to achieve sufficient point density at the ground surface. Vegetation will affect the ability of both lidar and orthophotos to view or model the ground surface.
Permitting and site access	Some DoD sites contain high-security areas, which can present higher costs for pre-flight planning and data collection. These costs result from restrictions on site access, time to acquire needed clearances, and longer flight times to avoid restricted areas. Sites with environmental constraints do not normally impose higher costs for lidar and orthophotography, due to the airborne nature of the technologies. However, the presence of sensitive species may affect pre-flight planning and scheduling (and thus costs) for projects that require landing to re-fuel on the site.

2.4 ADVANTAGES AND LIMITATIONS OF THE TECHNOLOGY

Advantages and limitations offered by use of lidar and orthophotos compared to the traditional approaches to MRS investigation as shown on Table 2-2.

Table 2-2
Technology Advantages and Limitations

Item	Advantages
Rate of coverage	In an operational setting, data collection rates of 5,000 acres per day can be expected for lidar and orthophotos. This compares favorably to maximum collection rates of around 500 acres per day for helicopter-based magnetometry, and 20 acres per day for towed-array magnetometry.
Ability to delineate MRS and MEC-related features	Lidar and orthophotography successfully revealed MRS and MEC-related surface features at both demonstration sites, even many years after their last use. In the case of the Kirtland site, these features were often not visible to observers on the ground.
Enhanced planning and risk assessment	Because they can cover entire sites relatively quickly and at lower cost, these technologies can be used to locate and prioritize appropriate areas for use of more costly ground-based technologies.
Other benefits	Both technologies provide highly detailed topographic data that can be integrated into a facility's CAD or GIS system and used in subsequent phases of site investigation, site remediation, and range management
Item	**Limitations**
MEC detection	Neither lidar nor orthophotography can directly detect small dimension shell casings or other MEC components. Consequently, further investigation with magnetometers or electromagnetic (EM) sensors is generally required.
Elevation data	Orthophotos do not contain elevation information. In practice, it is sometimes difficult to distinguish small surface depressions from small mounds or shadows using orthophotos alone.
Vegetation effects	Since both lidar and orthophotos are light-based technologies, neither will penetrate vegetation. Orthophotos do not "look through" vegetation, and lidar point densities will be lower in vegetated areas. However, lidar is frequently successful in penetrating small openings between and within vegetation, and this success has increased with the speed of lidar sensors and the development of the ability to measure multiple returns.

3.0 DEMONSTRATION DESIGN

3.1 PERFORMANCE OBJECTIVES

The primary performance objectives for these technologies were to:

- Clarify whether and to what extent lidar and orthophotos can delineate MRS boundaries and MEC-related features, and contribute to focusing and prioritizing subsequent low-altitude and ground-based work

- Reveal relationships between the density of lidar and orthophoto data, their levels of cost, and their ability to accurately locate MRS boundaries and MEC-related ground features

- Clarify whether and to what extent lidar and orthophotos can verify, reveal errors in, or improve the accuracy of the initial CSM

- Contribute data and analysis to the overall combination of technologies used in the WAA Pilot Program, in a manner that is timely to the application of the other technologies demonstrated, in formats useable by other demonstrators, and with sufficient positional accuracy compared to project control points to allow meaningful coordination and comparison

Specific performance criteria and performance metrics related to each of these objectives are established in the Technology Demonstration Plan for each site.

3.2 SELECTION OF TEST SITES

Both demonstration sites were chosen by the ESTCP Program Office. Details of the site selection process can be found in the final report for the WAA Pilot Program.

3.3 TEST SITE HISTORY, CHARACTERISTICS AND PRESENT OPERATIONS

The first demonstration site was located at the Kirtland Air Force Base Precision Bombing Range (PBR) located approximately 10 miles west of Albuquerque, New Mexico (Figure 3-1). The site is part of a much larger set of bombing ranges used for training purposes during World War II. The study site consisted of approximately 5,120 acres within the PBR located in two parcels to the north and south of the Double Eagle Airport, the primary small aircraft airport for the Albuquerque area. The study area itself is currently undeveloped, although portions are

planned for commercial or industrial development, and airport expansion into the study are is possible.

Figure 3-1
Kirtland Precision Bombing Range Site

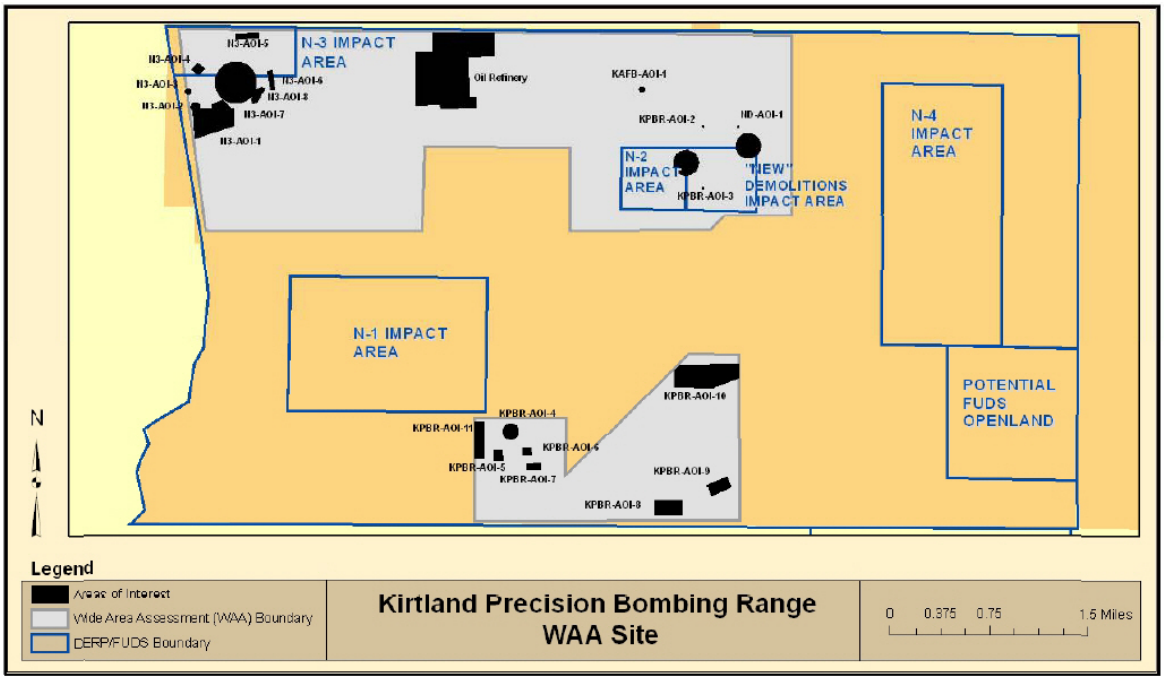

Source: ESTCP (2007a)

Munitions known or suspected to have been used at the site include 100-point practice bombs and 250-pound high explosive (HE) bombs. A certificate of clearance has been issued for one portion of the site, Target N3. Four target areas were identified in the initial CSM as within the study site:

- Target N-2, a 1,000-foot-diameter bull's-eye target used for 100-pound practice bombs
- Target N-3, a 1,000 -foot-diameter bull's-eye target used for 100-pound practice bombs and for scrap storage
- The New Demolitions Impact Area (NDIA), a 1,000 -foot-diameter HE bull's-eye target

- The Simulated Oil Refinery Target (SORT), a target consisting of 350-foot x 350-foot rectangular cells

Locations were given for the first three targets in the CSM. The approximate location of the SORT was given as "somewhere northwest of the Double Eagle airport."

The second demonstration site was located at the Former Victorville Army Air Force Demolition Bombing Target (DBT) Y and PBR 15 (Figure 3-2). The site is located in San Bernardino County, California, approximately 42 miles southeast of the town of Victorville, California. This site lies within a much larger complex of approximately 23 targets used between 1942 and 1945. The site is managed by the US Bureau of Land Management, and is used primarily as a recreation area for off-road vehicles, camping, and target shooting. The demonstration site encompasses approximately 5,640 acres.

Figure 3-2
Victorville DBT Y and PBR Target 15 Site

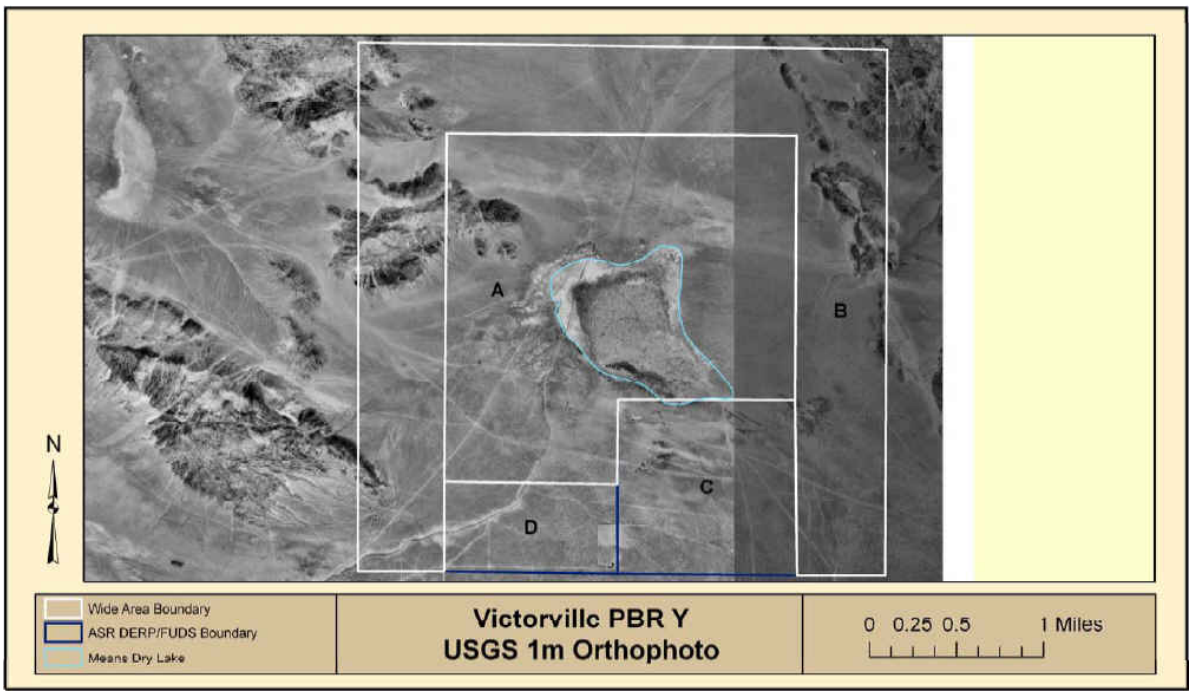

Source: ESTCP (2007b)

Two target areas were identified in the initial CSM for the Victorville site:

- Target DBT Y, located in Means Dry Lake bed in the center of the demonstration site, identified as a demolition bomb target area where bombs between 100 and 2,000 pounds were used.

- Target PBR 15, a suspected bull's-eye target located in the southeast portion of the demonstration site used for precision bombing practice. According to the initial CSM, PBR 15 was not visited during the archival search report site visit and little is known about the area.

3.4 PRE-DEMONSTRATION TESTING AND ANALYSIS

3.4.1 Kirtland Demonstration Site

Prior to mobilization, ESTCP established five survey control points on the Kirtland site (Figure 3-3). TRSI established four additional control points and independently occupied two of the ESTCP control points. Six vertical control structures were placed adjacent to the six control points established by TRSI, but two were vandalized prior to data collection. A test crater area was established in the south portion of the project site containing two test craters at 1.5 m diameter, two at 1.0 m diameter, and six at 0.32 m diameter (Figure 3-4).

Figure 3-3
Kirtland Control Points

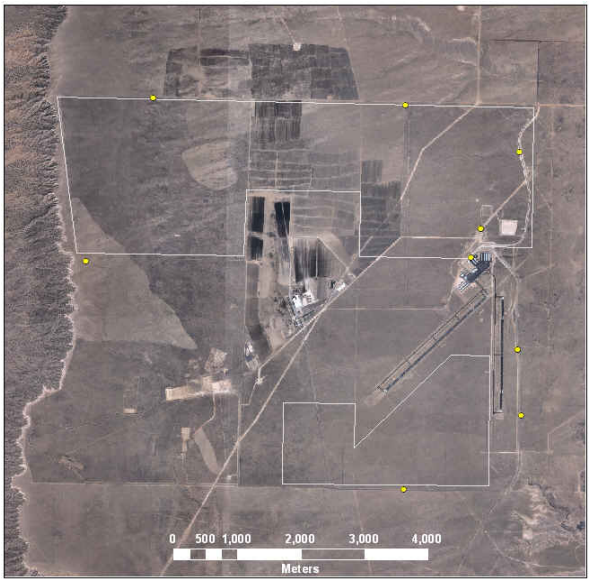

Control point locations

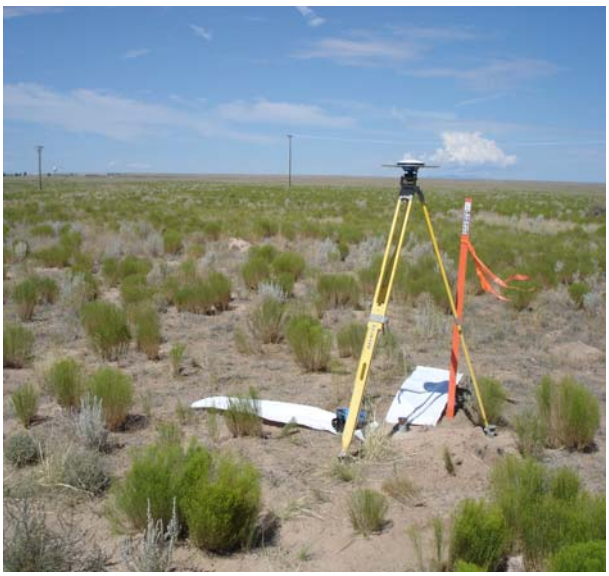

Example Kirtland control point

Figure 3-4
Kirtland Test Craters

0.32 m test craters

1.5 m test crater

On August 9, 2005, calibration flights were conducted to establish appropriate pitch, yaw, and roll correction factors and appropriate lidar sensor speeds. A laser pulse rate of 50 kHz was selected, based on performance at a variety of speeds tested. Lidar and orthophoto missions began the same day.

3.4.2 Victorville Demonstration Site

At the Victorville site, TRSI established eight survey control points on the site (Figure 3-5). These sites were later independently occupied by ESTCP. Four vertical control structures and 10 test craters were also established, at the same sizes as for the Kirtland site (Figure 3-6). Unlike at Kirtland, the Victorville test craters were not grouped together in one location. This revised configuration eliminated the observed tendency to infer the location of smaller test craters from the known location of the adjacent larger craters.

Figure 3-5
Victorville Control Points

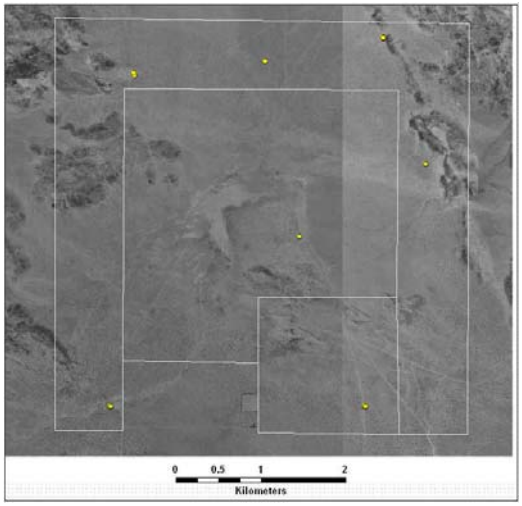

Control point locations

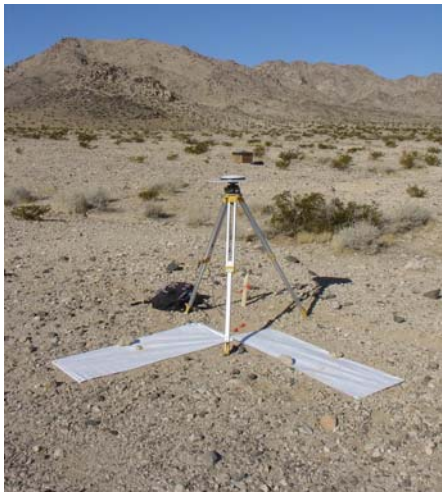

Example Victorville control point

On February 4, 2006, calibration flights were conducted. A laser pulse rate of 40 kHz was selected as most appropriate to meet overall point density targets. Orthophoto flights began on January 24, 2006 and lidar acquisition flights began on February 3, 2006.

Figure 3-6
Victorville Test Craters

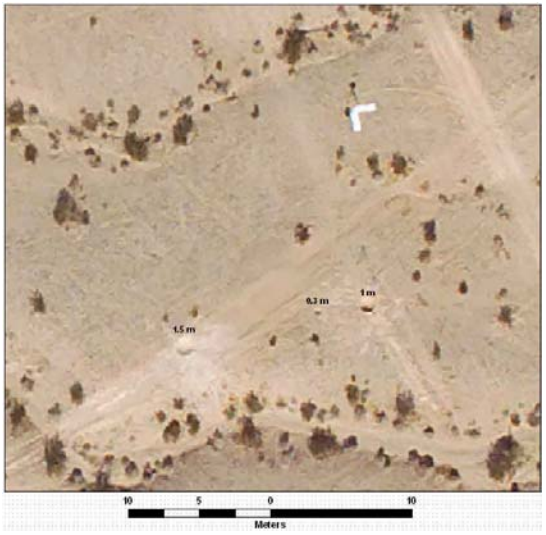

Sample test craters

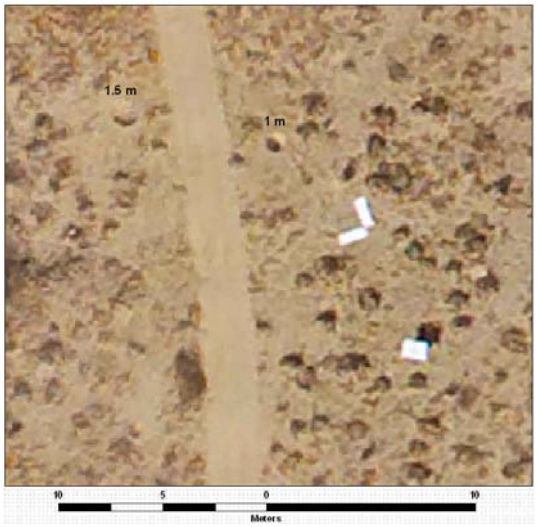

Sample test craters and vertical control structure

3.5 TESTING AND EVALUATION PLAN AND PROCEDURES

3.5.1 Demonstration Set-Up and Start-Up

At both sites, TRSI conducted flight line planning for the lidar/orthophoto and lidar only flights in the weeks prior to mobilization. Flight lines were planned to ensure complete site coverage, minimize the number of turns, and achieve planned overlap. At the Kirtland site, flight lines were planned to minimize interactions between data collection and air traffic at the Double Eagle Airport. Digital imagery was planned for acquisition at periods of low sun angle at both sites. Previous testing had shown that the shadows created by low sun angle were useful in detecting shallow features.

At each site, the lidar and orthophoto sensor system was installed into a Bell 206B helicopter owned by a local helicopter vendor (Figure 3-7). Renting helicopters (and pilots) using local vendors is a standard industry practice which allows the lidar vendor to ship only the sensor package rather than the aircraft. The use of local helicopter vendors also allows for the use of local pilots who have better knowledge of local weather patterns and flight clearance requirements.

Figure 3-7
Lidar Equipment Setup

Equipment installation

Sensor pod mounted below helicopter, control console visible through window

3.5.2 Period of Operation and Area Characterized

Data collection flights were begun once mobilization, sensor installation, and calibration flights were complete. The period for data collection included an additional day to allow for re-acquisition of any missed or erroneous areas discovered during daily quality assurance/quality control (QA/QC) review. Data collection periods were as shown on Table 3-1.

Table 3-1
Data Collection Periods

Period	Kirtland	Victorville
Preflight planning	July 2005	January 2006
Mobilization	August 8, 2005	February 7, 2006
Calibration flights	August 8, 2005	February 8, 2006
Data collection	August 9-11, 2005	January 24-25, 2006 February 3-4, 2006
Demobilization	August 1, 2005	February 5, 2006

At Kirtland, the area characterized was 1,914 hectares or 5,000 acres. At Victorville the area was 2,282 hectares or 5,640 acres.

3.5.3 Demobilization

Demobilization of the lidar and orthophoto equipment consisted of demounting the sensor system from the helicopter, packing and shipping. Demobilization required approximately a half day for each site.

3.6 SELECTION OF ANALYTICAL/TESTING METHODS

Analysis of lidar data is performed in two steps: conversion of sensor output to spatially correct lidar points, and then conversion of these points to useable GIS products such as surface models. Lidar data was processed into point files using a suite of software, including TerraSolid and custom algorithms written in this software by TRSI. TerraSolid is an industry standard software package for processing lidar data.

Creation of GIS products and their analysis were accomplished using ESRI's ArcGIS software suite. This package was chosen for two reasons. First, ArcGIS was the only standard CAD or GIS product reviewed that would successfully handle the large number of lidar points collected. Second, ArcGIS is the GIS package most widely used by US government agencies and private contractors. As such, it is appropriate to develop analysis methods and resulting products that can be duplicated by typical federal facilities managers.

Orthophoto data was analyzed in two steps: creation of a single orthorectified image from the large number of individual digital images collected, followed by visual examination of the image to locate potential MRS and munitions-related features. Processing of the digital imagery to create the orthophoto mosaic was accomplished using software from TerraSolid and PCI. This software is the industry standard.

3.7 RESULTS

3.7.1 Data Collection

At the Kirtland site, data collection flights took place on August 9, 10, and 11, 2005 with a total of 177 flight lines collected, totaling 555 km. Lidar data was collected at three altitudes: 900 meters, 450 meters, and 300 meters (Figure 3-8). Two sets of flight lines were flown at 300 meters. For the north portion of the project area the 300 meter flight lines were flown perpendicular to each other, for the south portion they were flown parallel. Orthophoto data was collected concurrently with lidar during the 900 meter and 450 meter flights.

Figure 3-8
Kirtland Sample Flight Lines

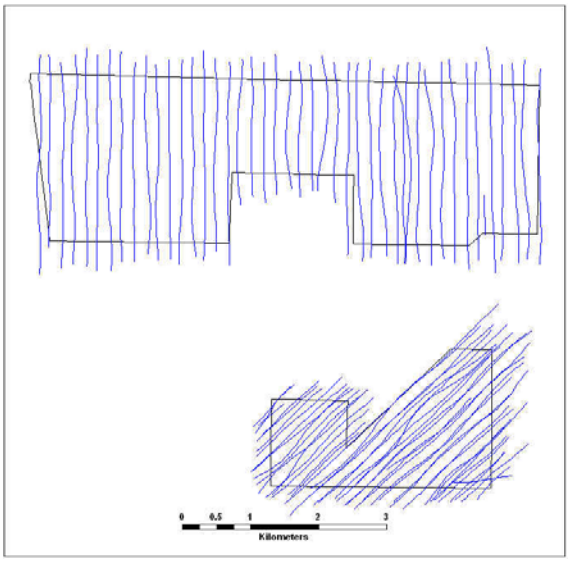

Kirtland flight lines, 300 m lidar flight 2

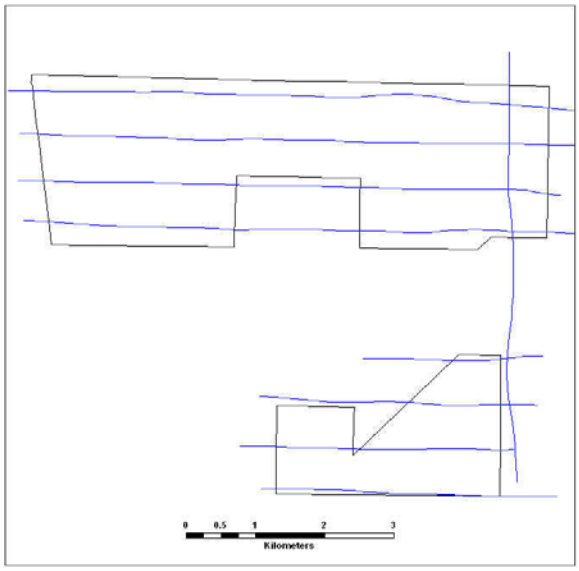

Kirtland flight lines, 900 m lidar and 20 cm orthophotos

Data was inspected each evening for GPS positional accuracy, completeness of lidar data coverage and imagery data coverage. During the final afternoon of data collection, flight lines that did not meet specifications were re-flown.

At the Victorville site, orthophoto data collection flights took place on January 24 and 25, 2006 and lidar data collection flights took place on February 3 and 4, 2006. A total of 45 flight lines were collected, totaling 601 km. Lidar data was collected at two altitudes: 450 meters and 300 meters (Figure 3-9). The two flights were flown perpendicular to each other. As at the Kirtland site, data was inspected each evening for accuracy and completeness, and data gaps were filled by additional flights prior to demobilization.

Figure 3-9
Victorville Sample Flight Lines and Example Image

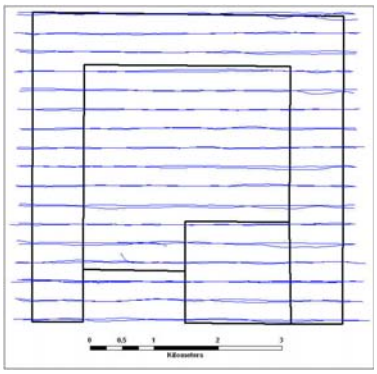

Victorville flight lines, 300 m lidar flight

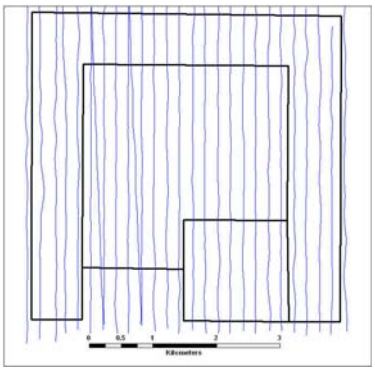

Victorville flight lines, 450 - m lidar and 10 cm orthophotos

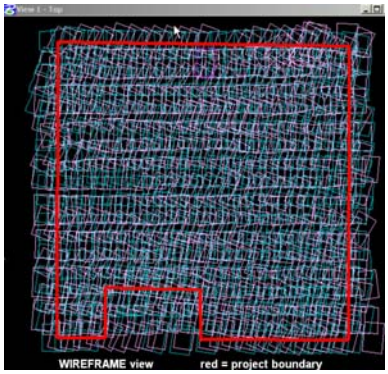

Example image from software used to check for complete coverage by digital imagery, 450 m flight

3.7.2 Safety Issues

At the Kirtland site, an important safety issue was the high level of air traffic at the Double Eagle Airport. This airport experiences more than 100,000 take-offs per year, and is located immediately adjacent to the study site between the north and south blocks. In response to the high level of air traffic, a second pilot was hired to be a spotter during data collection flights. This extra weight led to more frequent refueling and longer data collection work days. The air traffic situation also prevented the acquisition of perpendicular lidar flight lines for the south block, which would have required turning directly over the runway.

3.7.3 Data Processing Steps

TSRI processed the sensor output to create lidar points. Following return of the data to the office, calibration factors determined in the field were checked, fine-tuned, and applied to laser range, GPS, and IMU data to produce x,y,z values for each point. Lidar points were then transformed into the delivery datum and projection for each site, and coded to indicate returns from ground vs. non-ground surfaces. Lidar points were exported as text files for delivery to URS. Lidar data from each lidar flight was processed and delivered separately in order to allow for separate analysis of data from each flight altitude.

TSRI also processed digital images. The procedure included mosaicing the individual digital images collected during flight, transforming the consolidated image to the delivery datum and projection, orthorectification using the lidar data, color balancing, and trimming to the delivery tiles. For the Kirtland site, two sets of orthomosaics were created, one at 10 cm pixel size and one at 20 cm pixel size. For the Victorville site, a single set of orthophotos was created at 10 cm pixel size.

URS converted the random lidar point data to GIS products using the following steps:

- The lidar points were converted to ArcInfo point shape file format, with the horizontal locations determined by the northing and easting values in the lidar point file, and the elevation value, intensity value, and the code for ground or non-ground return retained as attributes.

- Point shape files were converted to Triangulated Irregular Network (TIN) files. A TIN is an elevation-based surface model where each point forms a vertex in a network of linked triangles. TINs were created from the lidar points coded as ground returns, using ArcInfo's TIN creation functions. A TIN was created for each lidar flight separately. For the Kirtland data, an additional TIN was created for the combined 300 meter flights, the combined 450 meter and 900 meter flights, and the points from all four flights. For the Victorville data, a TIN was created containing point from both flights. TINs were also created in selected areas using both ground and non-ground returns, in order to derive vegetation heights and to allow for QA/QC review of point classification as ground or non-ground returns.

- Digital elevation models (DEMs) were created from the TINs. A DEM is a regularly spaced, gridded array of elevation values. DEMs were created using the each of the TIN files as inputs. DEMs were created in the ArcInfo GRID file format, which allows for additional analysis that cannot be performed directly on the TIN file. All DEMs were created using 0.32 meter (1 foot) grid cell sizes. This value was chosen as the smallest cell size that would be supported by the lidar data densities acquired.

Automated GIS processing and analysis was used for many of the process steps.

Once the initial GIS products were created, the lidar data were examined to detect missing data, spatial discrepancies, or artifacts in the surface that would indicate improper calibration or other problems. Further data quality review, including review for spatial accuracy, was performed based on the parameters given in Appendix C of the Technology Demonstration Plan. All data met data quality specifications. Detailed results are given in Appendix A, Lidar and Orthophoto Positional Accuracy Results.

Following creation of initial GIS products and initial QA/QC review, analysis of the lidar and orthophoto data was conducted by URS:

- Hillshades were created for each of the DEMs. Hillshades are three-dimensional depictions of the surface with shadows formed by a simulated light source placed above the surface at an altitude and azimuth chosen by the operator. The default settings for hillshades in ArcGIS Spatial Analyst were used, then varied as needed during the analysis. Hillshades were saved in ArcInfo GRID format.

- Each lidar hillshade and orthophoto data set was visually inspected for potential MRS. Potential MRS were identified and drawn as ArcInfo line or polygon shape files for each data set.

- Each data set was visually inspected for potential munitions-related features. Potential features were drawn as ArcInfo line or polygon shape files for each data set. Potential features were classified according to naming standards provided by ESTCP.

- A slope model was created for each demonstration site. The process used the default setting for the ArcGIS SLOPE GRID command.

- Models of elevation above and below an average ground surface were created for each lidar data set. The process used the ArcInfo Focal Mean function.

3.7.4 Detection and Delineation of Munitions Response Sites

At the Kirtland site, all four of the MRS described in the Kirtland CSM were detected using lidar, and three of the four were detected using orthophotos. In addition, both technologies revealed additional potential sites of interest.

Table 3-2 presents Kirtland MRS detection results for each of the lidar and orthophoto data sets.

Table 3-2
MRS Detection – Kirtland

	MRS from CSM				Additional Sites of Interest
	N2	N3	NDIA	SORT	
Orthophotos					
20 cm	Y	Y	Y	N	1
10 cm	Y	Y	Y	N	1
Individual lidar flights					
900 m	Y	Y	Y	Y	6
450 m	Y	Y	Y	Y	7
300 m flight 1	Y	Y	Y	Y	7
300 m flight 2	Y	Y	Y	Y	7
Combined lidar flights					
450 and 900 m	Y	Y	N	Y	6
Both 300 m	Y	Y	Y	Y	5
All lidar	Y	Y	N	Y	5

As lidar data from different flights was combined, the number of additional potential MRS identified and the overall area mapped as MRS began to drop. This phenomenon is described more fully in Appendix B, Combining Lidar Data from Multiple Flights.

At the Victorville site, both MRS described in the initial CSM were detected, and were visible in both lidar data sets and the single orthophoto data set. No additional sites of interest were detected at Victorville using these technologies.

The following sections review data for each MRS listed in the Kirtland CSM in more detail.

3.7.5 Kirtland – Target N3 Results

Target N3 is described in the CSM as a 1,000-foot diameter bull's-eye target used for 100-pound practice bombs and scrap storage. In addition to the bull's-eye rings, three potential ancillary targets and one additional area of interest were identified that were not listed in the CSM: a ship target east of the bull's-eye, a simulated airfield target to the south, a diamond-shaped potential target to the west, and a small rectangular feature to the north. The bull's-eye rings consist of berms between 5 and 10 cm high and a mound at the center point approximately 80 cm high. The ship target consists of berms ranging from 60 cm in height on the north end to essentially flush with the ground surface on the south end. The diamond-shaped potential target consists of trenches from 20 to 70 cm deep in the corners.

Table 3-3
Target N3 Detection Results

	Rings	Ship	Airstrip	Diamond	Small Rectangle	Total Area of MRS (m^2)
Orthophotos						
10 cm	5	N	N	Y	N	195,258
20 cm	5	N	N	Y	N	195,258
Individual lidar						
900 m	4	Y	Y	Y	N	992,977
450 m	5	Y	Y	Y	N	1,226,982
300 m 1	5	Y	Y	Y	Y	1,226,982
300 m 2	5	Y	Y	Y	Y	1,226,982
Combined lidar						
450 and 900 m	5	Y	Y	Y	N	1,226,982
Both 300 m	5	Y				992,977
All lidar	5	Y	Y	Y	Y	992,977

Figure 3-10 shows the Target N3 target elements detected.

Figure 3-10
Target N3 Elements

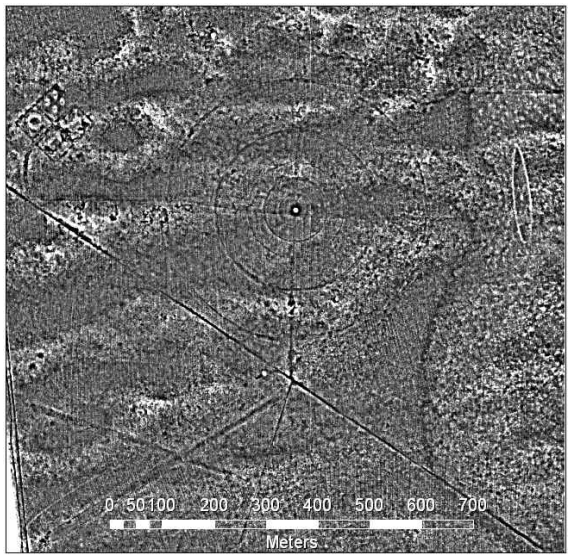

Target N3, 300 m lidar, showing target bull's-eye rings, ship target (east), diamond-shaped potential target (west), and simulated air strip (south).

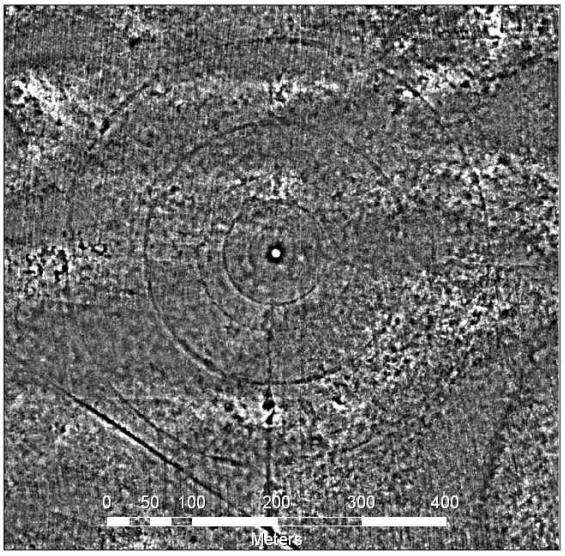

Target N3 bull's-eye rings, 450 m lidar displayed as elevations above an average ground surface.

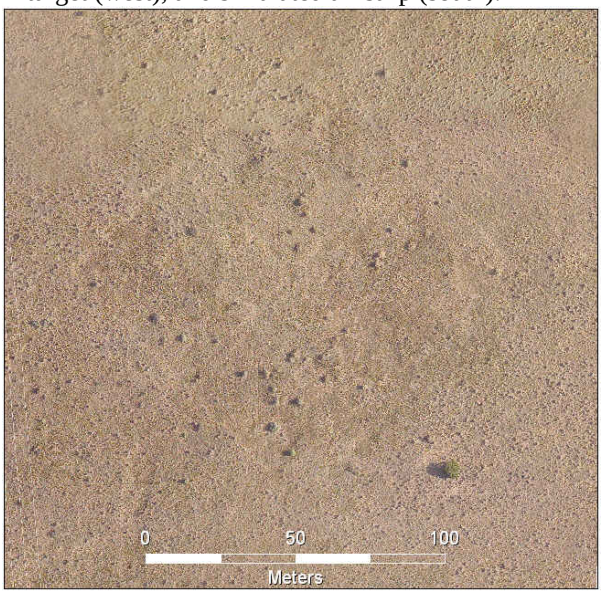

Diamond-shaped potential target west of N3 bull's-eye, 20 cm pixel orthophoto. Feature is approximately 100 m on each side.

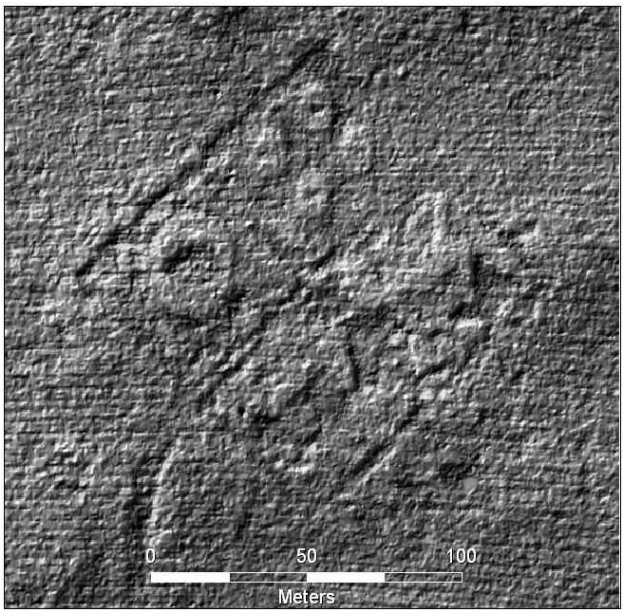

Diamond-shaped potential target west of N3 bull's-eye, 300 m lidar. Feature is similar in all lidar data sets.

Figure 3-10 (continued)
Target N3 Elements

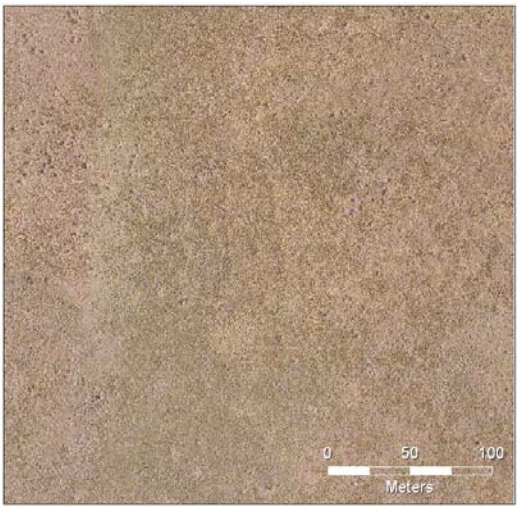

Ship target east of N3, 10 cm pixel orthophoto.

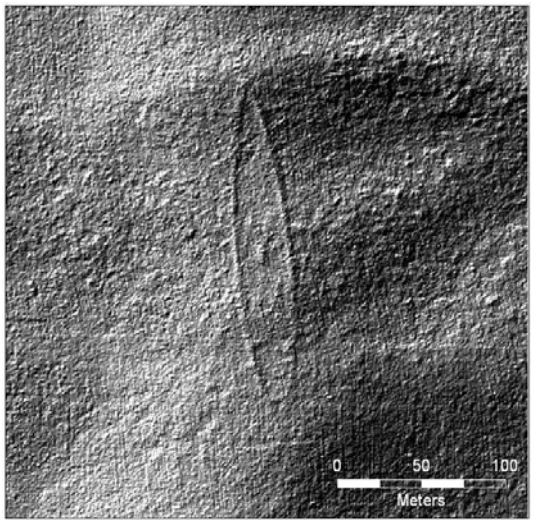

Ship target east of N3 shown in 300 m lidar surface combined with a 300 m lidar subtracted grid to enhance the image.

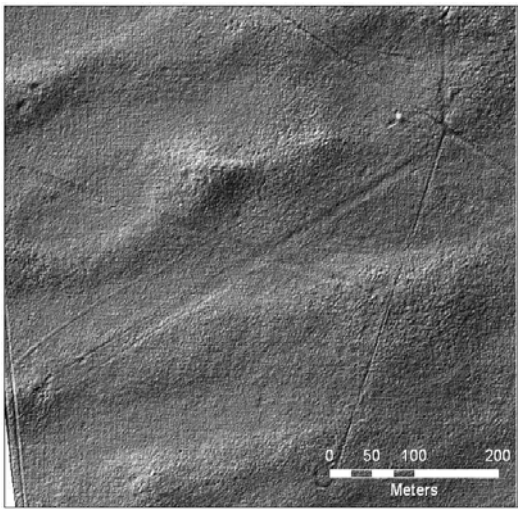

Airstrip target south of N3 bull's-eye.

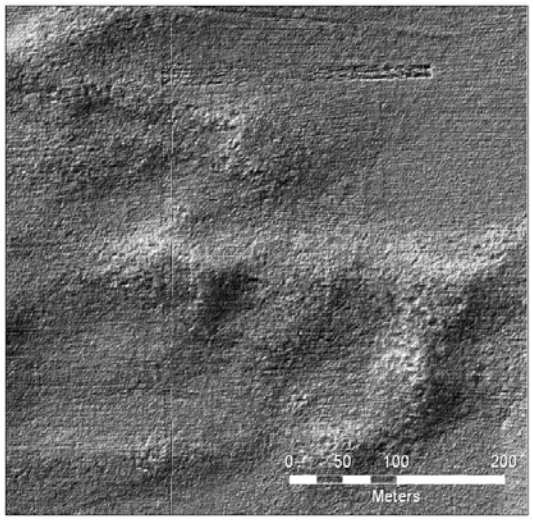

Small rectangular area of interest north of N3 bull's-eye.

3.7.6 Kirtland – Target N2 Results

Target N2 is described in the CSM as a bull's-eye target used for 100-pound practice bombs. The bull's-eye rings were visible using lidar data; there were few to no visible craters. Three rings were visible using the orthophotos at both pixel sizes, and four were visible in the lidar

data, regardless of data density. Because of the different number of rings visible, the total area of this MRS from the orthophotos was 26,234 m^2, while the total area from the lidar data was 74,753 m^2. The bull's-eye rings consist of berms between 5 and 10 cm high. Figure 3-11 shows the Target N2 target elements detected.

Figure 3-11
Target N2 Orthophoto and Lidar

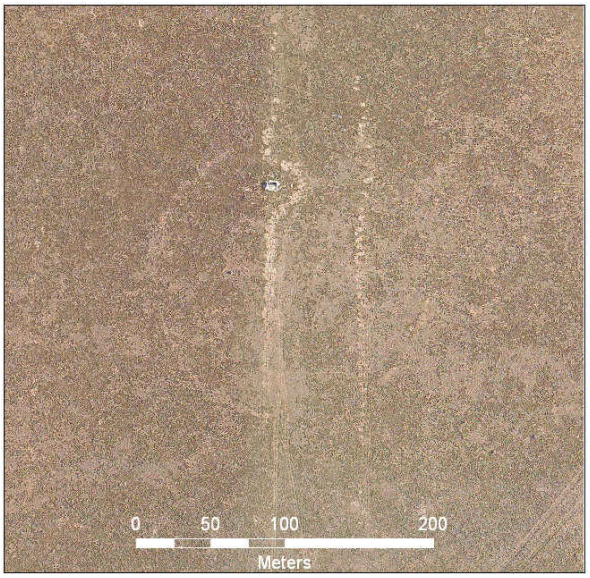

Target N2 bull's-eye, 20 cm pixel orthophoto

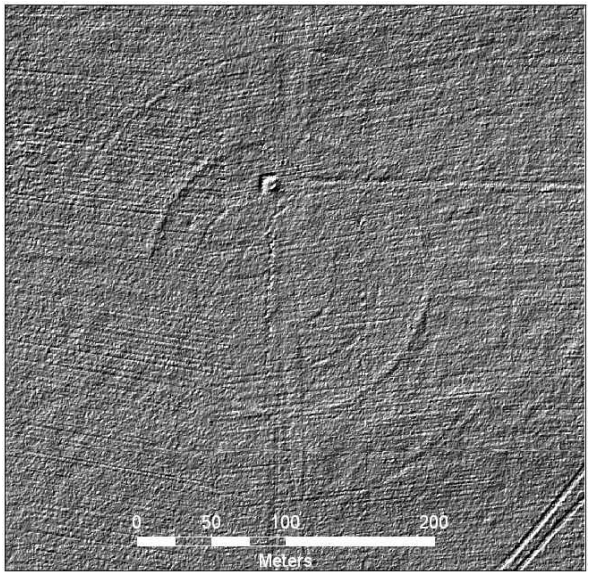

Target N2 bull's-eye, 300 m lidar

3.7.7 Kirtland – Target NDIA Results

The NDIA is described in the CSM as a 1,000 foot diameter HE bull's-eye target. Target cross-hairs and a single bull's-eye ring were visible in the orthophotos at both pixel sizes; neither was visible in the lidar data at any data density. A large number of probable craters was visible in the lidar data, with the number counted increasing with data density, then decreasing as data from the individual flights was combined. These craters were used to define the boundary of the MRS. Craters were not visible in the orthophoto data. Table 3-4 shows the features detected with each data set. Potential craters ranged from 1 to 3 meters in diameter and from 10 to 20 cm in depth.

Table 3-4
Target NDIA Detection Results

	Probable Craters	Rings	Cross-hairs	Total Area (m^2)
Orthophotos				
10 cm	0	1	2	78,251
20 cm	0	1	2	78,251
Individual lidar				
900 m	25	0	0	182,356
450 m	34	0	0	182,356
300 m 1	44	0	0	182,356
300 m 2	39	0	0	182,356
Combined lidar				
450 and 900 m	34	0	0	not found
Both 300 m	29	0	0	182,356
All lidar	33	0	0	not found

Figure 3-12 illustrates the complementary ability of lidar and orthophotos to define this target area, with the orthophoto image showing the cross-hairs and target rings, and the lidar data showing the probable craters.

Figure 3-12
Target NDIA Orthophoto and Lidar

Target NDIA 20 cm orthophoto showing target crosshairs and bull's-eye ring. Craters could not be seen in the orthophotos.

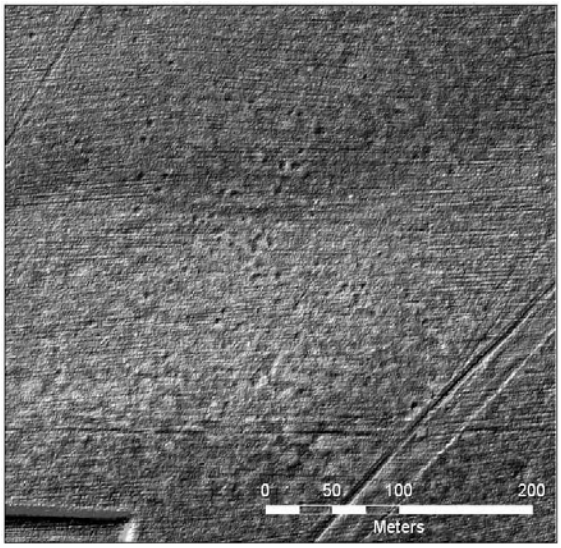

Target NDIA 300 m lidar showing craters. Cross-hairs and bull's-eye ring could not be seen using lidar.

3.7.8 Kirtland – Target SORT Results

The SORT is described in the CSM as a suspected target whose location is given as "somewhere northwest of the airport." The target was identified as a 23-acre rectangle subdivided into cells simulating an oil tank farm. This target was located using lidar data at all densities, but was not visible in either of the orthophoto sets (Figure 3-13). The target cells consist of berms from 0 to 20 cm in height.

Figure 3-13
Target SORT Orthophoto

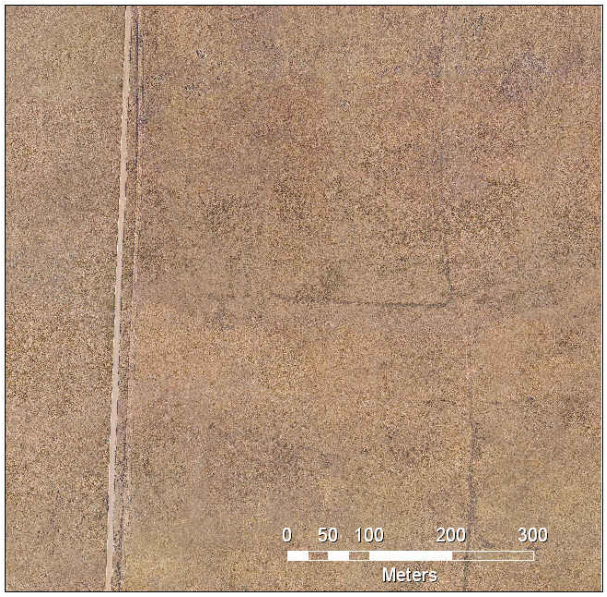

Target SORT, 10 cm pixel orthophotos. The target was not visible in either orthophoto data set.

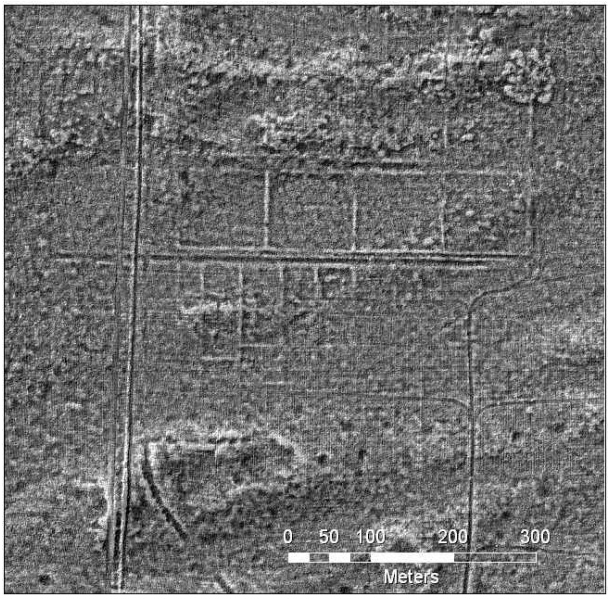

Target SORT, 300 m lidar. The target was visible in lidar data at all densities collected.

3.7.9 Kirtland – Other Sites of Interest

At the Kirtland site, 15 additional sites of interest were detected using the lidar data, including seven in the north portion of the site and eight in the south portion (Figure 3-14). One area in the south portion consisted of a previously unknown potential target bull's-eye; the remainder consisted of small groupings of potential craters and the small rectangular feature north of Target N3. All of these potential MRS were detected using lidar data; none was visible in the orthophotos. The potential craters are generally larger and more irregular than would be expected from any of the munitions mentioned in the initial CSM, and their sizes are irregular. It is possible that these features may be related to burial or other munitions management activities; however, the lidar data do not indicate a high confidence that these areas are related to munitions use. Rather, these are areas that warrant further investigation.

Figure 3-14
Sample Additional Sites of Interest

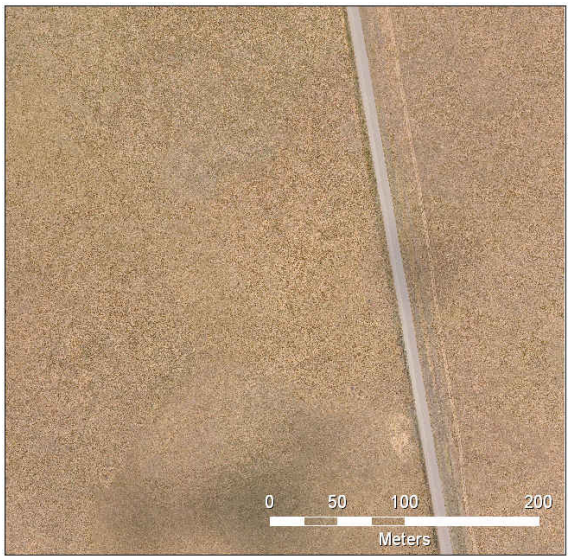

Previously unknown potential target bull's-eye, 10 cm pixel orthophoto. Potential target was not visible.

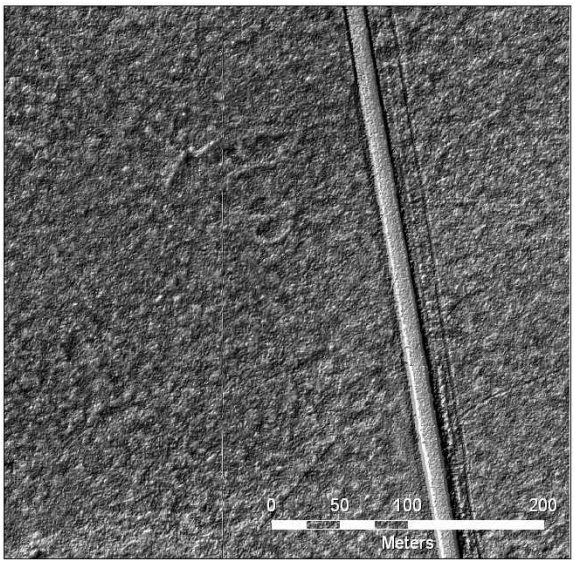

Previously unknown potential target bull's-eye, south portion of site, 300 m lidar. Identified in CSM as KPBR-AOI-4.

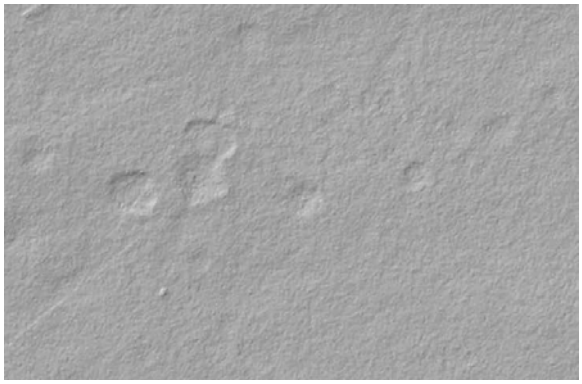

Craters forming potential MRS, 450 m lidar. This area is identified in the CSM as KPBR-AOI-10.

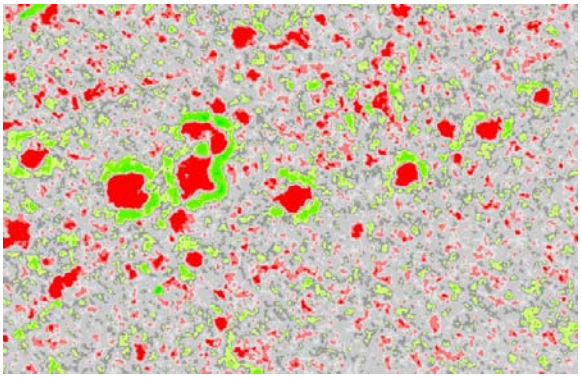

Craters forming potential MRS, elevations coded as below (red) and above (green) the ground surface.

3.7.10 Victorville – Target DBT Y Results

Target DBT Y is described in the CSM as the bed of Means Dry Lake, an area of approximately 345 acres. This area was clearly visible using both lidar and orthophotos, and the delineated boundary of the dry lake bed was not different between the lidar and orthophotos, nor for any of the lidar data densities tested (Figure 3-15).

Figure 3-15
Target DBT Y Orthophoto and Lidar

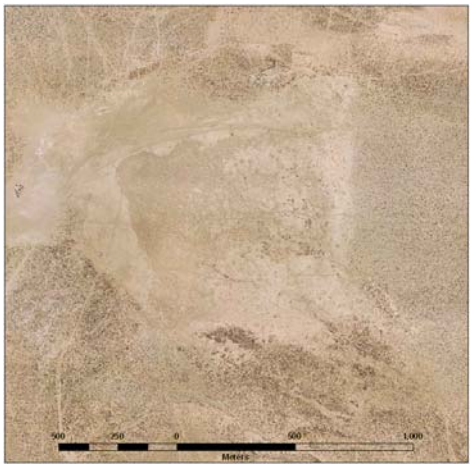

Target DBT Y, orthophoto

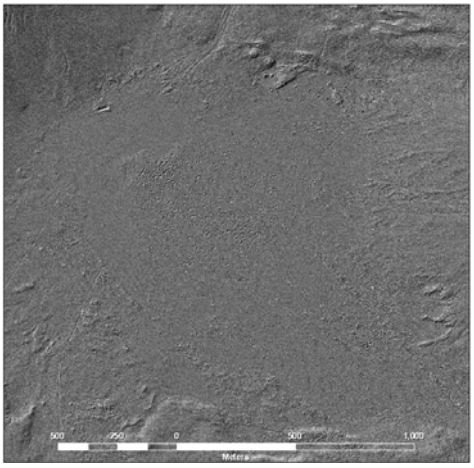

Target DBT Y, combined lidar

3.7.11 Victorville – Target PBR 15 Results

Target PBR 15 is described in the CSM as a bull's-eye target used for precision bombing practice. The target was clearly visible in the orthophotos. Initially, the target was difficult to detect using lidar, since the bull's-eye rings are formed from asphalt laid flat on the relatively flat ground surface. The target thus has very little vertical relief to be detected by lidar. However, an image of the area created using the lidar intensity values showed the target clearly (Figure 3-16). Target ring dimensions were 60 m (197 feet) for the smallest ring, 120 m (394 feet) for the middle ring, and 190 m (623 feet) for the outer ring.

Figure 3-16
Target PBR 15 Orthophotos, Lider Surface Model and Lidar Intensity Image

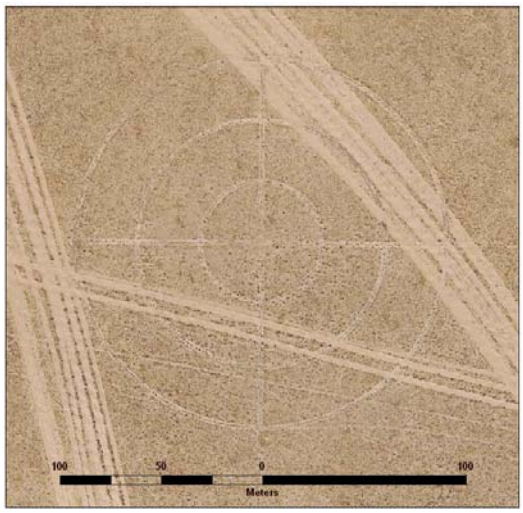

Target PBR 15, orthophoto.

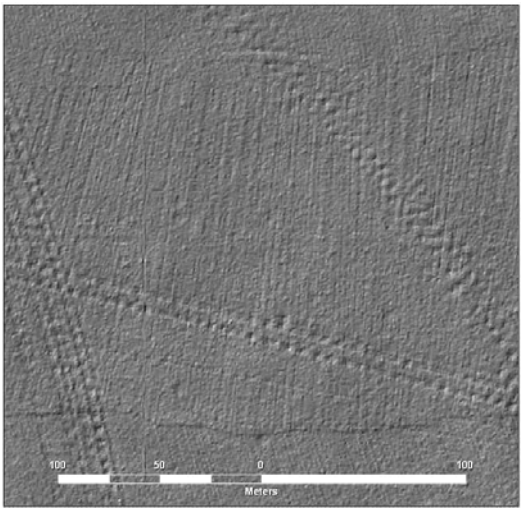

Target PBR 15, 300 m lidar.

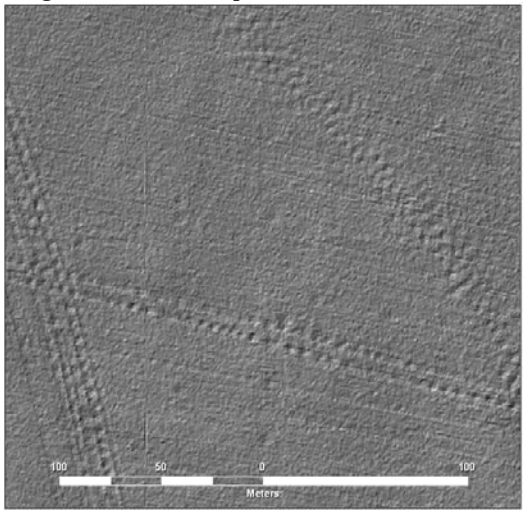

Target PBR 15, 450 m lidar.

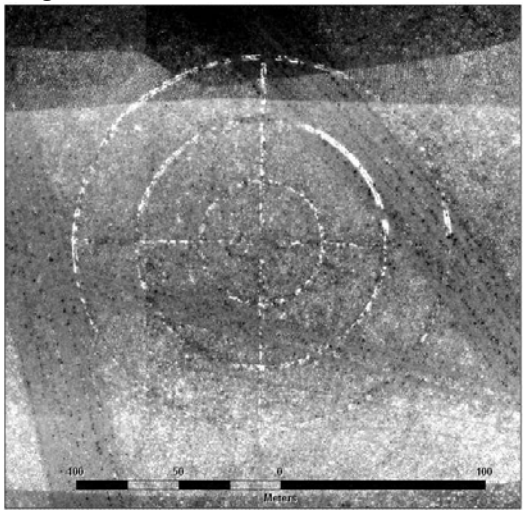

Target PBR 15, lidar intensity.

3.7.12 Detection of Potential Munitions-Related Ground Features

The Kirtland site contained just over one hundred small features that were potentially related to munitions use, mostly potential craters. The site also contained numerous linear features, mostly jeep trails and other vehicle tracks. Potential features were visually identified from the lidar hillshades and the orthophotos. The extremely shallow nature of the potential craters near Target NDIA (10 – 20 cm) made many of them difficult to distinguish with confidence from the natural ground surface. Consequently, the numbers given for objects detected should be understood as a comparison of the various data sets rather than a conclusive number of MEC-related features.

The number of features detected at the Kirtland site also varied depending on the method used to display the lidar data (Figure 3-17), particularly for the weathered craters near Target NDIA. This suggests that these potential craters were near the detection limit of this technology.

Figure 3-17
Kirtland Target NDIA Potential Crater Detection

Target NDIA, cross hairs and target center, 10 cm pixel orthophoto.

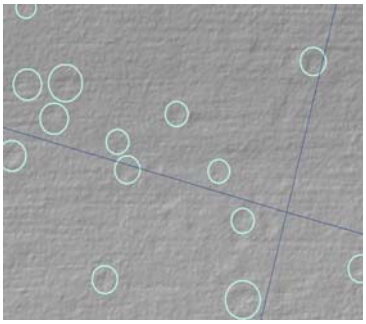

Target NDIA, craters identified from lidar hillshade alone.

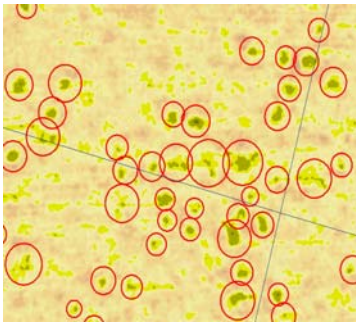

Target NDIA, craters identified from lidar surface model color-coded to show depths of depressions.

At Victorville, potential craters in Means Dry Lake were much larger than at any of the Kirtland targets, ranging from 5 to 8 m in diameter and up to 1 m deep. Unlike the smaller craters at Kirtland, the craters at Victorville were clearly visible in the orthophotos (Figure 3-18). A significant number of potential craters were located outside and northwest of the lake boundary.

Figure 3-18
Victorville Target DBT/Craters, Orthophotos and Lidar

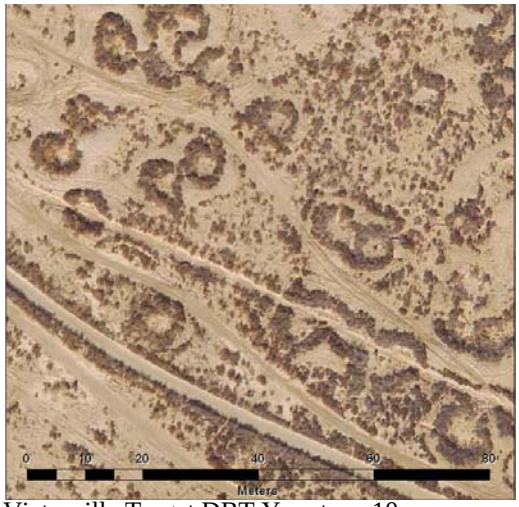

Victorville Target DBT Y craters, 10 cm orthophotos

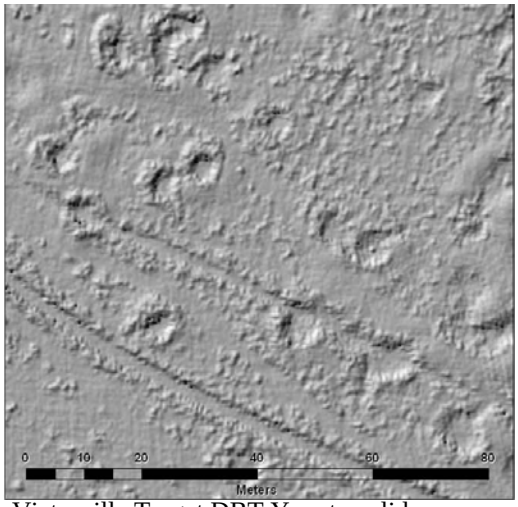

Victorville Target DBT Y craters, lidar surface model including vegetation point

Figure 3-18
Victorville Target DBT/Craters, Orthophotos and Lidar (continued)

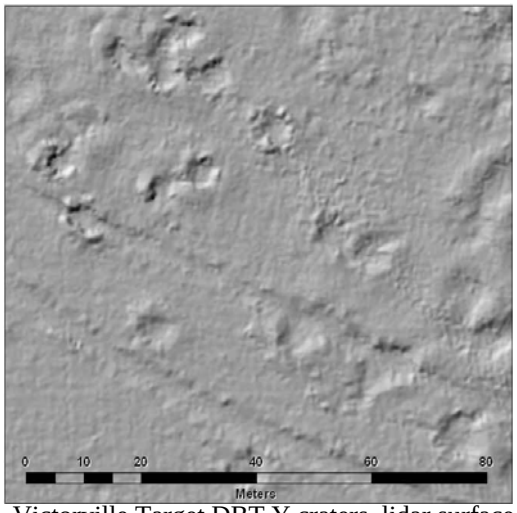

Victorville Target DBT Y craters, lidar surface model, ground points only

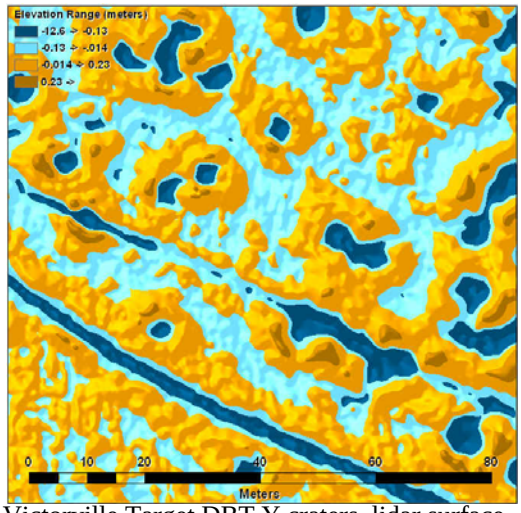

Victorville Target DBT Y craters, lidar surface model, ground points only, color-coded to show feature heights and depths.

The potential crater locations outside of the dry lake bed were used to modify the location of the target area boundary. Following this modification, the size of the potential MRS increased from the original 345 acres to 641 acres (Figure 3-19).

Figure 3-19
Victorville Target DBT Y - MRS Boundaries

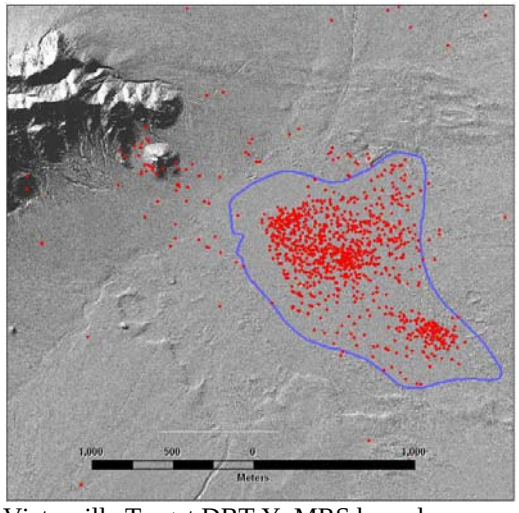

Victorville Target DBT Y, MRS boundary from CSM.

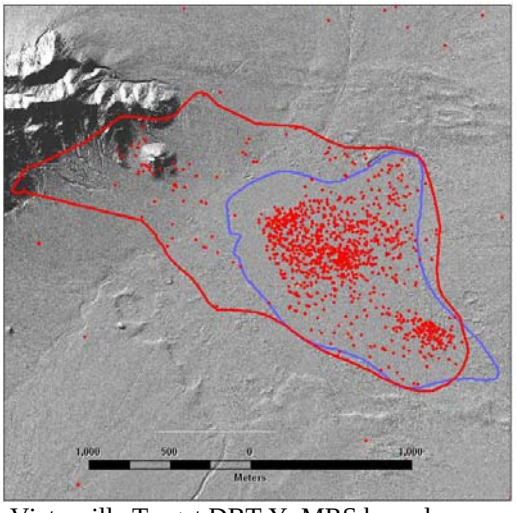

Victorville Target DBT Y, MRS boundary following modification using feature locations.

No craters were detected at Target PBR 15. This is consistent with its reported use as a practice bombing target. There were no other potential munitions-related features at the target, other than the asphalt target rings themselves.

3.7.13 Data Density Effects - General Results

The test crater area at the Kirtland site was used to examine the general effects of lidar and orthophoto data density. Orthophoto data density was examined first, based on the size of the image pixels. Figure 3-20 shows the test crater area in the 10-cm and 20-cm pixel data sets. The 10 cm orthophotos and the known dimensions of the test craters were used to create the "best" locations for the test craters; these were then superimposed on the 20 cm photo.

Figure 3-20
Kirtland Test Craters, Orthophotos

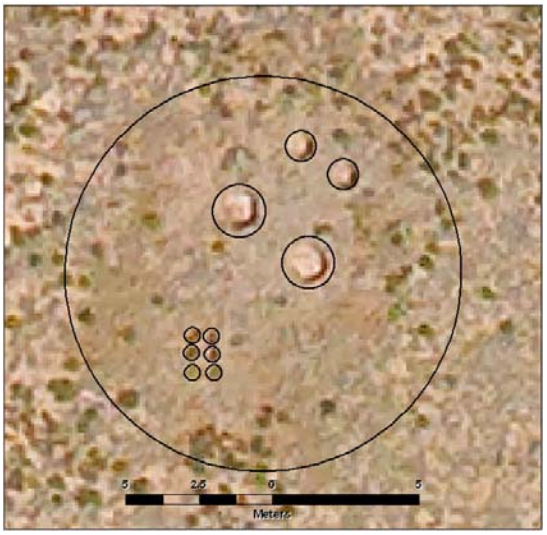

10 cm orthophoto with "best" crater locations.

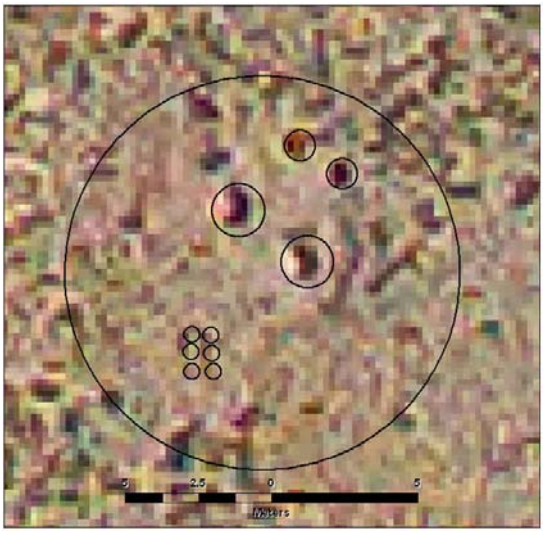

20 cm orthophoto with "best" crater locations.

These images illustrate the substantial difference in clarity between the 10 cm and 20 cm pixel orthophotos. All 10 test craters are visible in the 10 cm orthophoto, although the 0.32 m craters are distinguishable from surrounding objects primarily through their regular pattern. The 1.5 and 1.0 m craters are visible in the 20 cm pixel orthophoto; however, neither can be clearly distinguished from the surrounding ground features. This comparison led to the decision to acquire only 10 cm pixel orthophotos at the Victorville site.

Lidar data density was examined based on the average number of points per square meter. Lidar data was obtained at the overall data densities shown in Table 3-5.

Table 3-5
Achieved Lidar Data Densities

Demonstration Site	Flight	Point density (pts/m^2)
Kirtland	900 m North Block	1.4
	900 m South Block	1.6
	450 m north block	5.2
	450 m south block	4.1
	300 m east-west north block	5.2
	300 m north-south north block	6.5
	300 m flight 1 south block	5.9
	300 m flight 2 south block	6.1
Victorville	450 m flight	4.8
	300 m flight	6.4
	Combined 300 and 450 m flights	11.2

These overall lidar data densities are a general representation based on statistics for the site as a whole. In fact, lidar data density varies considerably over the ground surface, a complex phenomenon that is discussed in Appendix C.

Figure 3-21 shows hillshades of the four lidar data sets at the Kirtland test craters, using the ground returns only. The locations of the test craters are taken from the 10 cm orthophoto data and superimposed on the lidar images.

Figure 3-21
Kirtland Test Craters, Lidar Surface Models

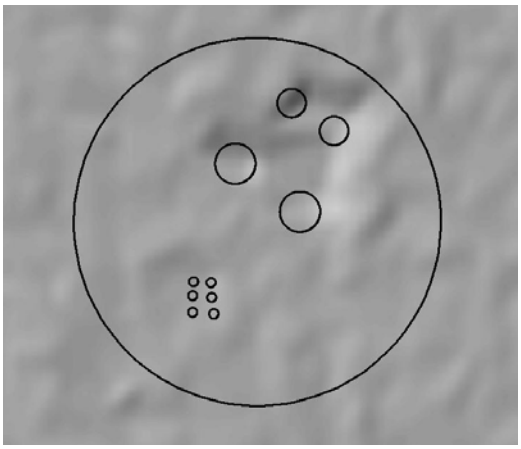

Kirtland test craters, 900 m (1.6 pts/ m^2) lidar hillshade, ground points only.

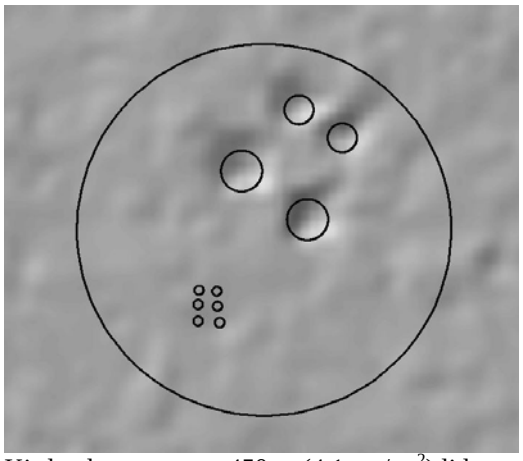

Kirtland test craters, 450 m (4.1 pts/ m^2) lidar hillshade, ground points only

Figure 3-21
Kirtland Test Craters, Lidar Surface Models (continued)

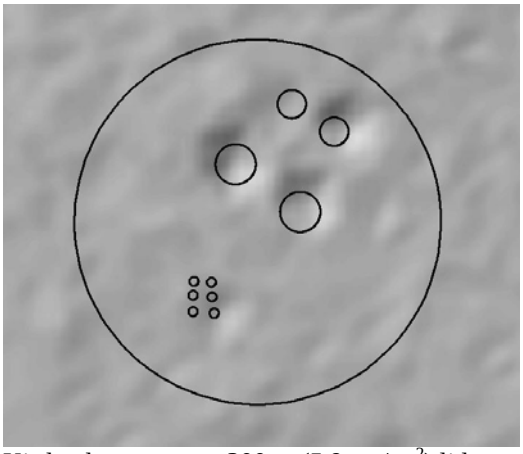

Kirtland test craters, 300 m (5.9 pts/ m^2) lidar flight 1 hillshade, ground points only.

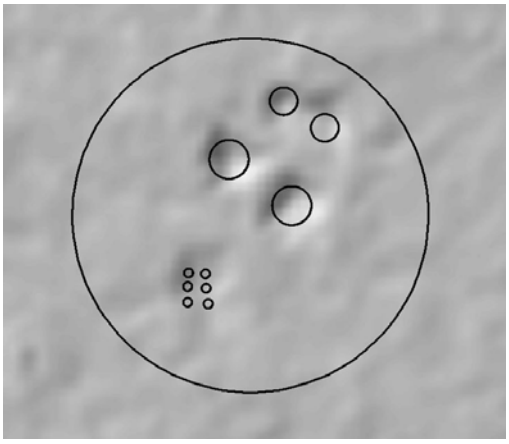

Kirtland test craters, 300 m (6.1 pts/ m^2) lidar flight 2 hillshade, ground points only.

These images show that craters are more clearly defined as the density of the lidar points increases. In the 900 m lidar data, the crater area appears as a single depression and the individual craters cannot be detected. In the 450 m lidar data, the 1.5 and 1.0 meter craters can be distinguished, but the 0.32 meter craters are not visible. In the 300 m lidar data, the 1.5 and 1.0 meter diameter craters are better defined, and the group of 0.32 meter craters begins to be seen as a single depression. None of the lidar data sets showed the 0.32 meter craters individually.

At the Victorville site, only one orthophoto data set was acquired. For the lidar data, the data from the 300 m and 450 m lidar flights were successfully aligned to create a combined data set, yielding a total of three lidar data densities (Figure 3-22). As at Kirtland, the data showed that feature definition increased with increasing lidar density.

Figure 3-22
Victorville Test Craters, Lidar Surface Models

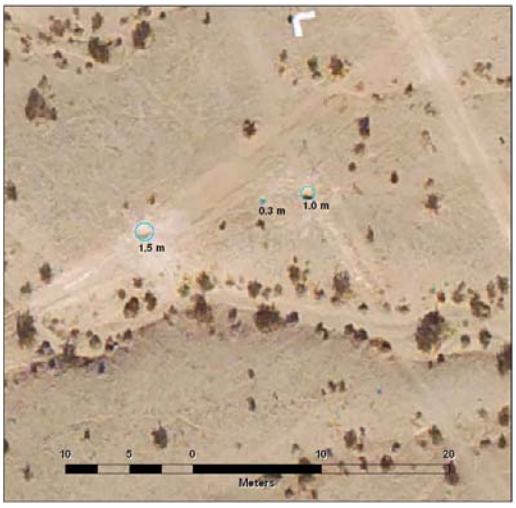

Victorville test craters – 10 cm orthophotos.

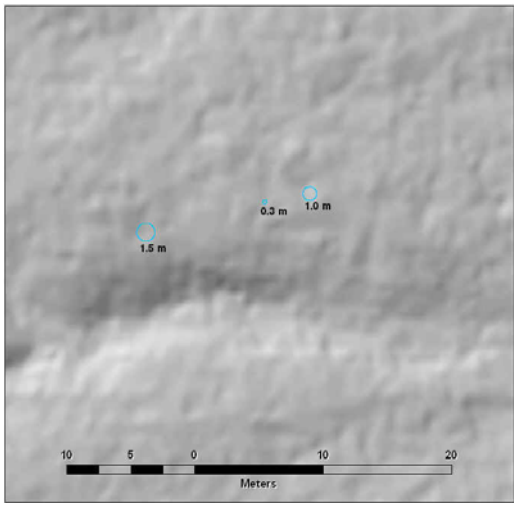

Victorville site test craters – 450 m (4.8 pts/ m^2) lidar flight, ground points only.

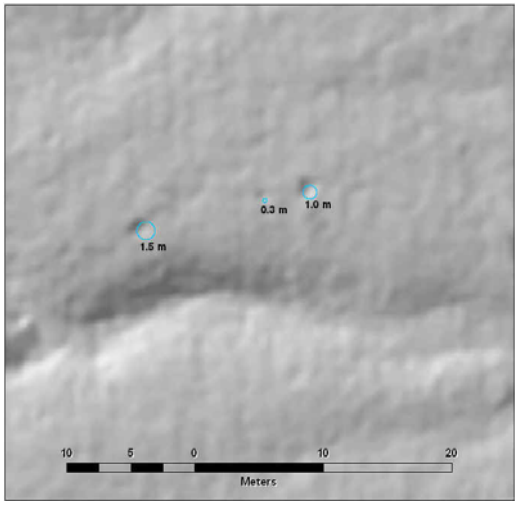

Victorville site test craters – 300 m (6.4 pts/ m^2) lidar flight, ground points only.

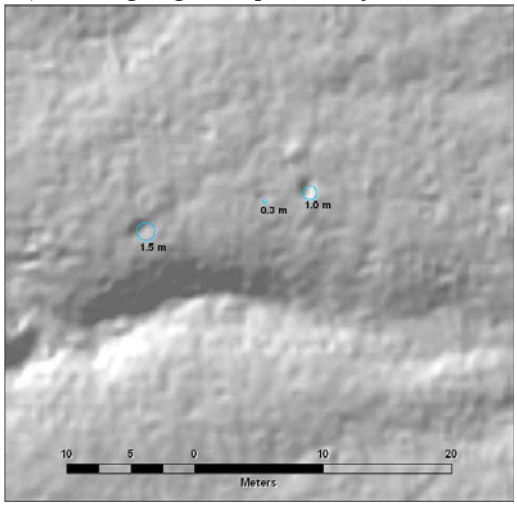

Victorville site test craters, combined (11.2 pts/ m^2) lidar data set, ground points only.

These images support the findings at the Kirtland site that increased lidar data density leads to better detection of smaller features. The Victorville test craters are somewhat harder to distinguish from the surrounding area because they are not grouped together. At the lower data density of the 450 m flight, the 1.0 and 1.5 m craters are difficult to distinguish, while both are clearly visible in the 300 m data and the combined data. The 0.32 m crater is discernable in the combined data set; however, without a group of craters in a regular pattern such as at Kirtland, it would be difficult to distinguish from the surrounding natural variation in the ground surface.

3.7.14 Data Density Effects - Quantitative Results

Counts were made of potential features identified in each lidar and orthophoto data set. For the Kirtland site, two classes of features were found: line features such as roads, trails and the target bull's-eye rings, and area features such as probable craters, isolated depressions that did not appear to be craters, and other items of interest including regularly-shaped mounds (Figure 3-23). The orthophotos area features included what appeared to be old building foundations and articles of debris on the surface. Table 3-6 presents results for each data set.

Figure 3-23
Kirtland Sample Features of Interest

Debris on the ground, approximately 1.0 x 0.5 m

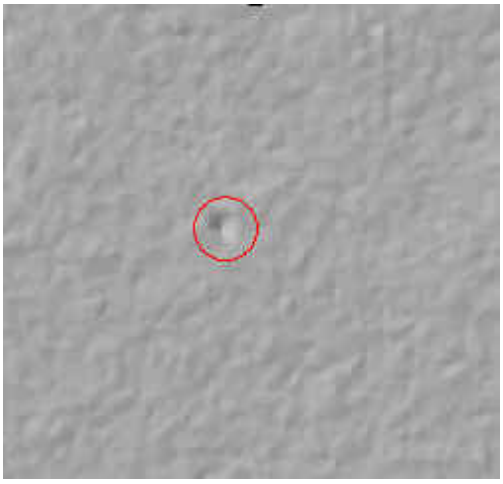

Unidentified depression, approximately 2 m in diameter

Table 3-6 summarizes the number of features identified for each data set at the Kirtland site. Figures 3-24 and 2-25 show the number of area features and the overall length of linear features detected for each orthophoto and lidar data set.

Area features included depressions that did not appear to be craters, probable craters, and other features of interest. Linear features were primarily dirt roads and jeep trails. The relatively small number of roads and trails at the Kirtland site, along with their faint and eroded character, make them appropriate subjects for comparison of the different data sets. Total length of features was used in place of the number of features to avoid problems with potentially arbitrary division of the roads and trails into segments.

Table 3-6
Kirtland Potential Features

	Area Features				Line Features
	Depressions	**Probable Craters**	**Other Features of Interest**	**Total Area Features**	**Total Length of Line Features (m)**
Orthophotos					
20 cm	0	0	29	29	92,325
10 cm	0	0	49	49	83,658
Individual lidar					
900 m	23	31	16	70	78,047
450 m	30	48	20	98	89,907
300 m 1	52	63	23	138	97,968
300 m 2	56	61	29	146	98,220
Combined lidar					
450 and 900 m	36	44	23	103	89,948
Both 300 m	51	49	29	129	89,974
All lidar	44	47	29	120	84,588

Figure 3-24
Kirtland Area Features by Data Source

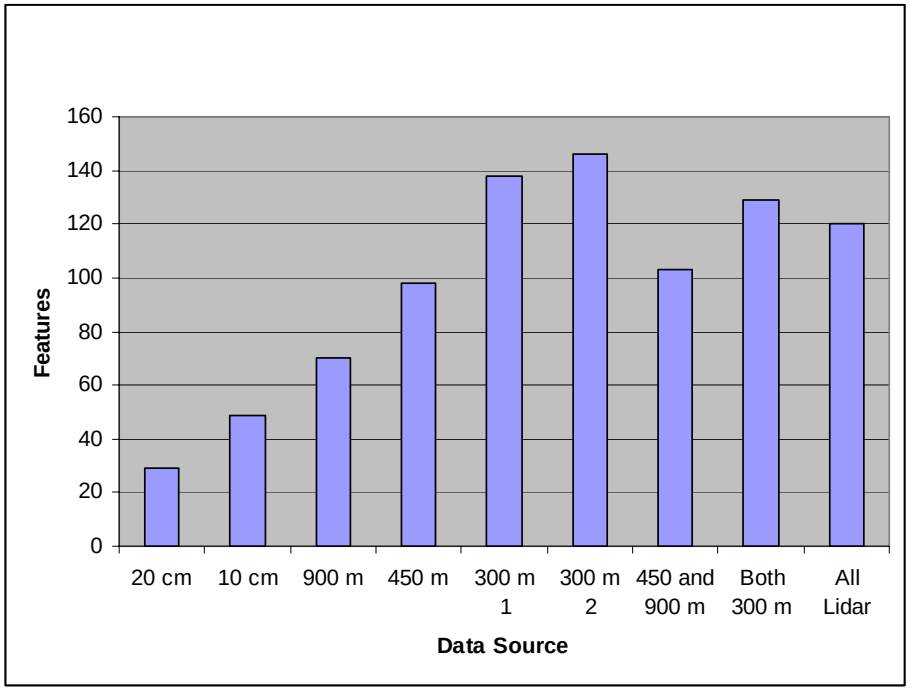

Figure 3-25
Kirtland Line Feature Length by Data Source

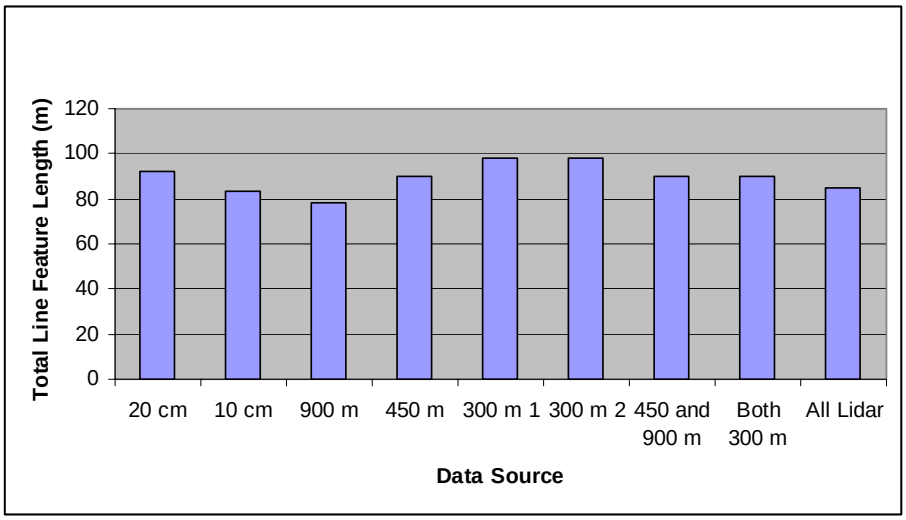

The data show that the number of area features such as potential craters was higher for lidar than for orthophotos, and the number of features identified increased with data density for both lidar and orthophotos. However, when lidar data from different altitudes was combined, the number of features detected decreased. Line features were detected roughly equally using either technology.

At the Victorville site, results were more equal between the two technologies, probably due to the larger size of the craters (Table 3-7). A slightly smaller number of craters was counted using the orthophotos, probably as a result of the vegetation in some parts of the Means Dry Lake bed that obscured the craters in the orthophotos but not the lidar data. A slightly higher number of additional features were identified using both the orthophotos and lidar together.

Table 3-7
Victorville Potential Features

	Total Features	Probable Craters
Orthophoto		
10 cm	1171	1108
Lidar		
450 m	1185	1108
300 m	1183	1106
300 and 450 m	1186	1105
Orthophoto and lidar	1198	1121

Figure 3-26 shows the number of area features for each orthophoto and lidar data set at the Victorville site.

Figure 3-26
Victorville Features by Data Source

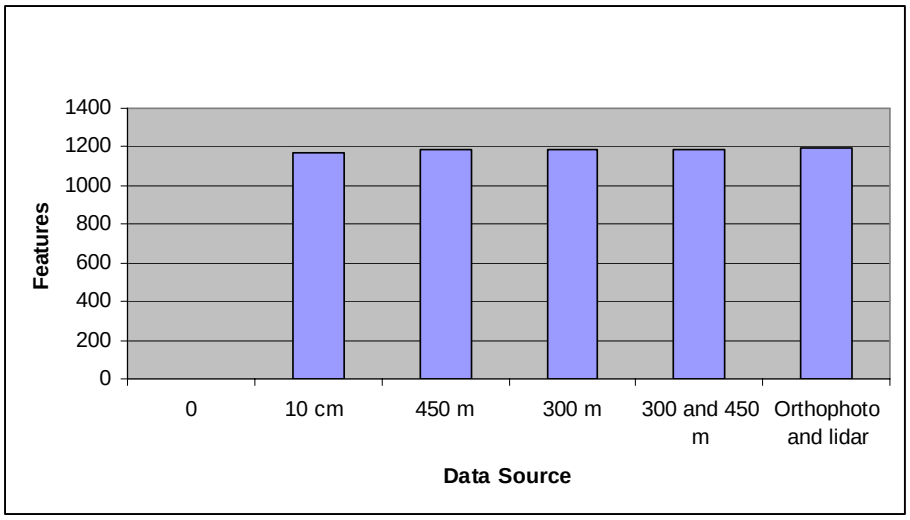

Line features were not quantitatively analyzed at Victorville, as the site is covered with off-road vehicle tracks at a density that made quantitative analysis difficult. However, roads and off-road vehicle tracks are clearly visible in both the lidar and orthophoto data at all data densities obtained.

3.7.15 Flight Line Orientation Effects

At the Kirtland site, the two 300 m lidar flights were flown perpendicular to each other in the north portion of the site (Figure 3-27). The resulting surface models were compared to determine whether flight line orientation would affect feature detection. The data showed that faint jeep roads running east-west were more clearly visible when the lidar flight lines are also east-west. This effect appears to be due to the orientation of the sweep of the laser either along or across these shallow roads. More distinct features, such as the larger north-south road in the images below, were equally visible in both data sets.

Figure 3-27
Kirtland Flightline Orientation Effects

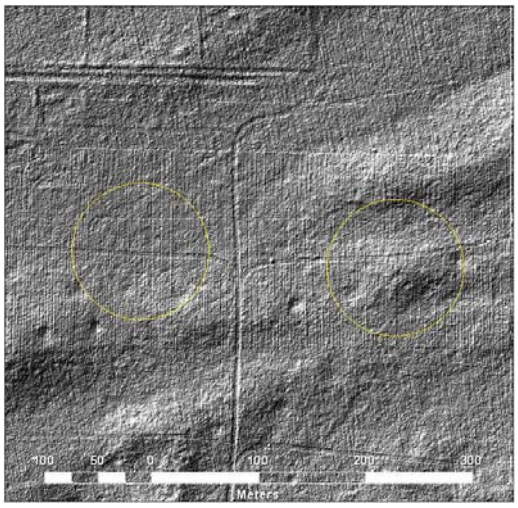

Roads, 300 m lidar east-west flight lines. Arrow shows flight line direction. East-west roads appear more clearly.

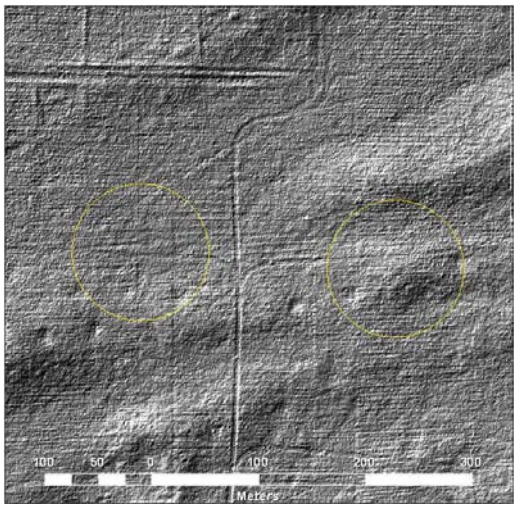

Roads, 300 m lidar, North-south flight lines. Arrow shows flight line direction. East-west roads appear less clearly.

3.7.16 Data Artifacts and Noise Effects

Two types of data artifacts were encountered in the lidar data. First, where data from two parallel flight lines overlapped, the surface occasionally showed very shallow (roughly 0.05 m) meandering linear features. This is a well-known type of noise effect caused by slight discrepancies between data between the two flight lines. The linear feature appears at the boundary of the overlap of the flight line overlap area (Figure 3-28). Such anomalies are probably the result of small errors in the GPS, IMU, and laser range finder that cannot be adjusted out during data processing.

Figure 3-28
Kirkland Flight Line Data Overlap Effect

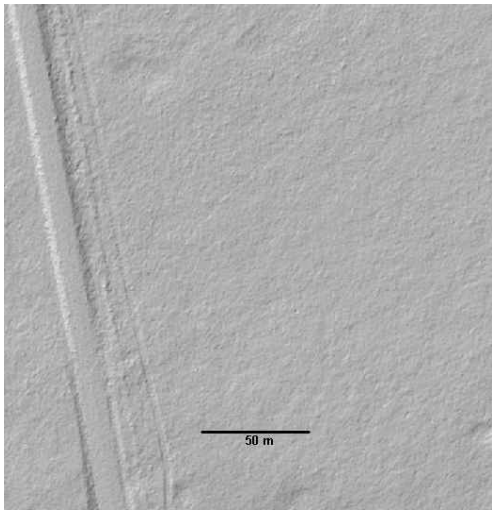

Flight line artifact, 300 m lidar. The faint linear feature shown does not appear in lidar surfaces with different flight line orientations.

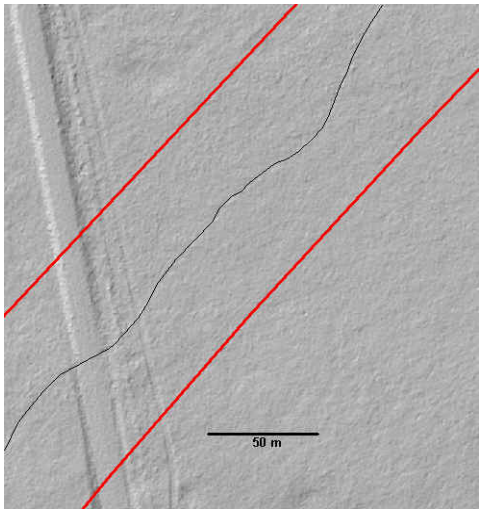

Flight line artifact, bold red lines represent flight lines.

Second, the lidar-derived ground surface often showed a “corduroy” effect consisting of shallow (roughly 0.05 m) ridges running perpendicular to the flight line and along the sweep of the laser (Figure 3-29). This is also a well-known lidar data artifact. This effect also likely results from small errors in the GPS, IMU and laser range finder. The size of both anomalies is well within the vertical accuracy specifications for the data.

Figure 3-29
Victorville Lidar "Corduroy" Effect

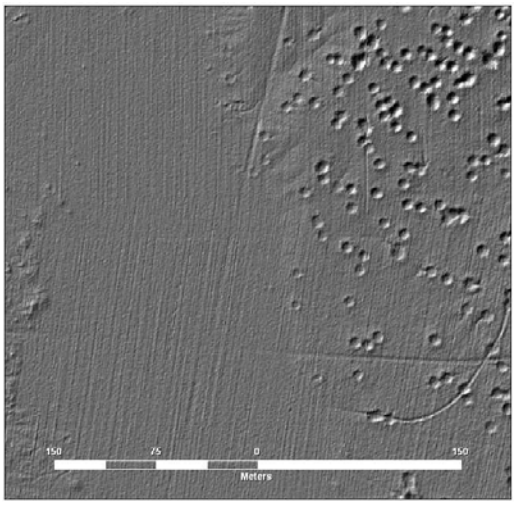

3.7.17 Vegetation Patterns

Vegetation at the Kirtland site was examined in both orthophotos and lidar data to determine whether vegetation patterns could reveal surface disturbances related to munitions use (Figure 3-30). Orthophotos were examined visually, and for the lidar data, vegetation heights were modeled. The bombing targets were occasionally very slightly discernable in the lidar vegetation height models; however, it is unlikely that vegetation data alone could be used to locate MRS or munitions-related features.

Figure 3-30
Kirtland Vegetation Patterns

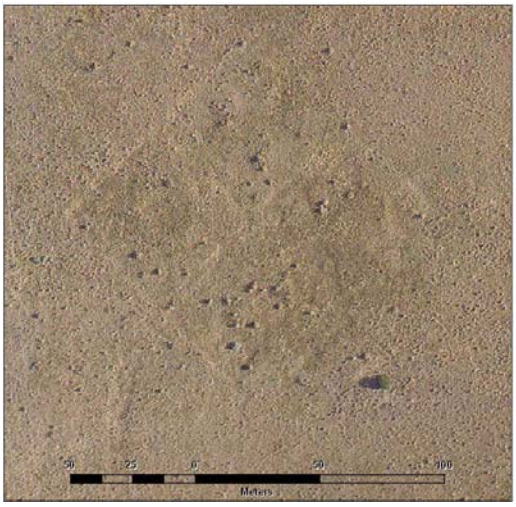

Target N3, diamond-shaped target to the west of main target area, 20 cm orthophoto.

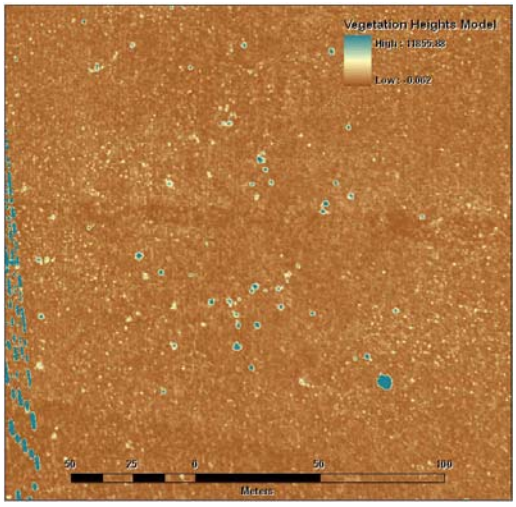

Target N3, diamond-shaped target to the west of main target area, lidar vegetation height model. The radiating bars to the west are power lines.

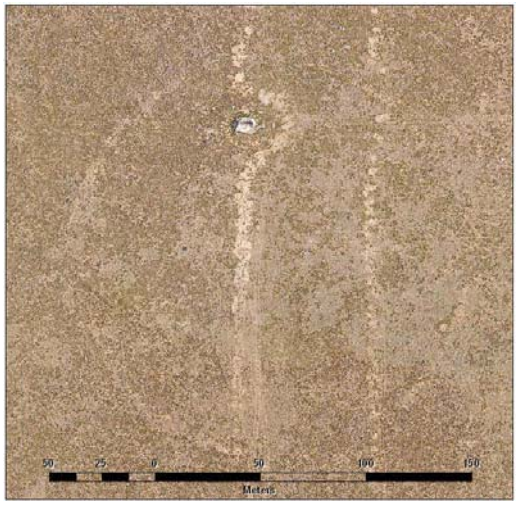

Target N2, bull's-eye.

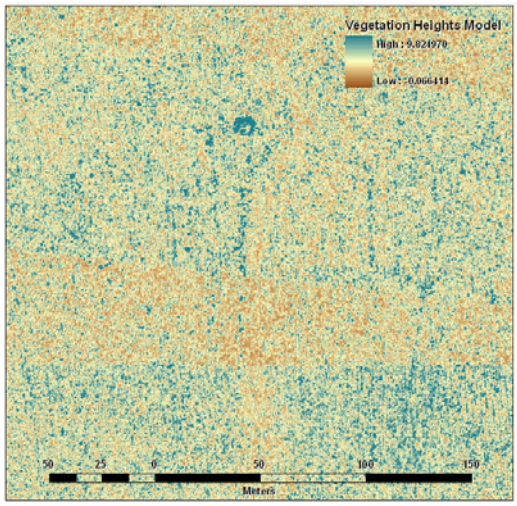

Target N2, bull's-eye, lidar vegetation height model.

3.7.18 Lidar and Orthophoto Positional Accuracy

Understanding the positional accuracy of lidar and orthophoto data is important since both data sets will be integrated with a wide variety of other spatial data. Positional accuracy specifications were established in the Demonstration Plan for each site, and are shown in Table

4-1 in Section 4. Positional accuracy verification methods are discussed in detail in Appendix A, Lidar and Orthophoto Positional Accuracy Results.

Lidar and orthophoto data met the positional accuracy criteria at both sites. Table 3-8 presents the overall positional accuracy results for the two sites.

Table 3-8
Overall Positional Accuracy Results

Item	Performance Criteria	Method	Results (m)
Lidar vertical accuracy	Ave. dz: +/- 0.15 m compared to control points	Kirtland: lidar to ESTCP control points	Ave. dz: 0.111
		Kirtland: lidar to TRSI control points	Ave. dz: 0.088
		Victorville: lidar to TRSI control points	Ave. dz: 0.102
Lidar horizontal accuracy	Ave. dx/y: +/- 0.65 m compared to control points	Kirtland: Average x and y displacement (dx and dy) for all control points and all lidar flights.	Ave. dx: 0.080 Ave. dy: 0.080
		Victorville: Average x and y displacement (dx and dy) for all control points for each flight.	300 m flight Ave. dx: 0.030 Ave. dy: 0.080 450 m flight Ave. dx: 0.060 Ave. dy: 0.030
Orthophoto horizontal accuracy	Ave. dx/y under 3 pixel widths compared to control points	Kirtland 20 cm orthophotos to control points	Ave. dx: 0.128 Ave. dy: 0.139
		Kirtland 10 cm orthophotos to control points	Ave. dx: 0.077 Ave. dy: 0.106
		Victorville 10 cm orthophotos to control points	Ave. dx: 0.027 Ave. dy: 0.037
Orthophoto to lidar alignment	Ave. dx/dz under 2 pixel widths	Kirtland 20 cm orthophotos to lidar positions	Ave. dx: 0.167 Ave. dy: 0.360
		Kirtland 10 cm orthophotos to lidar positions	Ave. dx: 0.137 Ave. dy: 0.167
		Victorville 10 cm orthophotos to lidar positions	Ave. dx: ~0.10 Ave. dy: ~0.10

3.7.19 Other Observations

Orthophotos were especially useful for providing additional information about potential surface features. In Figure 3-31, orthophotos were able to clarify a feature that appeared to have moved between two lidar flights. Orthophotos showed that the feature was related to construction and had in fact moved.

Figure 3-31
Use of Orthophotos to Resolve Apparent Lidar Data Discrepancy

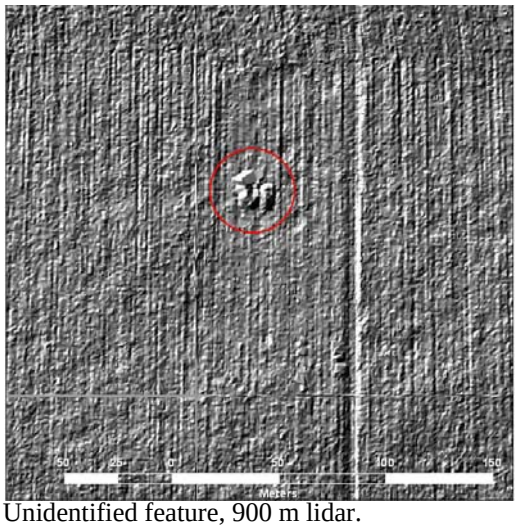

Unidentified feature, 900 m lidar.

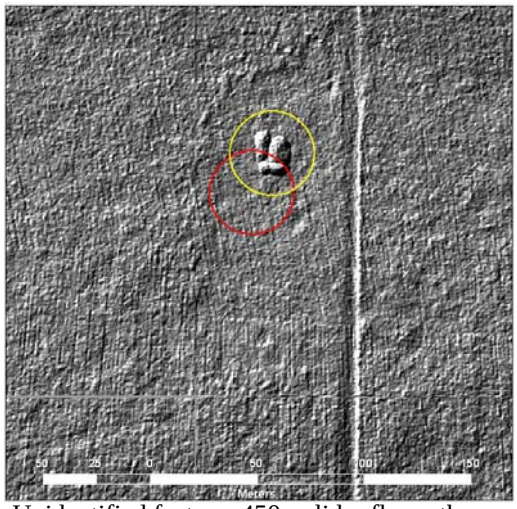

Unidentified feature, 450 m lidar flown the following day. The feature appears to have moved.

Unidentified feature, 20 cm ortho taken with the 900 m lidar flight, the orthophoto reveals that the feature is related to ongoing construction activity.

Unidentified feature, 10 cm ortho taken with the 450 m lidar flight.

4.0 PERFORMANCE ASSESSMENT

4.1 PERFORMANCE CRITERIA

Performance criteria for this demonstration were established in the Demonstration Plan for each site, and are shown in Table 4-1. The lidar and orthophoto data met these performance criteria, as shown in Tables 4-2 and 4-3. The results of validation activities and the implications of the validation results discussed in Section 4.2.

Table 4-1
Performance Criteria

Performance Criteria	Description	Primary or Secondary
Pre-mobilization		
Verification of survey control point positions	Verify survey control point locations within at least 3rd order accuracy	Primary
Lidar data collection and processing		
Area coverage	100% coverage for each flight	Primary
Lidar point density - Kirtland	Achieve overall lidar point densities of: 200 m flights (2) – 8 pts/m^2 each 450 m flight (1) – 3 pts/ m^2 900 m flight (1) – 2 pts/ m^2	Primary
Lidar point density - Victorville	Achieve overall lidar point densities of: 300 m flight (1) – 3 pts/ m^2 450 m flight (1) – 5 pts/ m^2	Primary
Lidar vertical accuracy	Vertical accuracy of +/- 15 cm compared to ground survey	Primary
Lidar horizontal accuracy	Horizontal accuracy of +/- 65 cm compared to ground survey	Primary
Orthophoto data collection and processing		
Orthophoto area coverage	100% coverage for each flight	Primary
Orthophoto flight altitude / pixel size	450 m (for 10 cm pixel flight) – Kirtland and Victorville 900 m (for 20 cm pixel flight)	Primary
Orthophoto horizontal alignment to Lidar	Lidar and orthophotos aligned so that target features are not displaced in the two data sets	Primary
Orthophoto horizontal alignment to survey control points	Orthophotos aligned to survey control points so that target features are not displaced	Primary
Munitions Response Site identification and analysis		
MRS identification	Correctly identify all previously identified MRS	Primary
MRS false alarm rate	No areas incorrectly identified as MRS	Primary
MRS boundary delineation	Correctly locate MRS boundaries to +/- 15% of ground-truthed area	Primary
MRS feature identification	Identify features presenting as munitions-related (anthropogenic)	Primary

Table 4-2
Data Quality Metrics—MRS Identification and Analysis

	Analytical Objective	Metric	Action to Achieve Metric	Sampling Frequency or Timing	Desired Result	Actual Result
MRS Identification and Analysis						
20	MRS identification	Correctly identify all previously identified MRS.	Identify and document MRS from lidar and orthophoto data sets.	Each lidar and orthophoto data set and combinations.	Correctly identify all MRS.	Kirtland Lidar: **Accomplished**. All previously identified MRS were correctly identified. Orthophotos: **Not Accomplished.** One of four MRS correctly identified.
						Victorville Lidar: **Accomplished**. Both previously identified MRS were correctly identified. Orthophotos: **Accomplished.** Both MRS were correctly identified.
21	MRS false alarm rate	No areas incorrectly identified as MRS.	Identify and document MRS from lidar and orthophoto data sets.	Each lidar and orthophoto data set and combinations.	No false MRS identification.	Kirtland **Not Accomplished.** 15 potential MRS were identified that appear not to be munitions-related.
						Victorville **Accomplished.** No additional potential MRS were identified from the lidar or orthophoto data.

Table 4-2
Data Quality Metrics—MRS Identification and Analysis (continued)

	Analytical Objective	Metric	Action to Achieve Metric	Sampling Frequency or Timing	Desired Result	Actual Result
22	MRS boundary delineation	Correctly locate MRS boundaries to +/– 15% of ground-truthed area.	Identify and document MRS boundaries from lidar and orthophoto data sets for a selected set of test MRS.	Each lidar and orthophoto data set and combinations.	Locate MRS boundaries within metrics.	Kirtland **Partially Accomplished.** For most targets, the lidar data formed the boundary of the MRS. However, at Targets N3 and SORT, additional areas were identified using mag and EM that changed the boundaries more than 15%.
						Victorville **Partially Accomplished.** For Target DBT Y, validation activities did not change the MRS boundary established using lidar. For Target PBR 15, mag data showed metal frag more accurately than the boundary established using lidar.
23	MRS feature identification	Identify features presenting as human-made (anthropogenic) not including craters (e.g., walls, berms, pits, small buildings).	Lidar and photo data sets will be examined for linear features.	Each lidar and orthophoto data set and combinations.	90% of features identified from selected field-identified features.	**Accomplished.** At both sites, potential human-made features were readily identifiable.

Table 4-2
Data Quality Metrics—MRS Identification and Analysis (continued)

	Analytical Objective	Metric	Action to Achieve Metric	Sampling Frequency or Timing	Desired Result	Actual Result
24	MRS feature identification	Identify craters. Count 90% of craters over 1.5 m diameter and .3 m depth.	Automated algorithms will be used to identify and count craters using lidar data.	Each lidar and orthophoto data set and combinations.	90% of craters identified outside of crater fields. 95% of craters identified inside crater fields.	Kirtland **Unknown.** Validation activities appear to be no more accurate than lidar and orthophotos in identifying the highly eroded craters at the site.
						Victorville **Unknown.** Validation activities do not appear to have been conducted to count individual craters. However, no concentrations of craters were reported in addition to those detected using lidar and orthophotos.
25	MRS feature identification	Identify vegetation patterns indicating previous disturbance.	Automated algorithms will be used to map vegetation heights and patterns from lidar data. Results will be examined for linearity or other regular shapes. Orthophotos will be examined for regular vegetation patterns.	Each lidar and orthophoto data set and combinations.	Identification of MRS.	**Not Accomplished**. Neither orthophotos nor lidar revealed patterns of vegetation indicating previous disturbance.

Table 4-2
Data Quality Metrics—MRS Identification and Analysis (continued)

	Analytical Objective	Metric	Action to Achieve Metric	Sampling Frequency or Timing	Desired Result	Actual Result
26	MRS feature identification	Identify established roads.	Lidar and photo data sets will be examined for linear features.	Each lidar and orthophoto data set and combinations.	100% identification of established roads.	**Accomplished.** Roads are clearly visible using lidar and orthophoto. Jeep tracks and other faint linear features were distinguishable from major roads.
27	MRS feature identification	Identify vehicle tracks.	Lidar and photo data sets will be examined for linear features.	Each lidar and orthophoto data set and combinations.	90% identification of field-identified vehicle tracks.	Lidar: **Unknown.** Vehicle tracks were visible using lidar data where such tracks are deeper than 5 – 10 cm. However, field validation was not conducted. Orthophotos: **Unknown**. Vehicle tracks are clearly visible including faint jeep trails. However, field validation was not conducted.
28	MRS feature identification	Identify topography that can limit access.	Lidar data sets will be used to map areas above designated slope.	Each lidar data set and combinations.	100% identification of steep slope areas.	**Accomplished**. Slopes were successfully modeled at both sites from lidar data.
Data management						
29	Data management	Data backup and storage to achieve redundancy and security.	Data will be backed up to separate redundant hard drives or tape drives.	Daily backup during field and data processing operations.	Data security, prevention of data loss.	**Partially Accomplished.** All data was and remains backed up to redundant hard drives. The only exception is the one orthophoto image at Kirtland that was lost, apparently during original data collection and before it was written to the hard drive in the aircraft.

Table 4-2
Data Quality Metrics—MRS Identification and Analysis (continued)

	Analytical Objective	Metric	Action to Achieve Metric	Sampling Frequency or Timing	Desired Result	Actual Result
30	Data transfer	Data transfer will be in appropriate formats and file sizes for ESTCP and Kirtland Air Force Base ongoing use.	Data will meet US Government Spatial Data Standard and fully comply with Versar electronic data deliverable specifications.	Each data transfer.	Data security and quality.	**Accomplished.** Data formats met ESTCP requirements. ESTCP staff requested that data not meet Spatial Data Standards, but only that it contain standard metadata files and use ESTCP-provided data codes. This was provided.
31	Data collection report	Standard flight reporting includes: calibration log, flight log, QA/QC log, and site photos .	The data collection report is a standard QA/QC product.	Calibration report: each flight day.	Full reporting is a required part of contract performance.	**Accomplished.** Calibration flights were accomplished and standard pitch, roll and heading adjustment values were calculated and recorded.
				Flight log: each flight.	Flight log: Full reporting.	**Accomplished.** Flight log data was recorded and delivered.
				QA/QC log: each flight.	QA/QC log: Full reporting.	**Accomplished.** Flight logs and QA/QC report were provided.
				Site photos: whole project.	Site photos: Full reporting.	**Accomplished.** Site photos were taken and delivered.
32	Data processing report	Standard data processing report includes: GPS control ties, accuracy verification report, and QA/QC report.	The data processing report is a standard QA/QC product.	Each lidar and orthophoto data set.	Full reporting is a required part of contract performance.	**Accomplished.** GPS control, accuracy verification report and QA/QC reports were delivered.

Table 4-2
Data Quality Metrics—MRS Identification and Analysis (continued)

	Analytical Objective	Metric	Action to Achieve Metric	Sampling Frequency or Timing	Desired Result	Actual Result
33	Metadata	Metadata to accurately describe data format and processing steps.	Data will meet US Government Spatial Data Standards and fully comply with Versar electronic data deliverable specifications including metadata standards.	Each data transfer.	Metadata meets required standards.	**Accomplished.** ESTCP staff stated that Spatial Data Standards would not apply but that metadata would be required. Standard GIS metadata files were delivered with all data.
34	QA/QC	All data and derived products will be subject to appropriate QA/QC review.	Data processing will follow the QA/QC plan described herein.	Each data transfer.	Data are valid useful for the intended purpose and defensible.	**Accomplished.** Each data deliverable was independently reviewed by the GIS Lead and a standard QA/QC form filled out and placed in the project files.
35	Data delivery	All data will be delivered in a timely and easy-to-transfer manner.	Data deliverables will be made using ftp where possible, but in all cases will be followed up with delivery on physical media, primarily external hard drives.	Each data transfer.	Meeting data deliverable deadlines.	**Accomplished.** Data was delivered on or before the dates given in the Demonstration Plan. Interim data deliveries were made by DVD or external hard drive. Final data delivery was accomplished through external hard drive.

Table 4-3
Data Quality Metrics, Individual Performance Measures

	Analytical Objective	Metric	Action to Achieve Metric	Sampling Frequency or Timing	Desired Result	Actual Result
Pre-flight Activities						
1	Study area boundary delineation	**Both Sites:** Site boundary polygon characteristics agreed on and documented to allow comparison with data collected.	Achieve stakeholder agreement to boundary parameters.	Once at beginning of program.	Document site boundary for measurement of future boundary metrics.	**Accomplished.** Boundaries were agreed on and utilized.
2	Survey control point confirmation measurement	**Both Sites:** Confirm coordinates of survey control points within at least third-order accuracy.	Perform and record GPS survey (static or kinematic).	Pre-flight (or during on-site acquisition).	Confirm coordinates of survey control points.	**Accomplished.** Control points were independently occupied by TRSI and ESTCP.
Lidar Data Collection and Processing						
3	Sensor calibration	**Both Sites:** Resolve roll/pitch/ heading for installation.	Perform opposing direction and orthogonal passes over baseline. Compare with nominal values from standard installation.	Prior to each flight day.	+/– 0.02 degrees	**Accomplished.** Standard roll, pitch and heading correction factors were established through calibration flights for both sites. See Appendix A.
4	Sensor speed	**Both Sites:** Laser pulse rate between 50 and 100 kHz.	Set laser pulse speed and the altitude of the low lidar passes depending on site conditions to achieve highest possible point density.	Prior to each flight day.	Achieve target sensor speed.	**Accomplished.** Laser pulse rate of 50 kHz was used at both sites.

Table 4-3
Data Quality Metrics, Individual Performance Measures (continued)

	Analytical Objective	Metric	Action to Achieve Metric	Sampling Frequency or Timing	Desired Result	Actual Result
5	Flight altitude, Kirtland	**Kirtland:** Flight altitudes of 900, 450, and 200 to 300 m.	Establish and fly appropriate flight altitudes for the desired lidar point densities and orthophoto pixel sizes. Lay out a series of flight lines for high-density lidar collection to be able to respond to site conditions.	Each flight line.	+/- 50 m from planned flight altitudes.	**Accomplished.** Lidar flight altitudes were 900, 450 and 300 m. Flight altitudes are documented through daily flight logs.
	Flight altitude, Victorville	**Victorville:** Flight altitudes of 450 and 300 m.	Establish and fly appropriate flight altitudes for the desired lidar point densities and orthophoto pixel sizes. Lay out a series of flight lines for high-density lidar collection to be able to respond to site conditions.	Each flight line.	+/- 50 m from planned flight altitudes.	**Accomplished.** Lidar flight altitudes were 900, 450 and 300 m. Flight altitudes are documented through daily flight logs.
6	Area coverage	**Both Sites:** 100% coverage for each flight.	Establish and fly flight lines so as to cover the entire target area. Data from each day's flights will be examined and data gaps will be filled.	Each flight.	100% coverage.	**Accomplished**. 100% coverage of the study area was accomplished for each flight at both sites.
					15% flightline overlap, 50m over area boundaries.	**Accomplished.** Flight line overlap met specifications for all flights.

Table 4-3
Data Quality Metrics, Individual Performance Measures (continued)

	Analytical Objective	Metric	Action to Achieve Metric	Sampling Frequency or Timing	Desired Result	Actual Result
7	Data collection rate	**Both Sites:** Collect data for the entire site within the established schedule. Reserve one additional day for QA/QC and re-flight.	Establish and review flight lines and flight schedule prior to data collection.	NA	Full data collection within planned schedule.	**Partially Accomplished**. Data was acquired as planned at Kirtland. At Victorville, data collection required two additional days due to high ambient air temperature.
8	Lidar point density	Achieve overall densities of:	Plan and accomplish appropriate sensor speed, flight altitude, and air speed. Flights more than 10% below target point densities will be repeated.	Each flight.	Data collection within 10% of target densities.	**Partially Accomplished.** At Kirtland, data for the 900 m and 450 m flights met or exceeded target densities. Data was below target density for the low-level flights. Lower densities resulted from 50 kHz laser pulse rate combined with 300 m flight altitude. At Victorville, data met target densities.
		Kirtland I 200 m flights (2) – 8 pts/m^2 each			200 m flights (2) – 8 pts/m^2 each	N block flight 1: 5.2 pts/m^2 N block flight 2: 6.5 pts/m^2 S block flight 1: 5.9 pts/m^2 S block flight 2: 6.1 pts/m^2
		Kirtland II 450 m flight (1) – 3 pts/m^2			450 m flight (1) – 3 pts/m^2	N block: 5.2 pts/m^2 S block: 4.1 pts/m^2
		Kirtland III 900 m flight (1) – 1.5pts/m^2.			900 m flight (1) – 1.5pts/m^2.	N block: 1.4 pts/m^2 S block: 1.6 pts/m^2

Table 4-3
Data Quality Metrics, Individual Performance Measures (continued)

	Analytical Objective	Metric	Action to Achieve Metric	Sampling Frequency or Timing	Desired Result	Actual Result
		Victorville I 300 m flight – 6 pts/m^2			300 m flight – 6 pts/m^2	6.4 pts/m^2
		Victorville II 450 m flight – 4.5 pts/m^2			450 m flight – 4.5 pts/m^2	4.8 pts/m^2
9	Lidar flight line alignment	**Kirtland** The two 200 m flights will be orthogonal.	Appropriate flight lines will be designed and flown. Planned flight lines will be submitted in advance.	Each flight.	Flight lines within 10^o of orthogonal.	**Partially Accomplished.** North block flights were orthogonal. South block flights were both flown northeast-southwest. The Double Eagle airport runway is just north of the south block. North-south flight lines would have required crossing and turning directly over the airstrip, which was impossible for safety reasons.
		Victorville: The 300 m and 450 m flights will be orthogonal.	Appropriate flight lines will be designed and flown. Planned flight lines will be submitted in advance.	Each flight.	Flight lines within 10° of orthogonal.	**Accomplished.** The two flights were flown orthogonal.

Table 4-3
Data Quality Metrics, Individual Performance Measures (continued)

	Analytical Objective	Metric	Action to Achieve Metric	Sampling Frequency or Timing	Desired Result	Actual Result
10	Lidar vertical accuracy	**Both Sites:** Vertical accuracy of +/– 15 cm compared to ground survey.	Steps:	Each flight		
			1. Perform sensor calibration as described above		As above.	**Accomplished.**
			2. Obtain ground elevations on identifiable points using ground based GPS methods (static and/or kinematic)		As above.	**Accomplished.** Control points were collected as described.
			3. Compare ground-based and airborne elevations.		Meet or exceed +/1 15 cm lidar to control point vertical accuracy.	**Accomplished.** Elevation comparisons were performed between control point elevations and the interpolated elevation of the lidar surface at that point. Results were within specifications. See Appendix A.
11	Lidar horizontal accuracy	**Both Sites:** Horizontal accuracy of +/– 65 cm compared to ground survey.	Steps:	Each flight.		**Accomplished.** Positions of control points were obtained in the Lidar data using intensity values. These positions were compared to the surveyed locations of these control points. Horizontal accuracy was well within specification. See Appendix A.
			1. Perform sensor calibration as described above		As above.	**Accomplished.**

Table 4-3
Data Quality Metrics, Individual Performance Measures (continued)

	Analytical Objective	Metric	Action to Achieve Metric	Sampling Frequency or Timing	Desired Result	Actual Result
			2. Obtain ground positions on identifiable points using ground based GPS methods (static and/or kinematic)		As above.	**Accomplished.**
			3. Compare ground-based and airborne positions.		Meet or exceed +/- 65 cm lidar to control point horizontal accuracy.	**Accomplished.**
12	Lidar data integration – flight lines	**Both Sites:** Achieve flight line to flight line edge match of +/– 12cm.	Review statistics from lidar processing software.	Line to line.	Achieve best possible match between individual lidar flight lines.	**Accomplished.**
13	Lidar point separation	**Both Sites:** Remove 100% of large features, (trees, buildings, vehicles)	Operators remove non-ground laser returns through automated separation routines followed by hand cleaning and inspection.	Lidar data set for each flight.	Satisfactory visual inspection of surface model of the ground surface.	**Accomplished.** Lidar points were classified as ground and non-ground returns. Visual inspection of the ground returns showed that all buildings, fences, and other larger features were successfully removed.
		Remove small features (grass, low brush) to the level where remaining data cannot distinguish ground from non-ground features.			Satisfactory visual inspection of surface model of the ground surface.	**Accomplished.** Inspection of ground and non-ground lidar points in conjunction with orthophotos showed that small brush and tall grass was removed within specification.

Table 4-3
Data Quality Metrics, Individual Performance Measures (continued)

	Analytical Objective	Metric	Action to Achieve Metric	Sampling Frequency or Timing	Desired Result	Actual Result
	Orthophoto Data Collection and Processing					
14	Orthophoto area coverage	**Both Sites:** 100% coverage for each flight.	Wireframes of "raw" images are compared to the project boundary to check for gaps or holes.	Each flight day as part of QA/QC checks.	100% coverage with sufficient image overlap for ortho-rectification.	**Partially Accomplished.** At Kirtland, complete coverage was obtained for both flights with the exception of one image in the 10 cm flight. The missing image is approximately 125 x 200 meters, located on the north boundary of the study area. The file appears to have been corrupted during collection. At Victorville, complete coverage was obtained.
15	Orthophoto flight altitude/ pixel size	Kirtland I 450 m (for 10 cm pixel flight)	Orthophoto pixel size is directly related to flight altitude. Flight lines are designed for the desired pixel sizes. Flight data will be examined during and after each flight and flight lines outside of the range will be repeated.	Each flight.	Achieve specified flight altitudes and pixel sizes.	**Accomplished.** 10 cm pixel sizes were achieved for 100% of the study area with the exception of the one missing image.

Table 4-3
Data Quality Metrics, Individual Performance Measures (continued)

	Analytical Objective	Metric	Action to Achieve Metric	Sampling Frequency or Timing	Desired Result	Actual Result
		Kirtland II 900 m (for 20 cm pixel flight).			Achieve specified flight altitudes and pixel sizes.	**Accomplished.** 20 cm pixel sizes were achieved for 100% of the study area.
		Victorville 450 m (for 10 cm pixel flight)			Achieve specified flight altitudes and pixel sizes.	**Accomplished.** 10 cm pixel sizes were achieved for 100% of the study area.
16	Orthophoto image mosaicing	**Both Sites:** No obvious seams between images in the final orthophoto.	Creation of an image mosaic from individual small images is largely an operator controlled rather than an automated process.	Each orthophoto composite image (10 cm and 20 cm).	Line features are continuous with no visible discontinuity at mosaic seams.	**Accomplished.** Visual inspection of the orthophoto images showed no obvious seams.
17	Orthophoto image color balancing	**Both Sites:** No obvious color imbalances within data for each session.	Color balancing is an operator controlled process based on viewing the mosaic to identify any areas of tonal imbalance.	Each orthophoto composite image (10 cm and 20 cm).	Continuity of tone such that individual images are not visible in mosaic.	**Accomplished.** Visual inspection of the orthophoto images showed no obvious color imbalances.
18	Orthophoto horizontal alignment to lidar	**Both Sites:** Lidar and orthophotos aligned so that target features are not displaced in the two data sets.	Orthorectification is performed using the lidar data and fiducial locations are control data sources, followed by operator adjustment.	Each orthophoto composite image.	Orthophotos aligned to +/– 2 pixel widths.	**Accomplished.** Positions of control targets were compared using the orthophoto and lidar intensity values. Locations were within specifications. See Appendix A.

Table 4-3
Data Quality Metrics, Individual Performance Measures (continued)

	Analytical Objective	Metric	Action to Achieve Metric	Sampling Frequency or Timing	Desired Result	Actual Result
19	Orthophoto horizontal alignment to fiducials	**Both Sites:** Orthophotos aligned to survey control points so that target features are not displaced.	Orthorectification is performed using the lidar data and fiducial locations are control data sources, followed by operator adjustment.	Each orthophoto composite image.	Orthophotos aligned to +/– 3 pixel widths.	**Accomplished.** Ortho image positions were compared to control targets visible in the images. In addition, lidar and orthophoto positions were compared for building corners and edges of pavement that were visible in both the orthophoto and lidar data. Positions were within specifications. See Appendix A.

4.2 PERFORMANCE CONFIRMATION METHODS

4.2.1 Demonstration-Level Confirmation Methods

At the demonstration level, the effectiveness of lidar and orthophotos was evaluated based on its ability to meet the stated performance criteria given in Table 4-1. The demonstration relied on proven industry methods to assure predictable results, including the use of survey controls, equipment calibration, alignment of lidar points to the survey control points and from one flight line to the next, and QA/QC checks throughout the project. Both lidar and orthophoto data met all data quality specifications.

During data analysis, standard GIS methods were used to create surface models from the lidar data. As a means to ensure objective results, staff assigned to initial feature identification was not provided with the CSM and did not know the history of munitions use at the site. All feature and MRS identification was subject to QA/QC review by project staff familiar with both the CSM and UXO/MEC generally.

4.2.2 Program Level Confirmation Methods

Lidar and orthophotos were evaluated for their ability to meet the goals of the WAA Pilot Program as a whole. Evaluation was based on comparing the results of the lidar and orthophoto data with the results of the other data collected at the two sites, including helicopter and transect magnetometry and transect-based EMI, along with validation data including 100% coverage magnetometry areas, site reconnaissance, and intrusive sampling. In general, these subsequent activities confirmed the findings and usefulness of lidar and orthophotos. They also revealed areas where lidar and orthophotos did not detect areas of concentrated munitions use, with implications for the appropriate use of these technologies at future sites.

For both of the sites, lidar, orthophotos, helicopter magnetometry, and towed-array magnetometry or EMI were collected on the entire demonstration site where terrain and vegetation allowed. This procedure was designed to facilitate comparison of the contributions of the various technologies in different site conditions. At production sites, it is assumed that the three technologies would be deployed in a manner that would consider time and budget constraints faced by site managers. In such a model, lidar and orthophotos would be deployed to the site first and the results used to guide the deployment of the subsequent magnetometry layers.

Validation activities included 100% coverage surveys of small parcels using the ground system, reconnaissance surveys, and a limited intrusive investigation. These were undertaken to validate both the data collected by the other technologies, and their conclusions, such as the conclusions as to the ordnance origin of features.

The reconnaissance survey team (an explosive ordnance disposal specialist and a geophysicist with a hand-held GPS and camera) located and confirmed anomalies observed in the helicopter data. The ground systems were used to survey smaller (tens of acres) patches near targets and in areas of no obvious munitions use, to determine the distributions of anomalies across the site. The intrusive investigation confirmed the identity of sub-surface features detected by the geophysical sensors and confirmed the reliability of feature classification using the geophysical results.

4.2.3 Results: Kirtland

At the Kirtland site, helicopter and ground-based magnetometry confirmed the ordnance origin of the MRS identified in the initial CSM. There was good general agreement between the lidar and orthophoto data and the helicopter magnetrometry data, as shown in Figure 4-1.

Figure 4-1
Kirtland Helicopter Magnetometry Density Grid

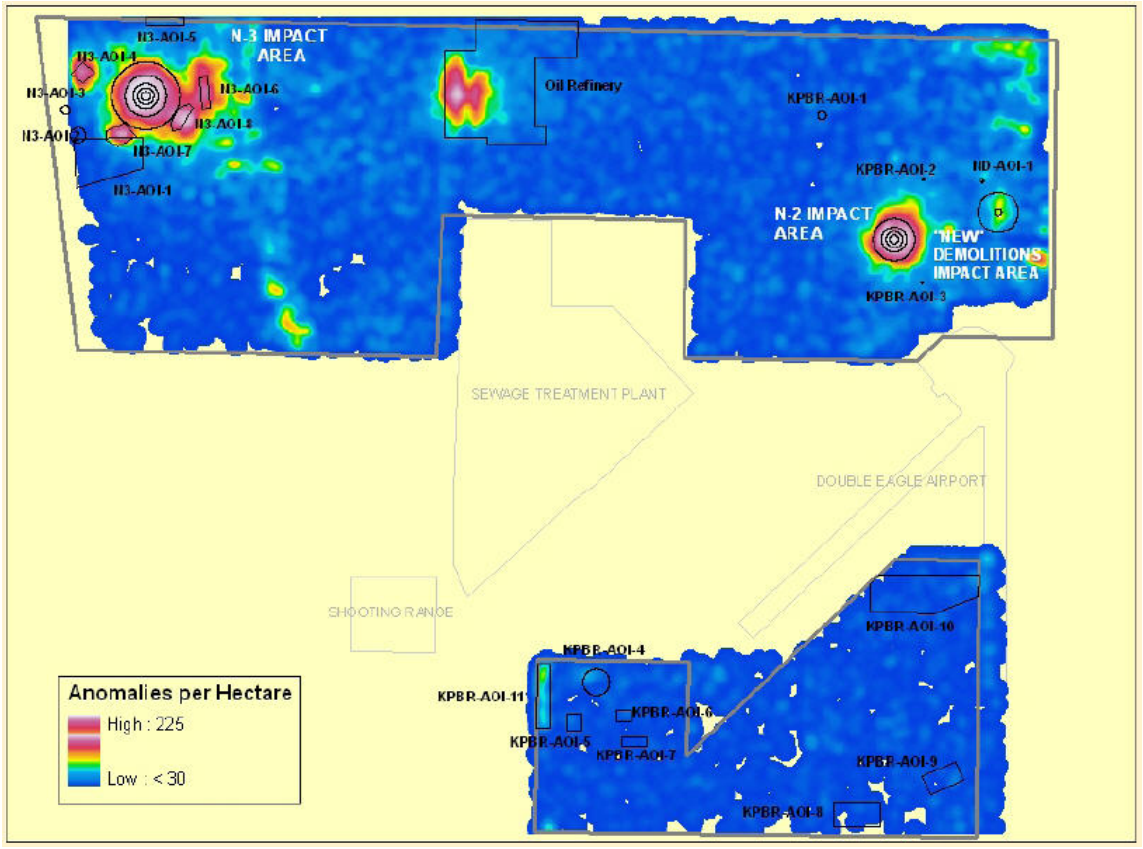

Source: ESTCP (2007a)

Results for the individual targets and areas of interest (AOIs) are discussed below.

Target N3

Target N3 is the most complex target area at the Kirtland demonstration site. For the main bombing target, the lidar and orthophoto data were very consistent with the validation data. Lidar and orthophoto data clearly showed the concentric circles of the bombing target. On-site reconnaissance located the target center but not the rings, which were too eroded to be visible from the ground. Helicopter magnetometry showed concentrations of anomalies within the target rings, as did the transect data. Intrusive sampling located abundant ordnance-related scrap along with four intact ordnance items.

There were no apparent craters within the aiming circles, and all ordnance-related scrap retrieved from the intrusive sampling was from 100-pound M38A2 practice rounds. The archival search report did not indicate any other munitions activity at this target. All data is consistent the CSM, which identified the area as a practice bombing target.

There were eight additional AOIs at Target N3, six of which were identified from the lidar and orthophoto data and two that were identified from the magnetometry data. The results using lidar and orthophotos, as well as from the relevant subsequent investigations are given below, using the AOI names given in the revised CSM:

- N3-AOI-1 is the possible crossed runway target southwest of the outer aiming circle. This area was identified in the lidar data as a potential additional target area. Portions of this area showed concentrations of geophysical anomalies.

- N3-AOI-2 and N3-AOI-3 were identified from the lidar data by possible craters. Site reconnaissance identified these as depressions with no evidence of ordnance scrap.

- N3-AOI-4 appears in the lidar data as a diamond-shaped potential target area west of the main target. (The CSM describes this as a “raised area shaped in a cloverleaf pattern.”) There were high concentrations of geophysical anomalies throughout the area and a large amount of ordnance-related scrap was retrieved.

- N3-AOI-5 appears in the lidar data as a long rectangular disturbance of the ground shaped like a single runway. Few anomalies were seen in the helicopter or transect magnetometry data; however, anomalies appeared in the 100% geophysical survey and some ordnance-related scrap was retrieved during the intrusive sampling.

- N3-AOI-6 appears in the lidar data ship-shaped potential target. The shape was confirmed by site reconnaissance, while geophysical data showed high concentrations

of anomalies and intrusive sampling located ordnance-related scrap and one intact ordnance item.

- N3-AOI-7 and N3-AOI-8 were not identified using the lidar or orthophoto data and were identified using helicopter magnetometry by concentrations of geophysical anomalies. Intrusive investigation showed that both areas had large amounts of ordnance-related scrap, and three intact ordnance items were located within N3-AOI-7.

The results of these activities at the AOIs are shown in Figures 4-2 and 4-3.

Figure 4-2
Kirtland Target N3 and Associated AOIs

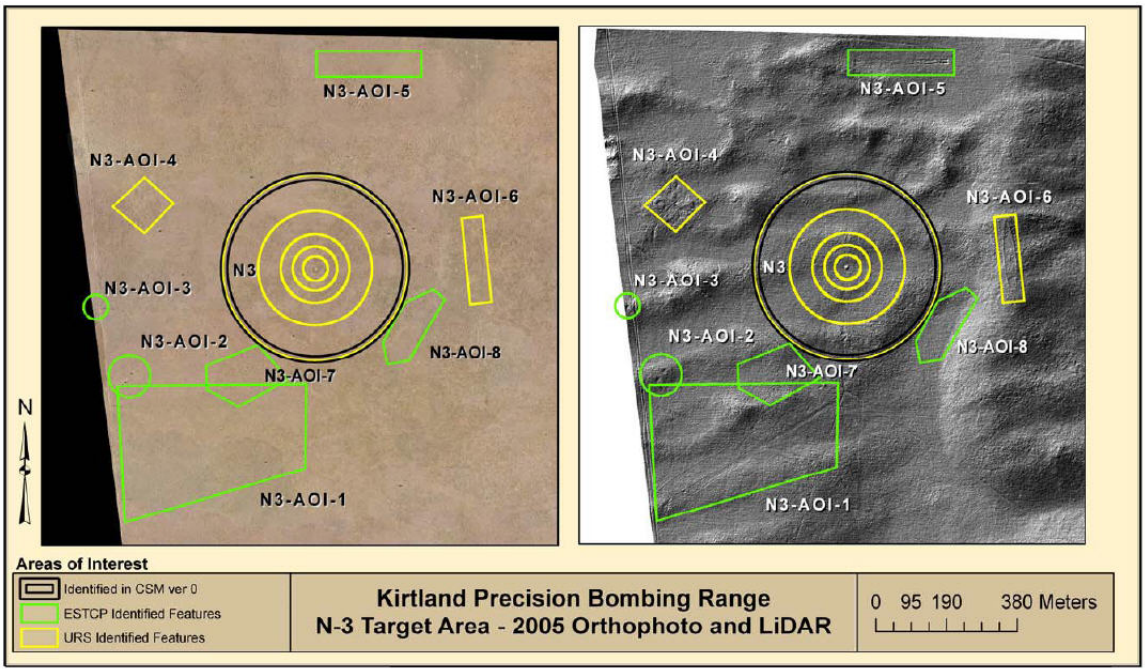

Source: ESTCP (2007a)

The location of N3-AOI-7 and N3-AOI-8, which were not detected using lidar and orthophotos, are shown, just southeast and southwest of the aiming circles.

Figure 4-3
Kirtland Target N3 and Associated AOIs, Geophysics Data

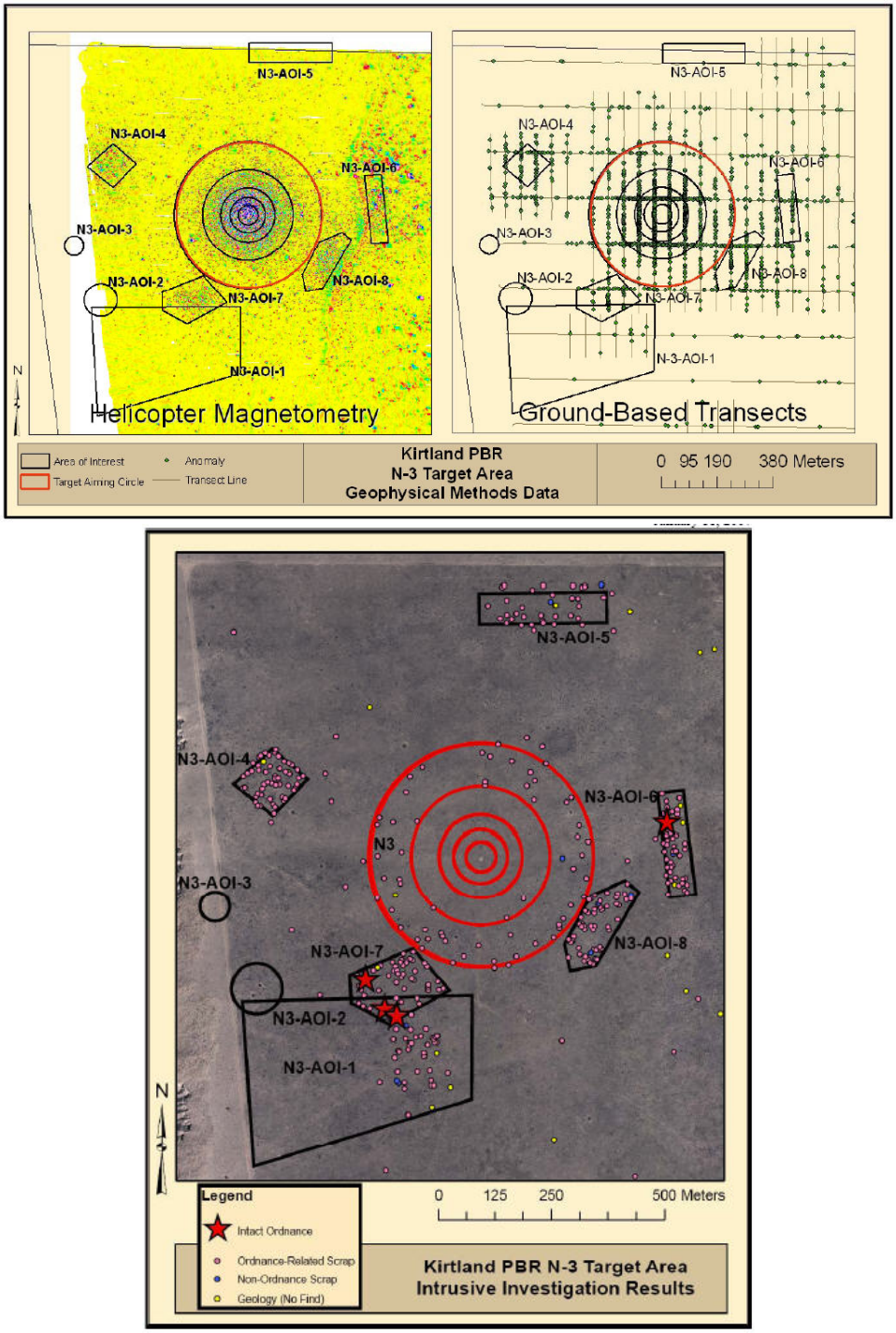

Source: ESTCP (2007a)

Simulated Oil Refinery

This SORT target is described in the initial CSM as a series of cells forming a rectangular shape. The target outline shown in Figures 4-4 and 4-5 is based on interpretation of the lidar and orthophoto data, in which rectangular cells and other berms are visible. The helicopter and transect magnetometry data showed a concentration of anomalies only in the western portion of the target area. The lack of craters and the nature of the ordnance scrap recovered support the conclusion that only 100-pound practice bombs were used at this target.

Figure 4-4
Kirtland Target SORT, Geophysics Data

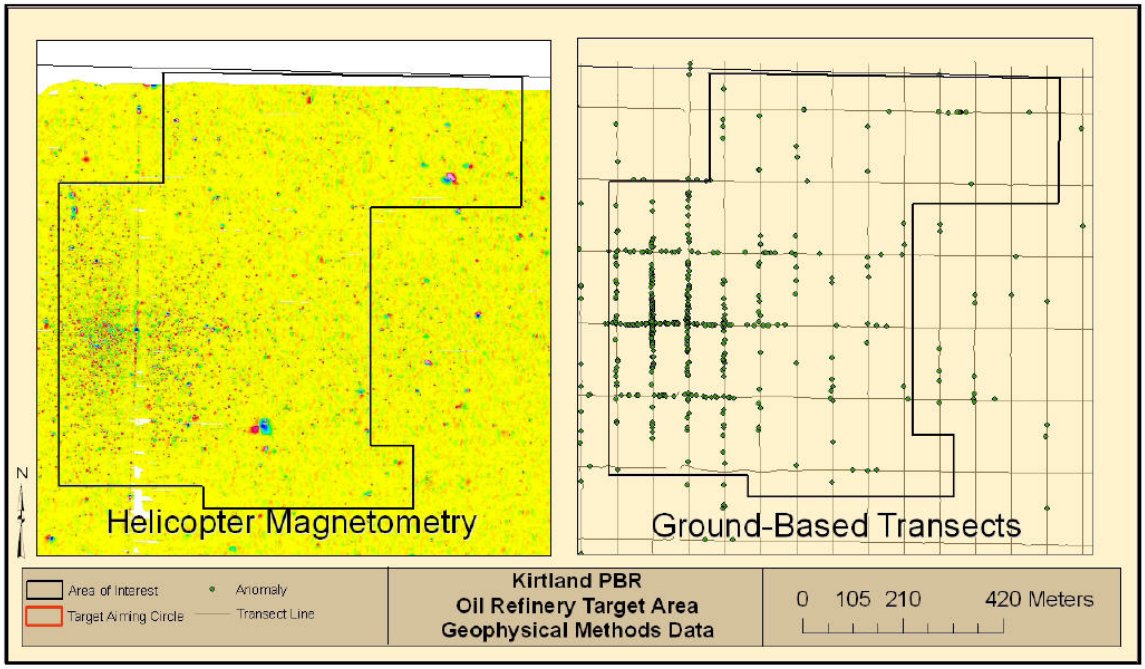

Source: ESTCP (2007a)

The transect and 100% coverage magnetometry data showed that anomalies extended past the boundaries of the target visible in the lidar and orthophoto data, though at low concentrations. Intrusive surveys confirmed that these anomalies included ordnance-related scrap, which extended to the farthest area surveyed.

Figure 4-5
Kirtland Target SORT, Intrusive Investigation Results

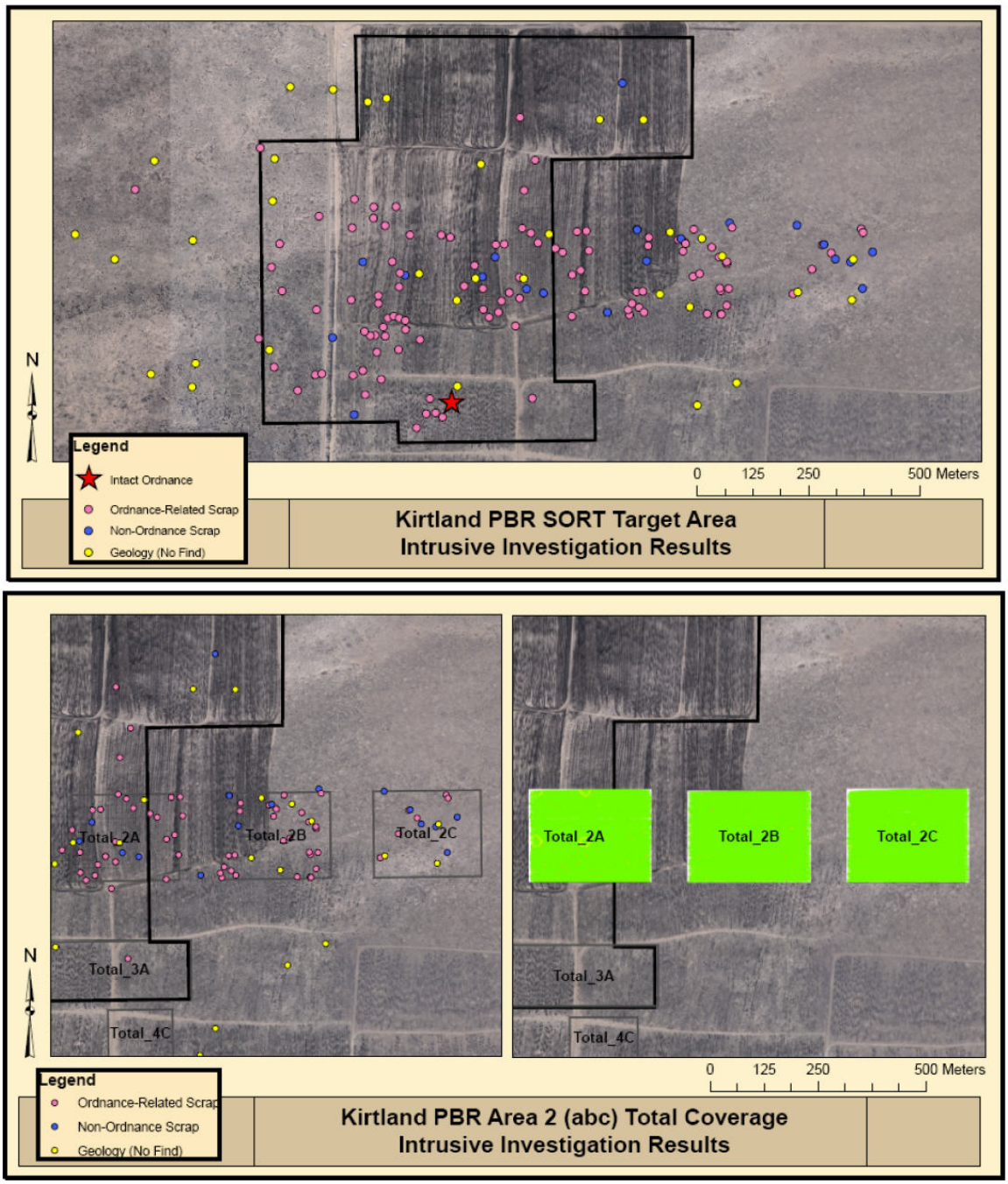

Source: ESTCP (2007a)

Target N2

Target N2 is described as a 1,000-foot bull's-eye target used for 100-pound practice bombs. Lidar and orthophoto data clearly showed the concentric circles making up this bombing target, although these were not visible from ground reconnaissance. No craters were seen in either the lidar data or site reconnaissance. Helicopter and ground-based magnetometry showed high concentrations of anomalies throughout the target circle to the outer ring (Figure 4-6). A large amount of small frag and ordnance-related scrap was observed at the surface. Ordnance-related scrap retrieved as part of the intrusive investigation was all from 100-pound M38A2 practice rounds or aerial flares. This data is all consistent with the conclusion that the target was used for practice bombing.

A structure located on the second inner ring to the north of the center is visible in both the orthophotography and the lidar data. Site reconnaissance identified this a razed cinderblock building.

The results of 100% magnetometry surveys and intrusive investigation were consistent with each other. There was a high concentration of ordnance-related anomalies and objects within the target, with the density falling off with distance but not to zero. These results indicate that, as at Target SORT, even the area considered background contained some ordnance-related material.

Figure 4-6
Kirtland Target N2, Geophysics Data

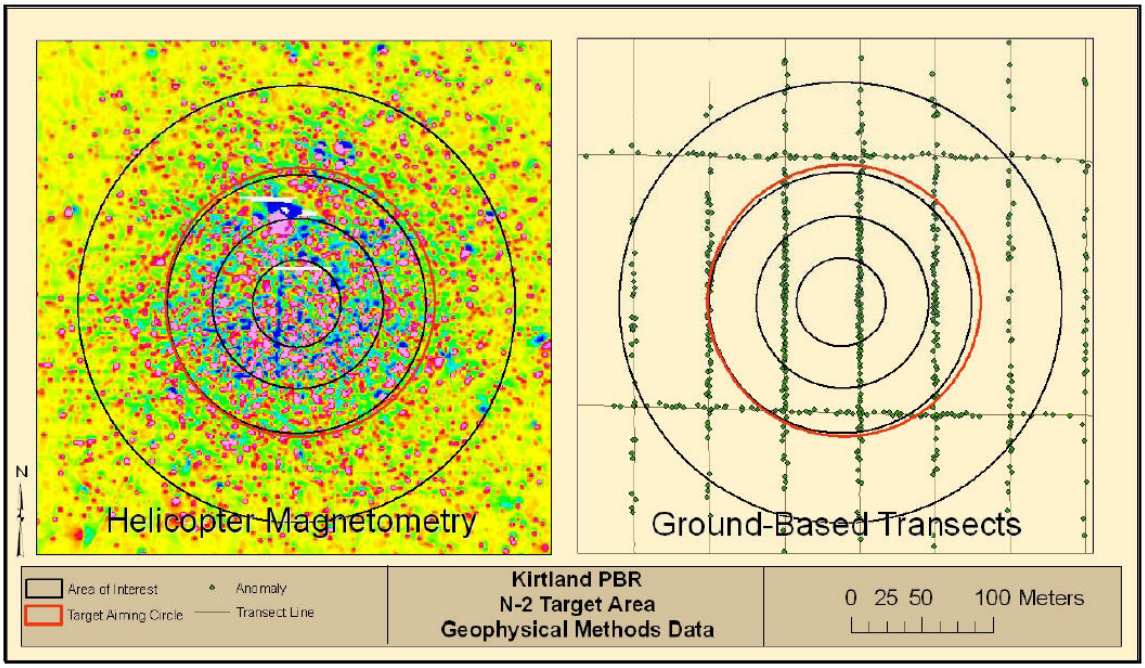

Source: ESTCP (2007a)

New Demolitions Impact Area

Target NDIA is described in the initial CSM as a 1,000-foot-diameter HE bull's-eye target. The lidar data did not show any evidence of target rings, but did show numerous potential craters. The orthophoto data showed target cross-hairs and one target ring. Helicopter and transect magnetometry both showed a low density of anomalies in and near the target area (Figure 4-7). The 100% ground geophysical surveys collected through the center of the inner target circle and at the northern edge of the outer circle showed concentrated anomalies at the center, getting more sparse further away. Intrusive sampling was not performed on these anomalies due to the possible presence of 250-pound HE bombs in close proximity to the airport. Field reconnaissance located craters and heavy walled frag. Both indicate of the use of HE at this site.

Figure 4-7
Kirtland Target NDIA, Geophysics Data

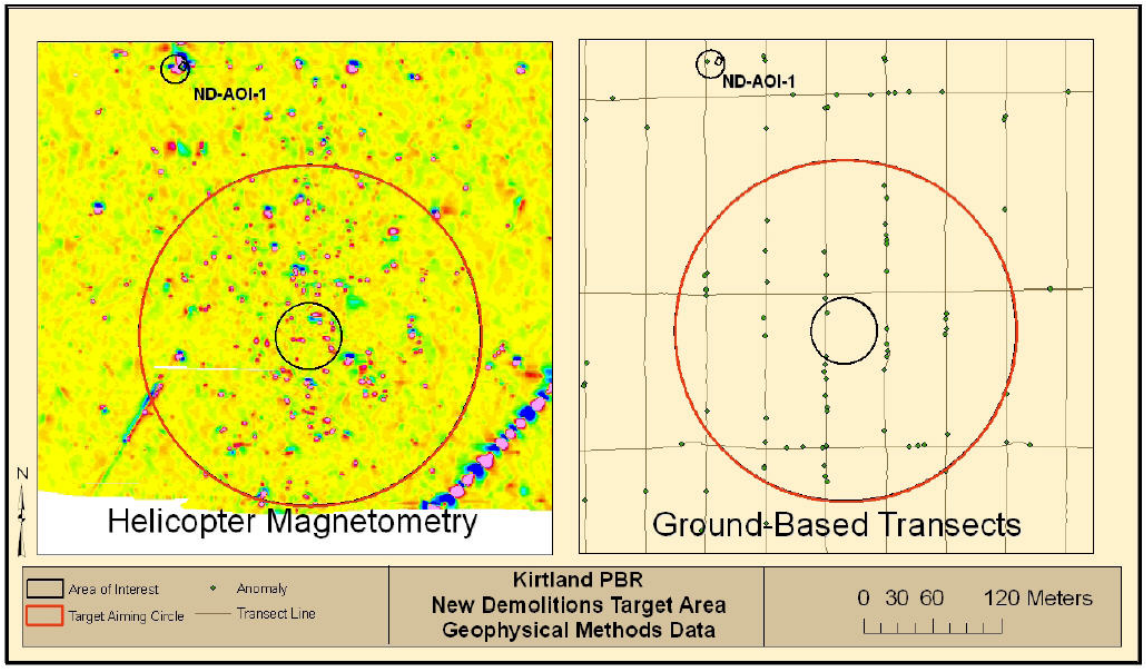

Source: ESTCP (2007a)

Additional Areas

Eleven additional AOIs were identified at the Kirtland site, nine of them in the southern portion of the study area and two in the northern portion near Target N2. The archival search report did not indicate any munitions-related activities in these areas, and subsequent surveys found all but one of these AOIs to be building foundations, animal burrows, or other areas with no evidence of ordnance use. The one exception was the potential bull's-eye target described in Section 3.7.9,

which was found to contain a small number of anomalies: two rings of light-colored pebbles and a small amount of ordnance-related scrap. The revised CSM describes this as a possible aiming circle, with a medium confidence level. The site is located relatively close to a known target area just outside of the study area, and it is possible that this is the source of the ordnance-related scrap found.

4.2.4 Results: Victorville

Target DBT Y

Target DBT Y is described as a HE bombing target, and large craters were clearly shown using both lidar and orthophotos. Helicopter and ground-based magnetometry and EMI found few anomalies at the site, and there was little evidence of munitions-related scrap. The revised CSM states that this is nevertheless consistent with potential HE use, which can leave few items large enough to result in either anomalies or visible scrap. The site has been the site of previous cleanup activities which may also account for the scarcity of items. Heavy-walled scrap indicative of HE use was found just outside of the dry lake bed near similar craters to those at the site.

Target PBR 15

Target PBR 15 is described as a bull's-eye target used for precision bombing practice. Orthophotos and lidar intensity imagery clearly showed the bull's eye rings. Concentrations of anomalies from both helicopter and ground-based magnetometry were found up to a circle of 1,000 feet in diameter surrounding the target. The lack of cratering at the target supported the conclusion that the target was used for practice bombing.

Figure 4-8 shows the ground magnetometry transect data as filtered for geologic noise. Target PBR 15 is clearly visible in the southeast portion of the site. Target DBT Y is faintly visible.

Figure 4-8
Victorville Filtered Geophysics Data

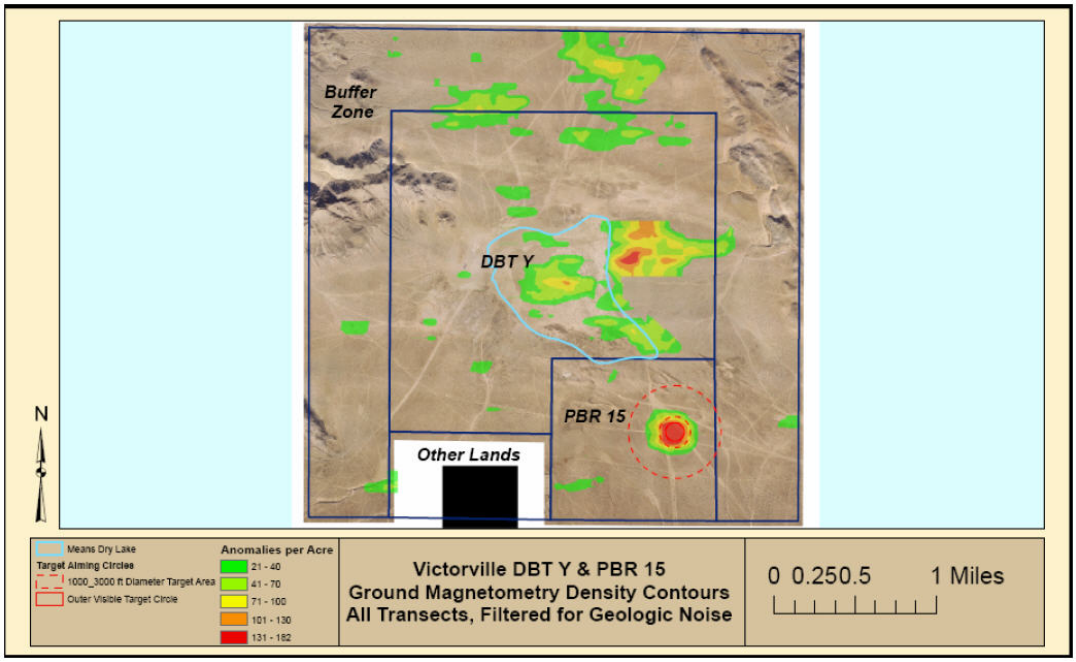

Source: ESTCP (2007b)

Additional AOIs

Figure 4-9 shows the additional AOIs identified at the Victorville site. All but the craters west of the dry lake bed were identified based on the magnetometry and EMI surveys. Lidar data showed a number of apparent craters west of the dry lake bed, and ESTCP conducted site reconnaissance of some of these features (labeled in the revised CSM as DBTY-AOI-1). The presence of heavy-walled ordnance frag confirmed that some of these features were craters from HEs. However, the small number of craters found suggested that these craters were from pilot error rather than a separate target. Others features to the far west in this area were identified as mining prospect pits or large boulder formations. The other AOIs were examined with ground-based magnetometry and EMI sensing, and were determined not to be ordnance-related.

Figure 4-9
Victorville Helicopter Magnetometry Density Grid

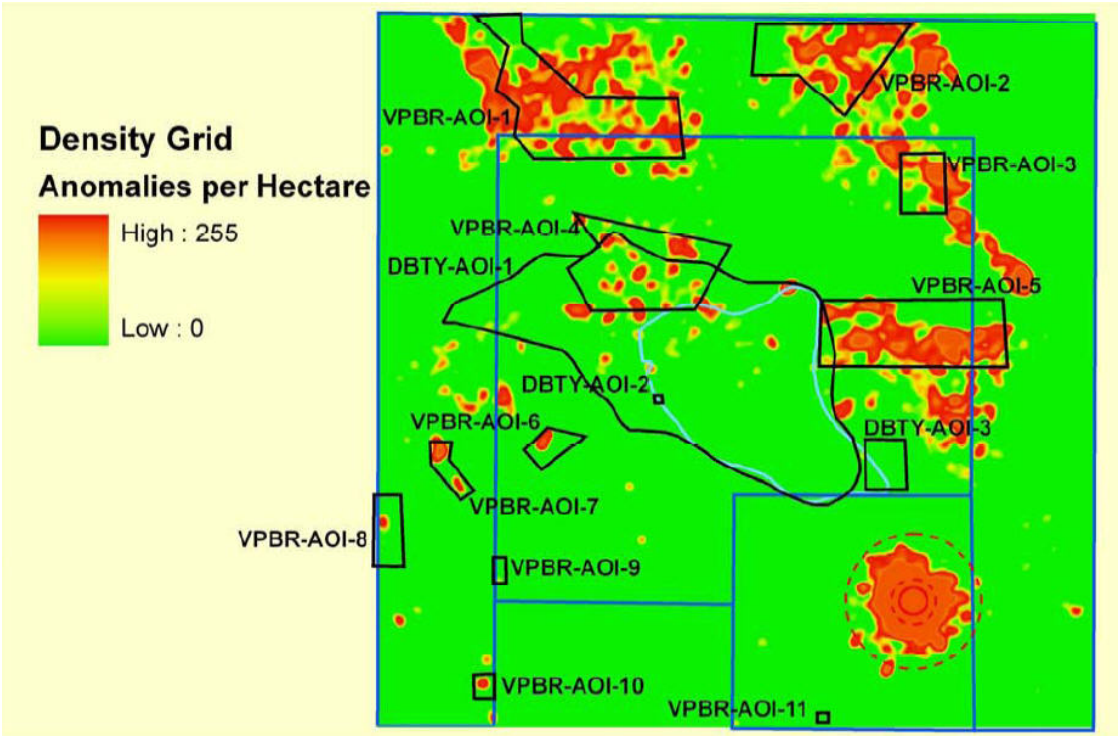

Source: ESTCP (2007b)

4.2.5 Findings and Conclusions

Examination of the lidar and orthophoto data in light of the subsequent activities at the two sites led to the following findings and conclusions:

- Lidar and orthophotos located all of the major target features. The general locations of these targets were consistent between the lidar and orthophoto data and that of the other technologies used.

- Lidar and orthophotos did not locate two ordnance-related areas associated with Kirtland Target N3, presumably because these areas did not show ground disturbances. These areas were detected using all of the magnetometry platforms, and were verified through intrusive investigation. This result points out a limitation of these light-based technologies: because they do not direct ordnance components directly, they can miss areas of munitions use that do not leave evidence on the ground surface. Consequently, use of lidar and orthophotos should be supplemented with other technologies where appropriate.

- Lidar and orthophotos tended to understate the extent of distribution of ordnance-related scrap at the Kirtland site. Ordnance-related scrap continued to be found in most of the areas of 100% coverage and intrusive investigation, well past what would have been estimated as conservative boundaries of the features using the lidar and orthophoto data. The reason for this wide distribution of ordnance scrap is not known. Because no intrusive sampling was done at the Victorville site, it is unknown whether this pattern would be found at the targets there. It is possible that methods could be developed to better extrapolate from features shown in lidar to the actual extent of ordnance-related scrap. However, this would require the examination of both lidar and orthophoto as well as validation data from a wider variety of sites.

- Lidar and orthophotos found targets using berms or craters that would not have been inferred from helicopter magnetometry data alone, including the main target ring at Kirtland Target N3 and Victorville Target DBT Y.

4.3 DATA ANALYSIS, INTERPRETATION, AND EVALUATION

4.3.1 Correlations with Operating Parameters and Required Performance Specifications

Of the operating parameters tested, lidar and orthophoto data density showed the strongest correlation with operational results. Of the two orthophoto pixel sizes tested, the 10 cm pixel images clearly outperformed the 20 cm images, allowing the detection of objects at or below 1 m in size. This is a significant result for two reasons: first, because the smaller pixel size is more expensive to acquire, and second, because both 10 cm and 20 cm pixel orthophotos are more dense than conventionally available orthophotography, which very seldom has pixel sizes smaller than 32 cm (1 foot).

Lidar data density clearly affected the detection of smaller craters. This effect was not as strong for the bombing targets, which were well detected using all but the lowest-density lidar data collected of 1.5 pts/ m^2. At this level, bull's-eye target rings began to be missed.

At future sites where detection of large features such as bombing targets is the principle objective, lidar data densities would not need to be as high as for reliable detection of craters. Nevertheless, additional lidar density should probably be acquired if the project budget and the vendor's equipment allow, since additional lidar density will help to define features more clearly. Additionally, this demonstration showed that lidar data density varied considerably over the project area. Increasing overall lidar density is one way to compensate for the possibility that some areas will be less dense than planned.

Data from this demonstration also suggests that if possible, increased lidar density should be acquired through use of faster sensors or lower flight elevations, rather than through multiple

overlapping flights. This is because in areas of flightline overlap, current equipment characteristics and data processing methods exclude significant numbers of lidar points from the ground surface model. In areas with very sparse vegetation, the point classification problem can be eliminating by making surface models using all lidar points, however this approach cannot be used on vegetated sites. Further investigation is appropriate in this area.

Flight line orientation also had a detectable effect on detection of very shallow linear features, indicating that if a second lidar flight is collected in addition to the primary lidar/orthophoto flight, it should be flown perpendicular to the first flight.

4.3.2 Optimum Operating Conditions and Appropriate Uses of the Technologies

Results from the Kirtland and Victorville sites support the general premise of the WAA Pilot Program: lidar and orthophotos should be the first technologies to be deployed after completion of the archival search report and the initial CSM. At both sites, lidar and orthophotos were successful at revealing and verifying the broad picture of munitions use. Lidar, especially, was very successful at delineating targets and crater fields, as well as additional areas of interest that warranted investigation. Areas of interest that warranted further investigation were delineated. The two technologies complemented each other well, each providing data that the other did not. Since vendors generally offer the two technologies together, it makes sense to acquire both at future production sites.

At the Kirtland site, two AOIs were identified using magnetometry that were not detected using lidar and orthophotos, presumably because these areas did not leave any indications on the ground surface. This finding supports the WAA Pilot Program approach that lidar and orthophoto acquisition should be followed with technologies that directly detect ordnance components.

5.0 COST ASSESSMENT

5.1 COST REPORTING

Table 5-1 presents actual costs for the Kirtland and Victorville demonstration sites, and estimated costs for production sites of three different sizes. Cost figures for the 18,000-acre demonstration site are based on preliminary project costs for the Former Camp Beale site, acquired in 2006. The remaining figures are planning-level estimates, assessed to be accurate within +/- 20%. Per-acre costs for the Kirtland site were higher since four rather than two lidar flights were conducted, and one rather than two orthophoto sets were created. The Victorville configuration, with one lidar/orthophoto flight and one additional lidar-only flight, is considered representative for a production site where it is important to detect both targets and individual small features. The "50,000-acre production site" estimate is based on URS' previous experience and interviews with industry sources, and the "115,000-acre production site" estimate is based on a cost proposal made by URS for a site in the western US in fall 2005. All projects listed can be completed in less than one year; therefore, no discount factor has been applied to the figures.

Table 5-1
Actual and Projected Costs

Project Parameters	Kirtland	Victorville	18,000-acre Production Site	50,000-acre Production Site	115,000-acre Production Site
Project area size (acres)	5,000	5,640	18,000	50,000	115,000
Project area size (hectares)	1,914	2,282	7,284	19,140	44,022
Lidar flights:					
300 m (Lidar only)	2	1	1	1	1
450 m (Lidar and 10 cm pixel imagery)	1	1	1	1	1
900 m (Lidar and 20 cm pixel imagery)	1	0	0	0	0
Total Lidar flights	4	2	2	2	2
Total Lidar point density (pts/m^2)	20	8-10	8-10	8-10	8-10
Orthophoto pixel size (cm)	10 and 20	10	10	10	10
Costs (2006 $)					
Fixed Costs					
Mob/demob	15,600	23,100	21,800	30,000	45,000
Planning/preparation	15,000	9,200	15,000	15,000	20,000
Project management	15,000	10,000	25,000	40,000	100,000
Site work	0	0	0	0	0
Equipment cost	0	0	0	0	0
Start-up and testing	0	0	0	0	0
Subtotal fixed costs	45,600	42,300	61,800	85,000	165,000
Variable Costs (2006 $)					
Data acquisition	39,900	34,100	85,300	160,000	355,000
Data processing	45,800	35,200	102,900	250,000	575,000
Data analysis and GIS products	94,300	30,000	68,100	150,000	220,000
Data reporting and documentation	13,600	8,500	12,000	15,000	25,000
Materials and consumables	1,500	1,000	1,500	5,000	10,000
Other direct costs	0	0	0	0	0
Subtotal variable costs	195,100	108,800	269,800	580,000	1,185,000
Total project cost (2006 $)	**240,700**	**151,100**	**331,679**	**665,000**	**1,350,000**
Total per/acre cost (2006 $)	**48.1**	**26.8**	**18.43**	**13.3**	**11.7**
Total per/hectare cost (2006 $)	**125.8**	**66.2**	**45.53**	**34.7**	**30.7**

5.2 COST ANALYSIS

5.2.1 Cost drivers

The major cost drivers for the two demonstration sites were:

- **Lidar data density required.** For the Kirtland site, four lidar flights were conducted; two concurrently with digital imagery collection, and two lidar-only flights. For the Victorville site, one lidar/orthophoto flight and one lidar-only flight were conducted.

- **Orthophoto data density required.** For the Kirtland site, two sets of digital images were collected, and orthophotos were created at 10 cm and 20 cm pixel sizes. For the Victorville site, only 10 cm pixel size was collected.

- **Accuracy and precision requirements.** A higher level of survey control was needed at the Kirtland PBR site than for production sites, in order to verify the accuracy and precision of the lidar and orthophoto data and to confirm that data could be successfully integrated with the other technologies demonstrated. It is estimated that during production projects fewer survey control points and vertical control structures would be needed.

- **Site location/logistics.** The Kirtland PBR site location affected project costs both positively and negatively. Positive effects were that the Double Eagle Airport was immediately adjacent to the project site and the helicopter vendor used was based at this site. These factors lowered mobilization and equipment rental costs and eliminated fees for fuel transport. Negative factors were that the high level of air traffic at the airport required hiring a second pilot. In addition to the additional labor cost, the additional weight resulted in higher fuel costs. At the Victorville site, fuel had to be transported to the site and helicopter flight times were longer, creating somewhat higher site-related costs than for Kirtland.

In addition to the cost drivers listed above, costs for production sites will be affected by the following additional factors:

- **Site size.** Larger sites achieve cost savings through amortization of fixed costs such as mobilization and project planning, as well as through increased efficiency in data acquisition and processing.

- **Vegetation conditions.** Highly vegetated sites will have higher costs due to the requirement for additional lidar passes to achieve sufficient density of points reaching the ground surface.

- **Permitting and site access constraints.** DoD sites with sensitive, high-security areas may have higher costs. However, such conditions would typically affect only pre-flight planning and equipment mobilization costs rather than data acquisition, processing and analysis costs. Sites with environmental constraints do not normally impose significantly higher costs for lidar and orthophotography, since the airborne nature of the technologies does not typically affect sensitive species or environments.

5.2.2 Cost Sensitivities and Additional Potential Savings

Additional savings could be realized through either of the following methods:

- **Acquiring orthophotography with a larger pixel size.** The cost of acquiring and processing orthophotography rises dramatically for smaller pixel sizes, and acquiring orthophotos at 20 cm pixel size rather than 10 cm would reduce the data acquisition and processing costs by 30 to 35%. The utility of such photos would be lower since their resolution will not allow discrimination of smaller features. Nevertheless, this may be an appropriate solution for sites where orthophotography is inherently less useful, such as sites with heavy tree cover. At such sites, pre-existing orthophotography from other sources may be acceptable if its positional accuracy can be verified.

- **Acquiring lower-density lidar data.** Eliminating the assumed second lidar flight, and thus only collecting lidar with the 10 cm orthophoto imagery, would reduce costs by 25 to 30%. The ability of the resulting lidar data set to discriminate features would be reduced; however, this might be appropriate if the lidar data was to be used only to discriminate large features such as bombing targets or roads, rather than smaller features such as craters. Alternatively, DoD could specify use of a faster lidar sensor, which could meet lidar data density requirements from a single pass.

Some additional cost savings could potentially be achieved by establishing Service- or DoD-wide standards for data acquisition, GIS data product creation, data delivery formats, and project reporting.

5.3 COST COMPARISON

Cost comparisons with the other innovative technologies demonstrated as part of the ESTCP WAA Pilot Program will be made in the Final Report for the WAA Pilot Program.

6.0 IMPLEMENTATION ISSUES

6.1 ENVIRONMENTAL CHECKLIST

No environmental regulations applied to the demonstration and no permits were required.

6.2 OTHER REGULATORY ISSUES

Both lidar and orthophotography are in wide commercial use. Within the United States, no regulatory restrictions are known that would impede the wide use of either technology. Outside of the United States, use of advanced IMU equipment may be restricted in certain countries. The IMU used in lidar systems is military dual use technology and international use requires a permit under the International Traffic in Arms Regulations (22 CFR 120-130). Additionally, some countries impose a variety of restrictions on the acquisition, processing and subsequent use of lidar and orthophoto data collected within their borders, particularly in border or military-use areas. Potential users of lidar in such situations should investigate such restrictions as part of project planning.

6.3 END-USER ISSUES

Both lidar and orthophotos are in wide commercial use and do not face substantial end-user issues.

7.0 REFERENCES

URS Corporation. 2001. *Quality Assurance Manual.* January.

———. 2005. Final Demonstration Plan, Project Number UX-0534, High Density LiDAR and Orthophotography in UXO Wide Area Assessment. July.

———. 2006a. Demonstration Plan Addendum for Victorville PBR Y Demonstration Site. January.

———. 2006b. Demonstration Plan Addendum for Former Camp Beale Demonstration Site. July.

Environmental Security Technology Certification Program. 2007a. Former Kirtland Precision Bombing Range, Conceptual Site Model. Draft Version 3.1. January.

———. 2007b. Victorville Precision Bombing Range: Demolition Bombing Target "Y" and Precision Bombing Range Target 15, Conceptual Site Model. Draft Version 2. January.

———. 2006a. Draft Reconnaissance Plan, Wide Area Assessment Pilot Program Demonstration at Victorville Precision Bombing Ranges Y & 15, CA. September.

———. 2006b. Draft Validation Plan, Wide Area Assessment Pilot Program Demonstration at Former Kirtland Precision Bombing Range, NM. January.

APPENDIX A

Lidar and Orthophoto Positional Accuracy Results

LIDAR AND ORTHOPHOTO POSITIONAL ACCURACY RESULTS

INTRODUCTION

Verification of the positional accuracy of lidar and orthophoto data was a key performance metric for the demonstration. To be useful in Wide Area Assessment, lidar and orthophotos must have positional accuracies that allow integration with other spatial data sets. Lidar and orthophotos must allow for meaningful measurement of object sizes in order to make conclusions about historic munitions use. The data must be sufficiently accurate to allow field verification of their results. Quality Assurance/Quality Control (QA/QC) methods for lidar and orthophotos have been well established, and standard methods were applied at both sites. At both sites, primary performance metrics for both technologies were met.

DISCUSSION

In the Demonstration Plan, performance specifications are established in Table 4-2, Performance Confirmation Methods, and Section 4.3, Data Analysis, Interpretation and Evaluation. Positional confirmation was accomplished through comparison of lidar and orthophoto positions to surveyed control points, vertical control structures, and comparison of lidar and orthophoto positions to each other.

RESULTS

Surveyed Control Points

Surveyed control points formed the basis for analysis of positional accuracy. At the Kirtland site, ESTCP established five control points on the site; TRSI established four additional control points and independently occupied two of the ESTCP control points. Both control point sets were referenced to NGS Q424, the local High Accuracy Reference Network (HARN) point, located approximately 6 km south of the study area.

At the Victorville site, TRSI established eight survey control points on the site. These were independently occupied by ESTCP. Control point locations and typical control points are shown in Section 3.4, and are available in the project QAQC reports.

Lidar vertical accuracies – Control points

Comparisons were made between the elevations of the control points and the lidar points, by comparing the surveyed elevations to the elevation of the modeled lidar surface at that point. All values were within the target accuracy of +/- 0.150 meters. Values for the Kirtland site were

calculated using both ESTCP and TRSI control point values. Values shown in the chart below were calculated using both sets of survey values. At the Victorville site, the ESTCP values were not used to calculate positional accuracies. This was because the TRSI and ESTCP surveyors had a vertical discrepancy in their surveyed values for the control points of approximately 1 meter (across all points) which could not be resolved. This discrepancy was probably the result of differences in survey datums used. All values were within the specified accuracy standard. At the Kirtland site, results followed the general industry expectation that lidar data flown at lower elevations will be more accurate than at higher elevations, however the correlation was not strong, and at the Victorville site the accuracy at the two elevations flown was essentially equivalent.

Kirtland

	Lowest Dz (m)	**Highest Dz (m)**	**Mean Dz (m)**
900 m flight	0.002	0.333	0.107
450 m flight	0.043	0.197	0.113
300 m flight 1	0.011	0.227	0.082
300 m flight 2	0.012	0.217	0.087

Victorville

	Lowest Dz (m)	**Highest Dz (m)**	**Mean Dz (m)**
300 m flight	0.021	0.333	0.107
450 m flight	0.021	0.197	0.113

Lidar Horizontal Accuracy

The horizontal accuracy of the lidar data was evaluated by comparison with the control points. The method was slightly different at the two sites. At the Kirtland site, the control point positions were inferred from the lidar data by using the intensity value of the lidar returns. Intensity is the measured value of the strength of the lidar return signal, and this value varies directly with the reflectivity of the surface. Lidar points that returned from the white targets were distinguishable from those that reflected from the darker colored ground surface. These points were used to infer the position of the intersection of the two target legs, which was the location of the control point. This location was then compared to the surveyed location of the measured control point.

At the Victorville site, the lidar points reflected (by chance) from the antenna of the GPS base station at one control point, giving an excellent location for the control point. This location was used for the comparison and inference of the other control points was not needed.

The method is illustrated below.

Figure A-1
Method for Evaluating Lidar Horizontal Accuracy

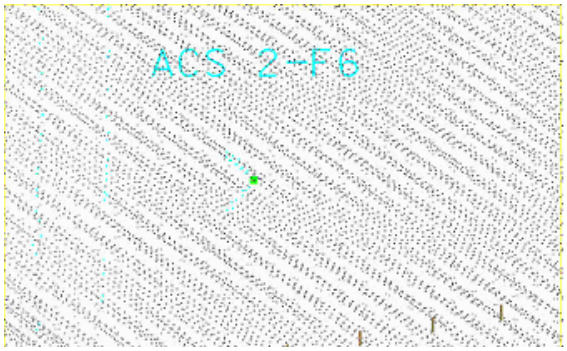

Lidar points classified by intensity, blue points are reflections from the target legs. Kirtland

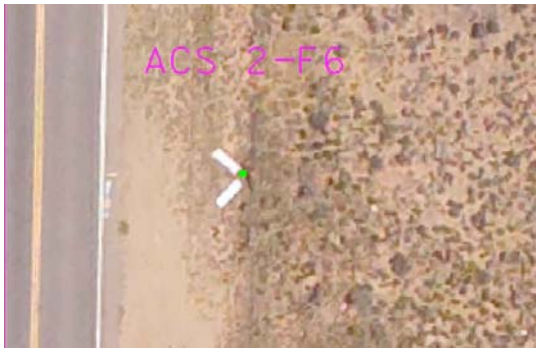

Orthophoto image with lidar-derived point added.

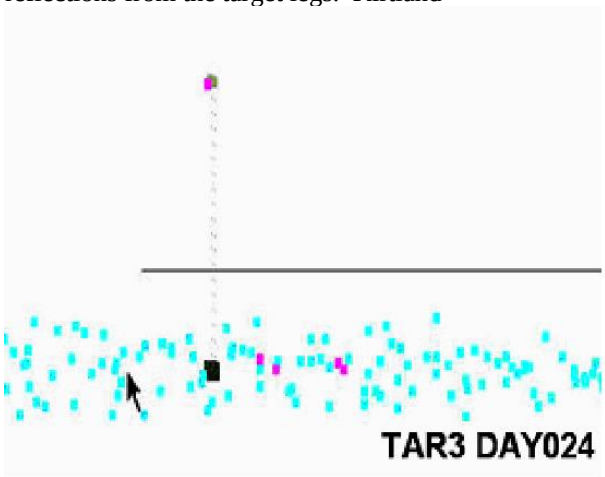

Profile view of lidar points showing reflection from the antenna of the GPS base station and the fiberglass target legs.

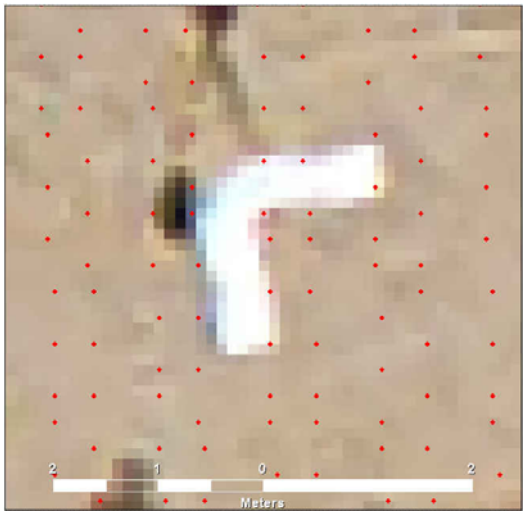

Orthophoto view of the target showing the same lidar points.

At the Kirtland site, the average x and y displacement (dx and dy) for all targets were both 0.08 m. At the Victorville site, the average x and y displacements were 0.03 m and 0.08 m for 300 m lidar flight and 0.06 m and -0.03 m for the 450 m flight. All values are well within the 0.65 m horizontal accuracy specification.

Lidar to Orthophoto Positional Alignment

Lidar to orthophoto positional alignment was evaluated by comparing the locations of features with hard edges such as buildings and pavement in the lidar and orthophoto images. The edges of buildings and pavement were located visually on the orthophotos. In the lidar data, building

edges were located by examining the elevation values of the returns, and edges of pavement were located using the intensity values. The process is illustrated in the figures below:

Figure A-2
Method for Evaluating Lidar Positional Alignment

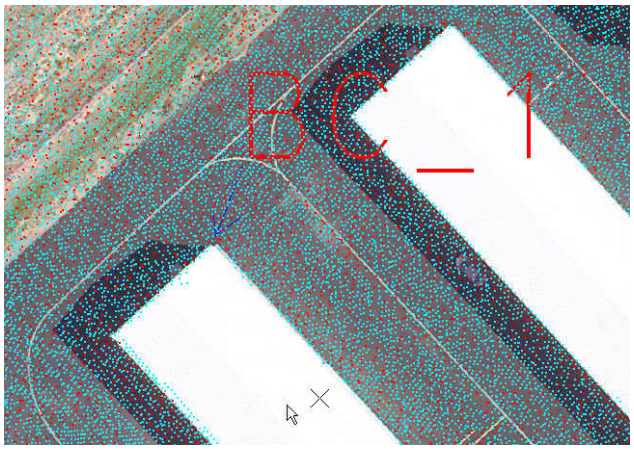

Kirtland site, Double Eagle Airport. Buildings in lidar are identified by elevation values of the lidar returns.

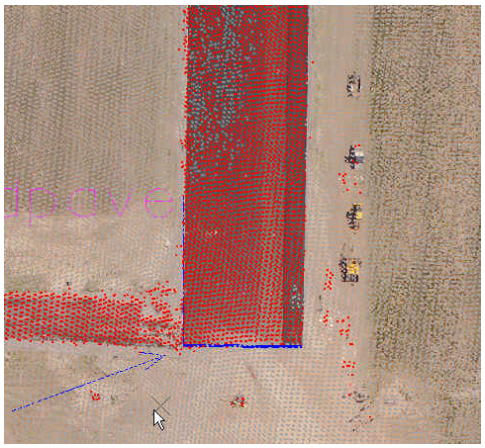

Kirtland site, Double Eagle Airport Runway. Pavement edges in lidar are identified by intensity value.

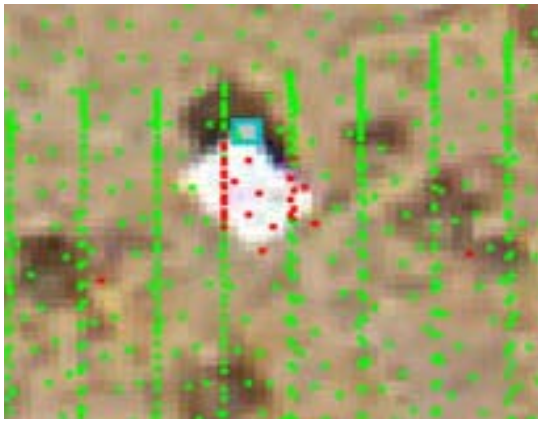

Victorville site, vertical control structure, lidar points classified by elevation.

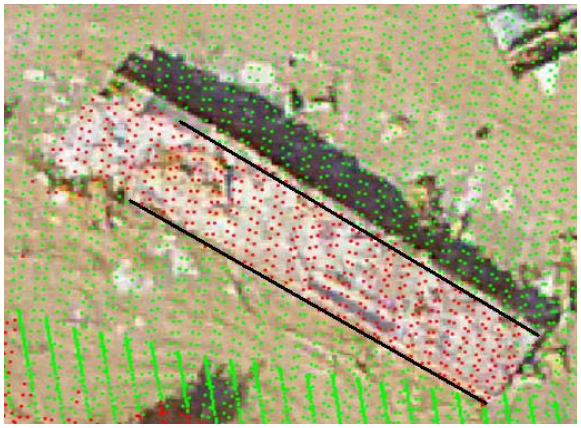

Victorville site, old RV, lidar points classified by elevation.

At the Victorville site, this calculation was more difficult, since the site did not contain buildings or paved roads. The vertical control structures and an abandoned RV were examined. Results from this comparison are considered less reliable than for the Kirtland site. This is due partially to the fact that the vertical control structures are too small to reliably derive a corner location from the lidar data alone. (The example shown is the best case).

Results are shown for the two sites:

	Specification (m)	Average Dx (m)	Average Dy (m)
Kirtland 20 cm pixels	0.40	0.167	0.360
Kirtland 10 cm pixels	0.20	0.137	0.167
Victorville 10 cm pixels	0.20	0.10	0.10

Orthophoto Positional Accuracy

Orthophoto horizontal accuracy was evaluated by deriving the location of the surveyed control points in the orthophoto images, and then comparing these to their surveyed locations. The method is illustrated in the figure below.

Figure A-3
Orthophoto Comparison to Control Points

The red star represents the control point location in the orthophoto; the blue star is its surveyed location. The points are approximately 1 pixel width (10 cm) apart.

The established accuracy specification was 2 pixel widths; all orthophoto data met this specification, as shown below.

	Specification (m)	Maximum offset (m)	Mean offset (m)
Kirtland 20 cm pixels	0.60	0.561	0.210
Kirtland 10 cm pixels	0.30	0.279	0.146
Victorville 10 cm pixels	0.30	0.143	0.072

CONCLUSIONS

Lidar and orthophoto data at both sites met the established positional accuracy specifications.

APPENDIX B

Combining Lidar Data from Multiple Flights

COMBINING LIDAR DATA FROM MULTIPLE FLIGHTS

INTRODUCTION

When lidar data from different flights at the Kirtland site was combined, the resulting surface models showed serious degradation. Features that were clearly shown in the data from individual flights were obscured in the combined data. This effect was particularly pronounced when flights from different altitudes were combined. The cause of this effect has implications for the acquisition of lidar data, including appropriate contract specifications.

DISCUSSION

All lidar data acquisition contracts specify the vertical datum of the output data; normally the datum specified is the North American Vertical Datum of 1988 (NAVD 88). In the case of the Kirtland site, the lidar vendor was requested to deliver each of the four flights as a separate data set, each in NAVD 88. This specification was met.

However, this contract specifications, with adjustment of each individual flight to the contract vertical datum, is not standard industry practice. Rather, standard practice is to choose only one of the flights which will be calibrated to the specified vertical datum, after which data from the rest of the flights is calibrated, not to the vertical datum, but to data from the first flight. It is also more standard practice to deliver only one, combined data set. The contract specification used for the Kirtland site resulted from the decision to deliver the lidar at each elevation as a separate date file. Delivery of the Demonstration Plan appeared to be the most conservative approach and to introduce the fewest additional variables. In fact, this approach illustrated the wisdom of the standard industry practice.

The Kirtland data illustrates the results of specifying that each flight be adjusted only to the project vertical datum. Despite the fact that each flight's data set was correctly calibrated to the vertical datum, and each was well within contract specifications, small errors in the equipment lead to each flight being slightly out of alignment with the next. These slight misalignments create a "blurring" of the resulting ground surface in the combined data set.

Figure B-1
Kirtland Individual and Combined Lidar Data As Delivered

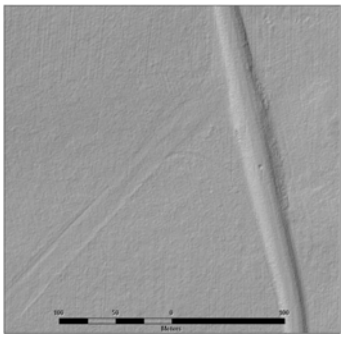

300 m lidar, single flight.

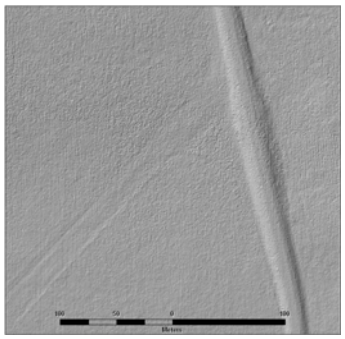

Combined 900 m and 450 m lidar flights.

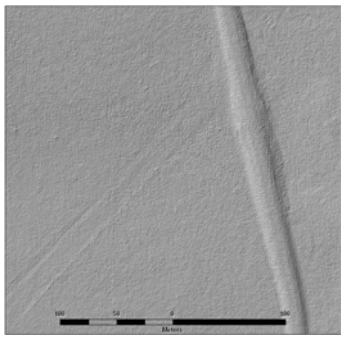

Combined lidar, all flights.

Figure B-2
Kirtland Combined Lidar Data Following Reprocessing

As a test, a small sample of the Kirtland data was reprocessed to achieve the best fit possible between the two data sets. Results were promising, with the reprocessed data yielding a much more useable surface model.

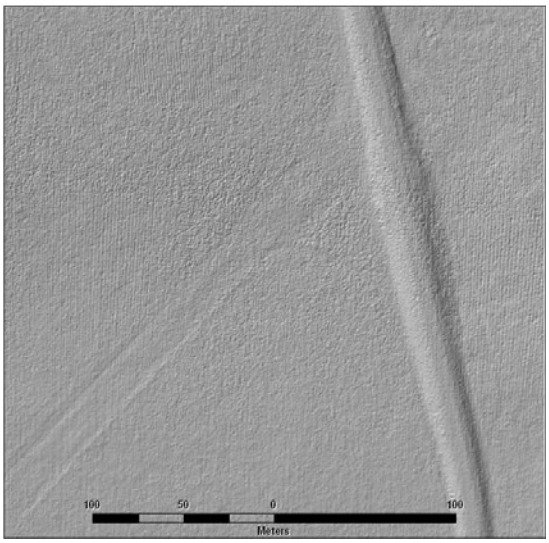

Combined 900 and 450 m lidar flights.

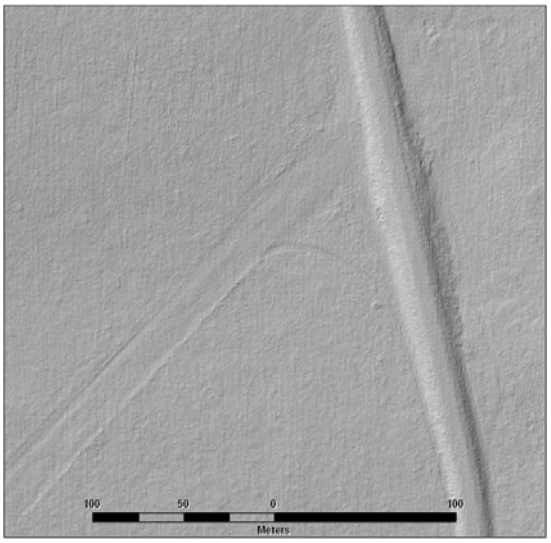

Combined 900 and 450 m lidar, following adjustment of the two flights for best fit.

At the Victorville site, contract specifications were changed. The two flights were delivered as separate data sets, as with the Kirtland data. However, the 900 m flight was calibrated to NAVD 88, and the 450 m flight was adjusted to the best possible fit with the 900 m data set. As a result, the 450 m data was not truly in NAVD 88. However, the two data sets could then be combined

to create a higher-density combined data set that could be used to examine the effects of higher overall point density.

Figure B-3
Victorville Individual and Combined Lidar Data

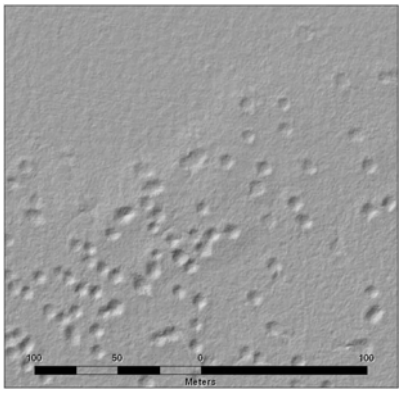

450 m lidar flight.

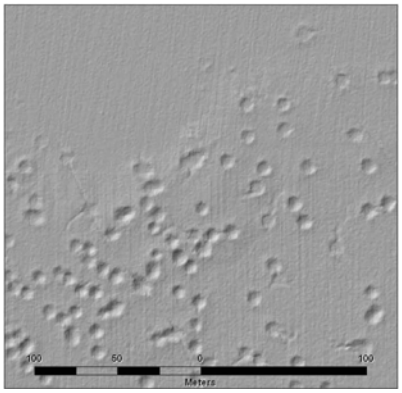

300 m lidar flight.

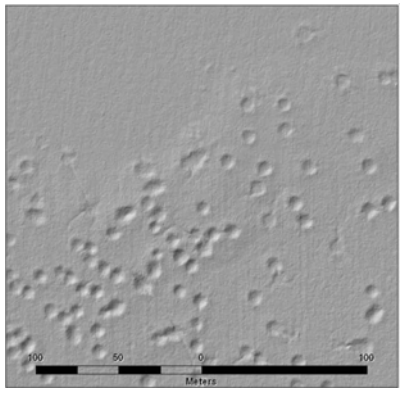

Combined 300 m and 450 m flights.

CONCLUSIONS

In projects where multiple lidar flights will be conducted, acquisition specifications should be written to recognize current industry practice for combining lidar data sets. Contracts should not specify that each individual flight should be independently calibrated to the specified vertical datum. Rather, the vertical datum requirement should be applied to data from one flight, with subsequent data sets adjusted to the first.

APPENDIX C

Variation in Lidar Data Density and Potential Effect on Feature Identification

VARIATION IN LIDAR DATA DENSITY AND POTENTIAL EFFECT ON FEATURE DETECTION

INTRODUCTION

Lidar data density is generally expressed as either points per square meter or average spacing between lidar points, averaged over the entire site. In practice, lidar point density was found to vary considerably over the site depending on factors such as flight line overlap and wind conditions. These variations probably do not affect the ability of lidar to detect large features such as bombing targets, but may affect the ability to detect smaller objects, particularly those at or below 1 meter in size. Measures of overall density remain useful as general indicators of the effectiveness of lidar. However, data density specifications may need to be adjusted where detecting small objects is a priority.

DISCUSSION

Lidar data density is affected by at least five operational factors, including the following:

- flight altitude,
- flight speed,
- flight line overlap,
- laser pulse rate, and
- mirror rotation speed.

Data density is also affected by at least three site factors:
density of vegetation cover,
steepness of terrain, and
wind speed during data collection.

Finally, the density of lidar points used to create the ground surface model is very substantially affected by how lidar points are classified as ground or non-ground reflections.

At both demonstration sites, the intention of the demonstration was to vary only flight altitude, as a means to vary the overall lidar point density. Other parameters were held as constant as possible, including flight speed, flight line overlap, laser pulse rate and mirror rotation speed. Slopes on the site did not vary sufficiently to affect data density. Vegetation on the site was relatively sparse and also relatively constant throughout the site, and it was assumed that vegetation classification rates would be relatively constant.

Nevertheless, flight line overlap and vegetation classification had a very significant impact on lidar point density. In some cases these factors had a much larger impacts than flight altitude in determining lidar data density.

Lidar data densities achieved for the four Kirtland flights and two Victorville flights are given in the table below. These are overall densities, derived by dividing the number of lidar points by the area of the site, for the entire lidar point data set before classification as ground and non-ground returns.

Table C-1
Overall Lidar Data Densities

Demonstration Site	Flight	Point density (pts/m^2)
Kirtland	900 m North Block	1.4
	900 m South Block	1.6
	450 m north block	5.2
	450 m south block	4.1
	300 m east-west north block	5.2
	300 m north-south north block	6.5
	300 m flight 1 south block	5.9
	300 m flight 2 south block	6.1
Victorville	450 m flight	4.8
	300 m flight	6.4

When examined more closely, lidar point density was found to vary considerably within each flight. The following figures give a graphical illustration of some of the ways that lidar point density varied. In all of the following figures, darker colors indicate higher point density, and the fine blue lines indicate the lidar flight lines.

Figure C-1
Kirtland Site Lidar Point Density Maps – All Lidar Points

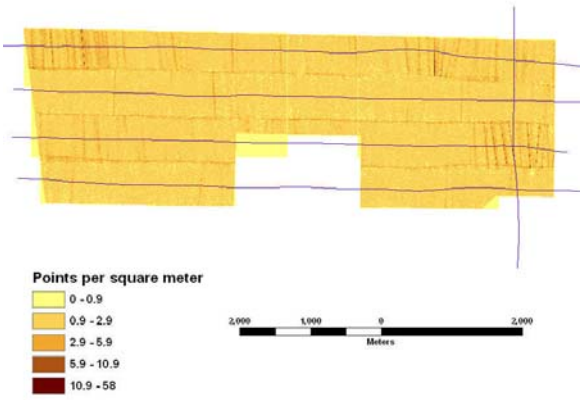

900 m north block, all points.

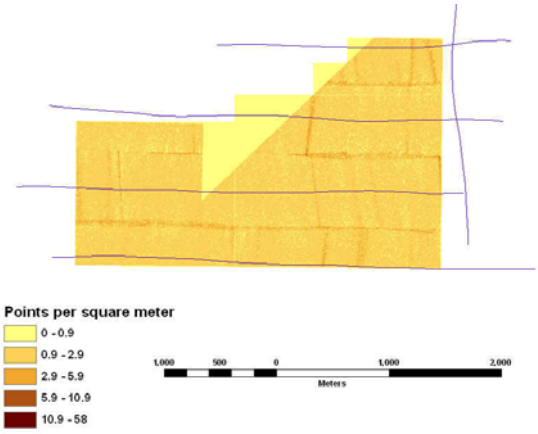

900 m south block, all points.

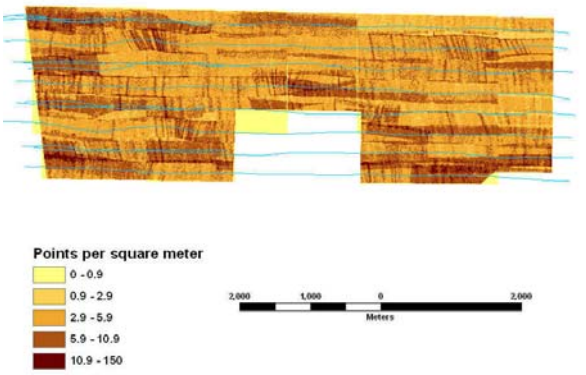

450 m north block, all points.

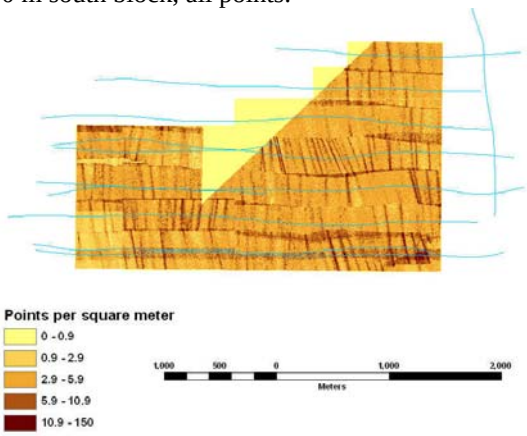

450 m south block, all points.

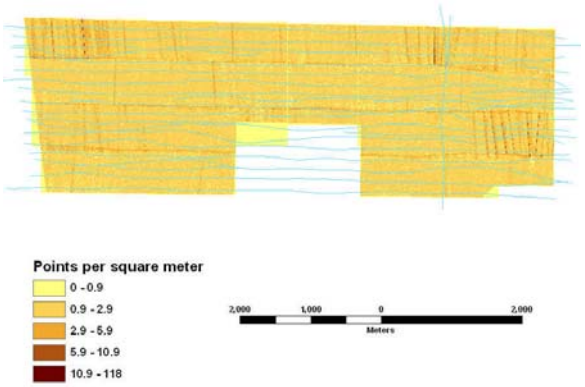

300 m north block East-West flight, all points.

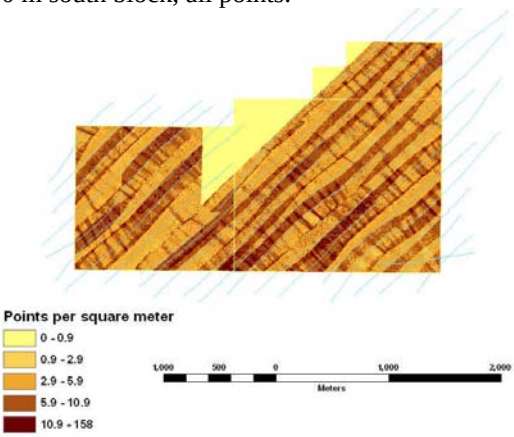

300 m south block, Flight 1, all points.

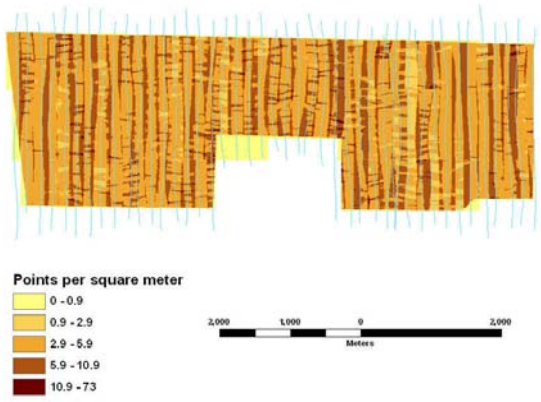

300 m north block North-South flight, all points.

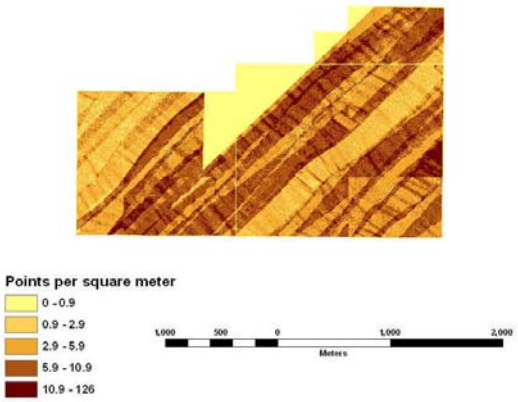

300 m south block, Flight 2, all points.

The images above are for all lidar points regardless of classification as ground or non-ground reflections. Once the points classified as vegetation are removed, both overall point density and the variability of the point density is reduced, as shown in the following figures.

Figure C-2
Kirtland Site Lidar Point Density Maps – Ground Returns Only

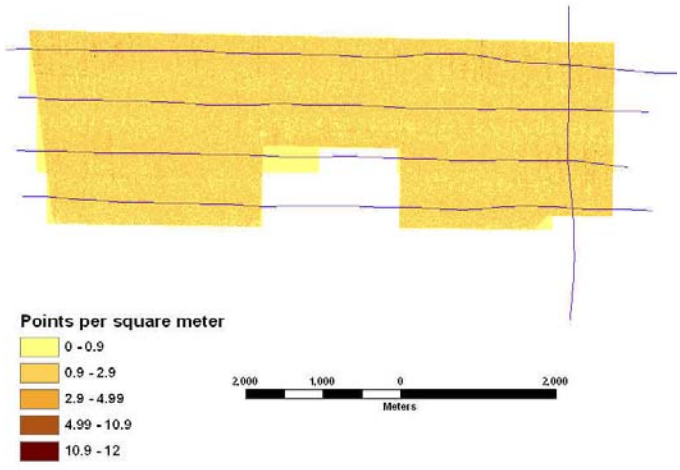

900 m north block, ground points.

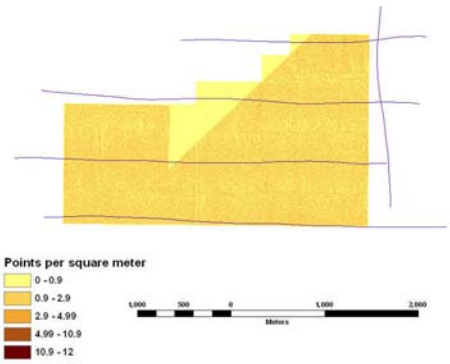

900 m south block, ground points.

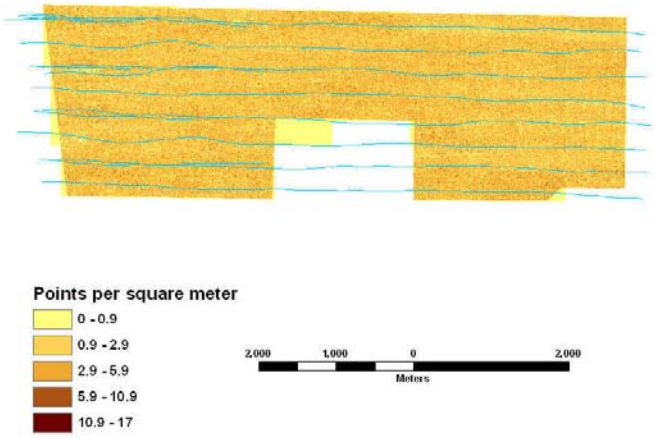

450 m north block, ground points.

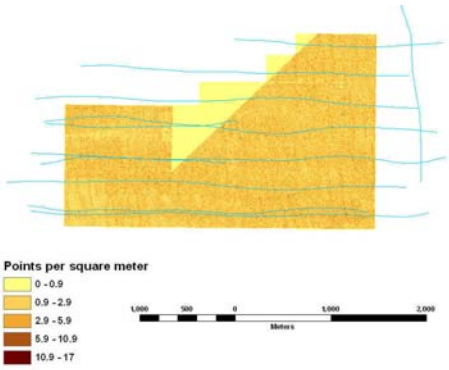

450 m south block, ground points.

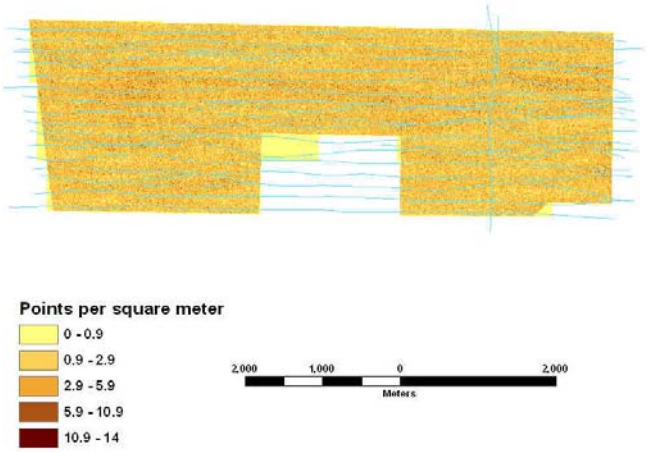

300 m north block EW, ground points.

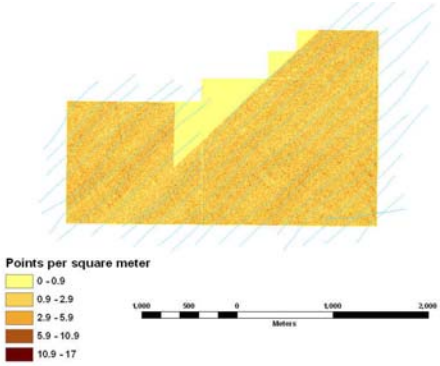

300 m south block, Flight 1, ground points.

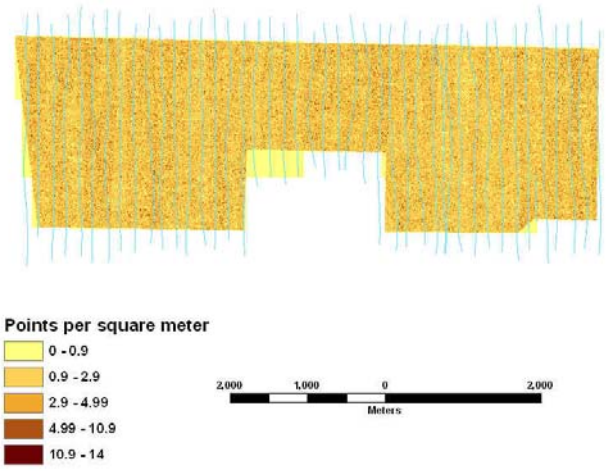

300 m north block NS, ground points.

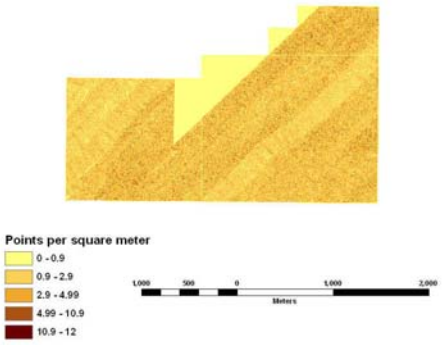

300 m south block F2, ground points.

The following figures present close-up views of the point density maps for one of the 300 meter lidar data sets, including images for both all lidar points and ground points only.

These results illustrate one limitation of measuring lidar point density for the site as a whole: some areas of the site have a higher point density than specified, while other areas have a lower density.

Figure C-3
Lidar Point Density Maps – Detailed Views

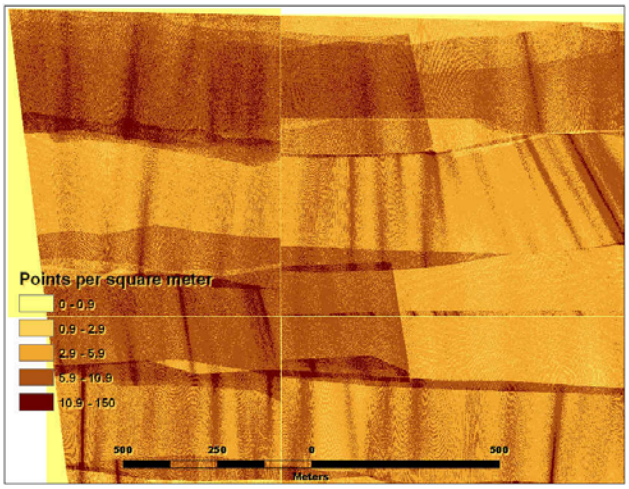

450 m all points, scale 1-6,000.

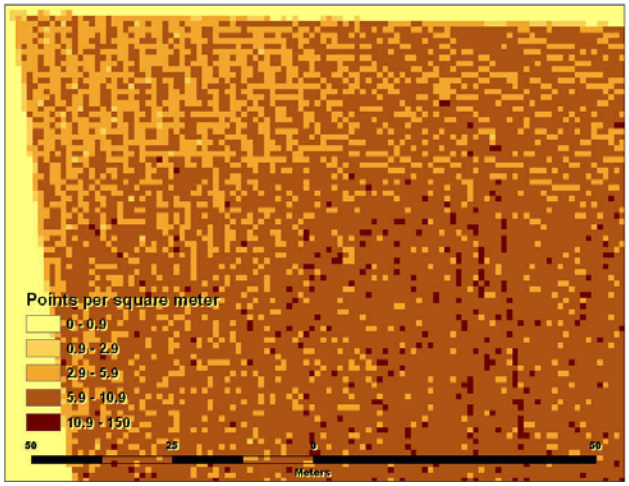

450 m all points, scale: 1-400.

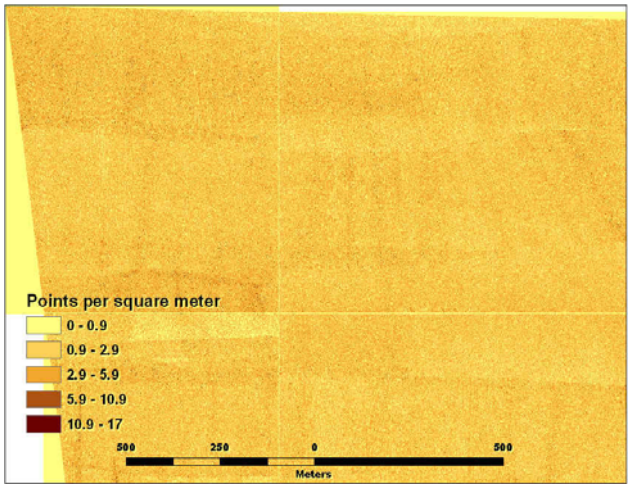

300 m east-west, ground points, scale 1-6,000.

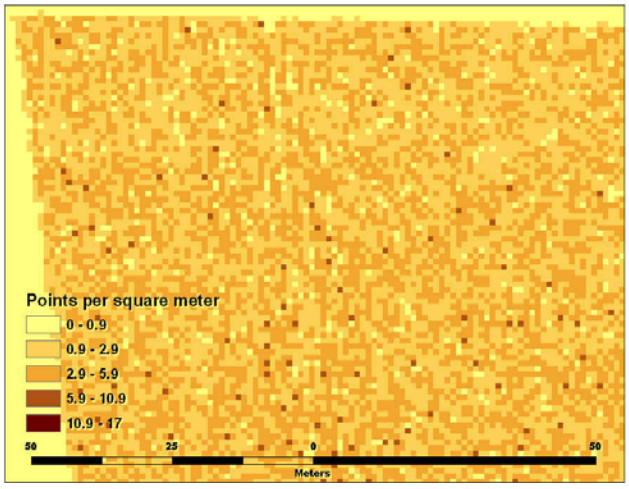

300 m east-west, ground points, scale: 1-400.

Similar results were obtained for the Victorville site, as shown below:

Figure C-4
Victorville Site Data Density Maps

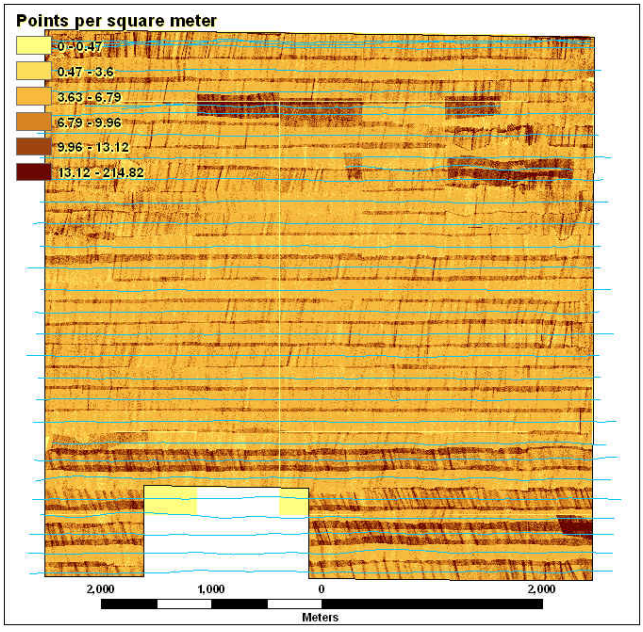

300 m all points.

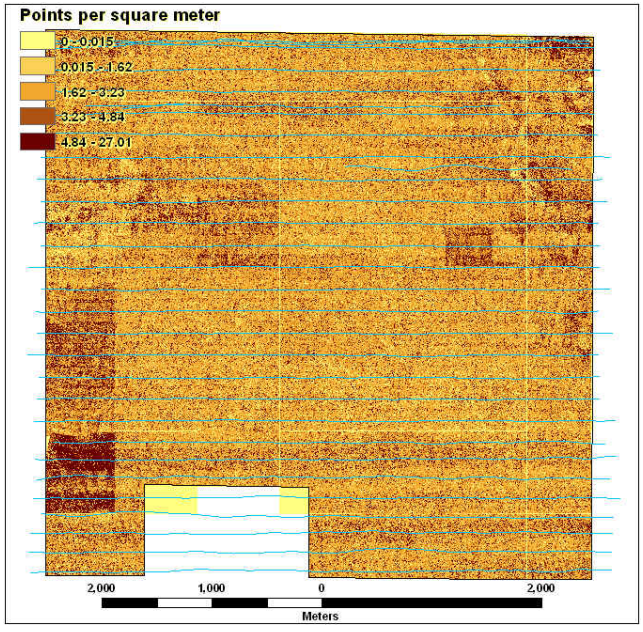

300 m ground points only.

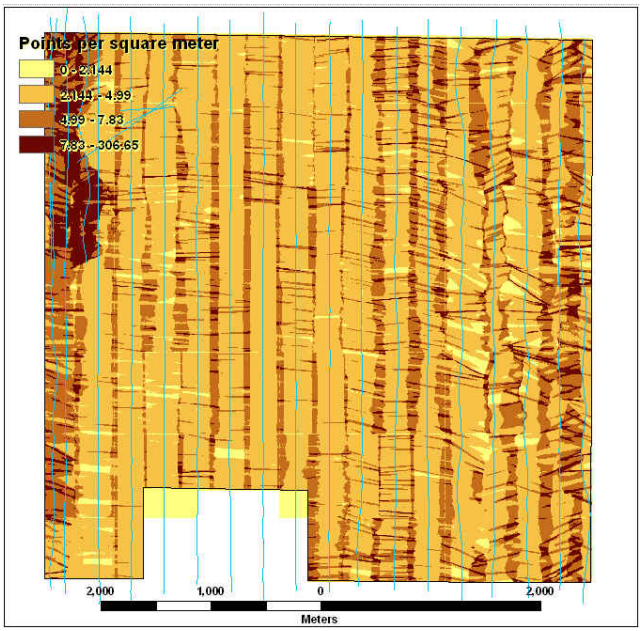

450 m all points.

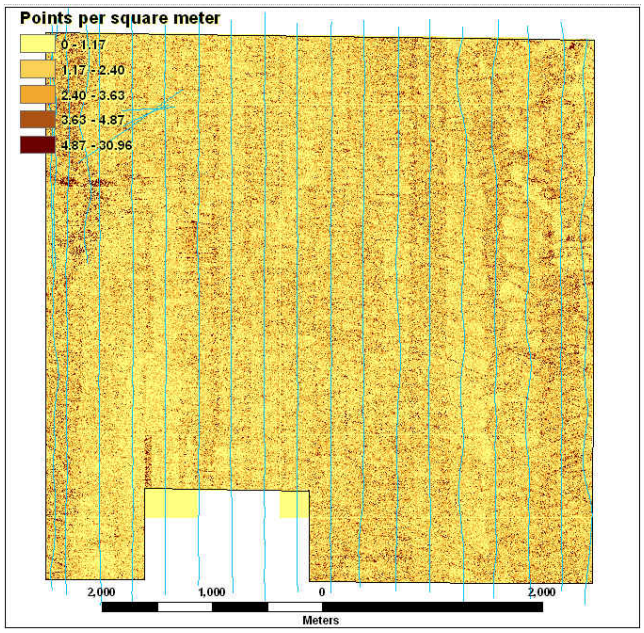

450 m ground points only.

All of these figures show that lidar point density in the overall lidar data set is highly influenced by flight line overlap. Point density also varies along the flight line, with bands of higher and lower point density. These bands are the result of flight conditions such as wind gusts or sudden changes in pitch of the aircraft, which result in wider or narrower spacing between the lines of lidar points. This effect is particularly pronounced in the all points data set.

DATA DENSITY AND POINT CLASSIFICATION

Data density variation appears to fall significantly as vegetation is removed, even for these two relatively sparsely-vegetated sites. This result was unexpected: vegetation conditions were relatively uniform on both sites, so variation in data density caused by flight line overlap should theoretically be the same for either all points or ground points. This effect results from the methods used to classify points.

Classification of lidar points as ground or non-ground is performed using automated algorithms followed by operator inspection and editing. Standard point classification methods are aimed at creating an accurate ground surface model free of vegetation artifacts. As such, they are biased towards vegetation removal. The following table shows the percentages of points classified as ground and non-ground for the four lidar flights at the Kirtland demonstration site.

Table C-2
Percentages, Ground and Non-Ground Lidar Returns

Lidar Flight	Total Points	Ground Points	Ground %	Non-Ground Points	Non-Ground %
900 m	31,212,625	22,503,996	72.1%	8,708,629	27.9%
450 n	102,136,027	42,849,155	42.0%	59,286,872	58.0%
300 m NS and SB F2	110,320,328	42,863,611	38.9%	67,456,717	61.1%
300 m EW and SB F1	129,953,682	45,906,149	35.3%	84,047,533	64.7%

This table shows that as the number of overall lidar points increased, the percentage classified as ground points decreased. That is, part of the increased overall data density was lost from the ground surface model. This finding is unexpected since vegetation was identical for each flight. In order to examine this phenomenon in more detail, ten sample blocks were selected, each 25 x 25 m, covering a range of data densities. The sample blocks are shown in the following figure.

Figure C-5
Data Density Analysis Blocks

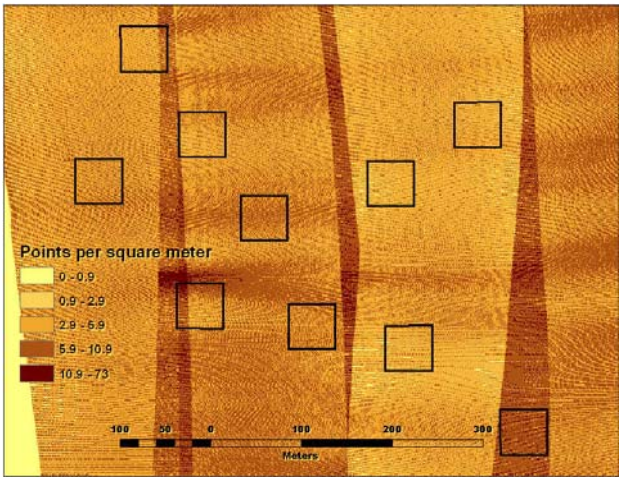

Point density test blocks with 300 m lidar point density map.

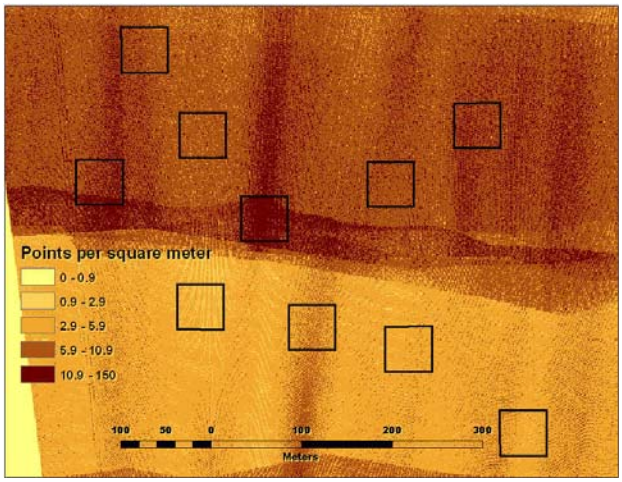

Point density test blocks with 450 m lidar point density map.

For each sample block, the total number of lidar points was calculated, along with the percentage of ground and non-ground returns. Similar calculations were performed for each of the four lidar flights. The data showed a strong correlation between overall data density (total number of points) and percentage of points classified as non-ground. As the total number of points increased, the percentage of non-ground points rose from around 30% to around 80%.

Figure C-6
Lidar Point Classification vs. Point Density

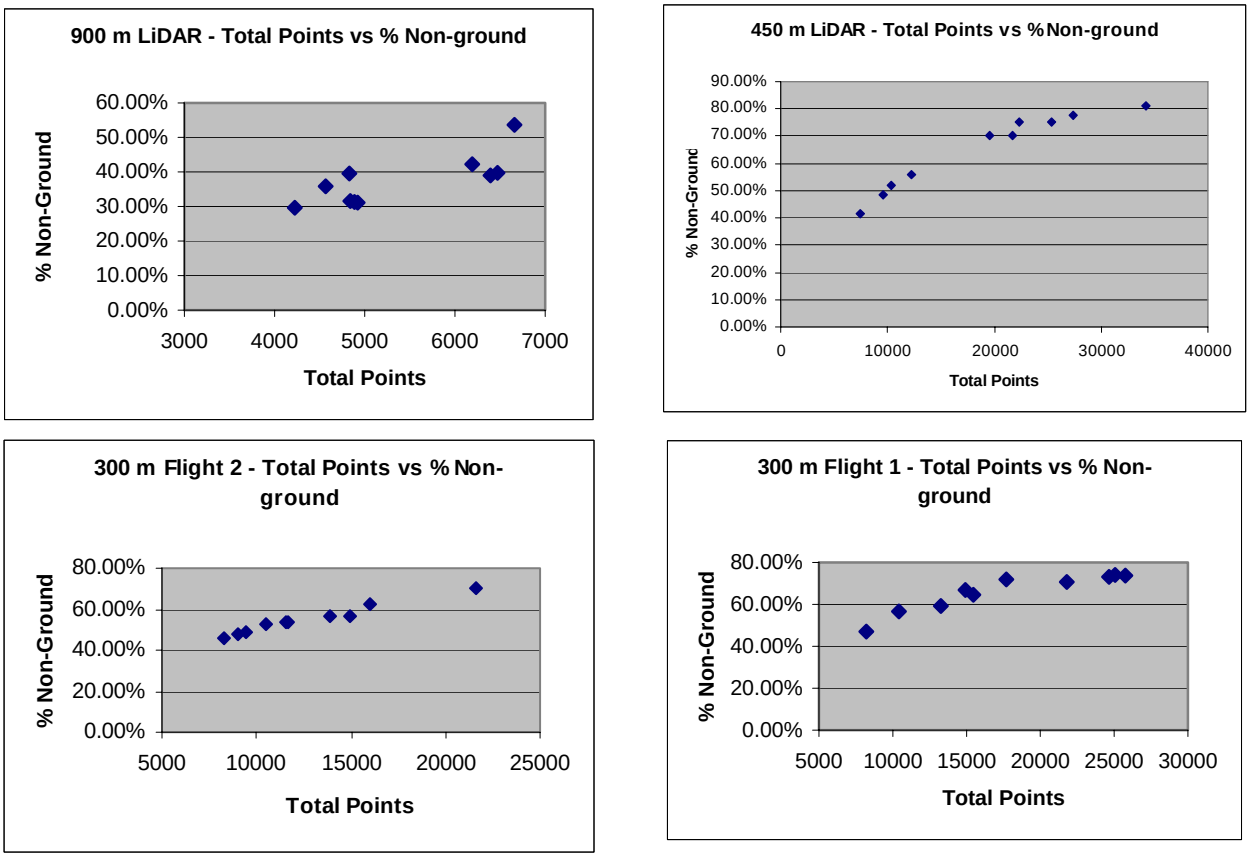

This result is significant since acquiring more lidar density raises the project costs. These results appear to indicate that at least a significant portion of the additional lidar points being acquired is not reaching the ground surface models.

The most likely explanation for this effect is based on the fact that, as shown in the point density maps, the highest areas of point density occur where flight lines overlap. In these areas, lidar points from the different flight lines are always very slightly misaligned, (even when the data is well within the vertical accuracy specification), with one data set slightly below and the other slightly above each other. This causes the surface in this overlap area to be "rough", and it is this roughness that the automated point classification algorithm uses as an indicator of non-ground points such as low vegetation. This phenomenon deserves further investigation.

LIDAR DATA DENSITY DISTRIBUTION AND FEATURE DETECTION

Detecting MEC features using lidar requires that the lidar points be dense enough to reflect from both the feature and its surroundings. Variations in lidar point density should affect the size of features that can reliably be detected.

To examine this variation more closely, the lidar density maps shown above were queried to determine the number of lidar points in each square meter of the study area. The analysis was performed for both the entire point set and for ground returns only. Results were as follows:

Table C-3
Kirtland lidar Data Density Distribution – All Points

All values are in points per square meter.					
Flight	**Min**	**Max**	**Mean**	**Standard Deviation**	**% Value = 0**
900 m all points	0	58	1.43	0.89	24.28
450 m all points	0	150	4.68	2.74	0.19
300 m north block east-west all points	0	118	6.22	3.25	0.14
300 m north block north-south all points	0	73	4.98	2.57	0.36
300 m south block flight 1 all points	0	158	5.34	3.20	0.12
300 m south block flight 2 all points	0	126	5.49	3.70	1.26

Table C-4
Kirtland lidar Data Density Distribution – Ground Points Only

All values are in points per square meter.					
Flight	**Min**	**Max**	**Mean**	**Standard Deviation**	**% Value = 0**
900 m ground points	0	12	1.03	0.72	38.46
450 m ground points	0	17	1.98	1.23	11.10
300 m north block east-west ground points	0	14	2.21	1.38	10.20
300 m north block north-south ground points	0	14	2.03	1.38	12.59
300 m south block flight 1 ground points	0	17	1.86	1.32	14.51
300 m north block flight 2 ground points	0	12	1.83	1.35	16.62

Table C-5
Victorville lidar Data Density Distribution – All Points

All values are in points per square meter.					
Flight	**Min**	**Max**	**Mean**	**Standard Deviation**	**% Value = 0**
450 m all points	0	346	4.48	2.80	1.60%
300 m all points	0	220	6.02	2.96	1.54%

Table C-6
Victorville lidar Data Density Distribution – Ground Points Only

All values are in points per square meter.					
Flight	**Min**	**Max**	**Mean**	**Standard Deviation**	**% Value = 0**
450 m ground points	0	42	1.91	1.21	10.87%
300 m ground points	0	28	2.59	1.56	7.89%

These tables illustrate that even at the highest overall data densities achieved; there are nevertheless one-meter grid cells where there are no lidar points. For ground points – the data most typically used to create surface models - the percentage of one-meter cells with no lidar points ranges from 7.89% to 38.46%. This is a potentially significant finding since one use of lidar is to detect small features in order to delineate MRS boundaries. An examination of the actual lidar point patterns on the ground demonstrates that in some circumstances, objects in the 1.0 – 1.5 m range could easily be missed in the 900 m flight.

The following figures show the Kirtland test crater area with surface models created from the various lidar data sets. Surfaces were created using both the full lidar data set and the points classified as ground reflections. This approach was taken in order to determine whether vegetation removal significantly affected the ability of the lidar data to distinguish the craters. Darker green colors represent lower elevations.

Figure C-7
Test Craters and lidar Data Density

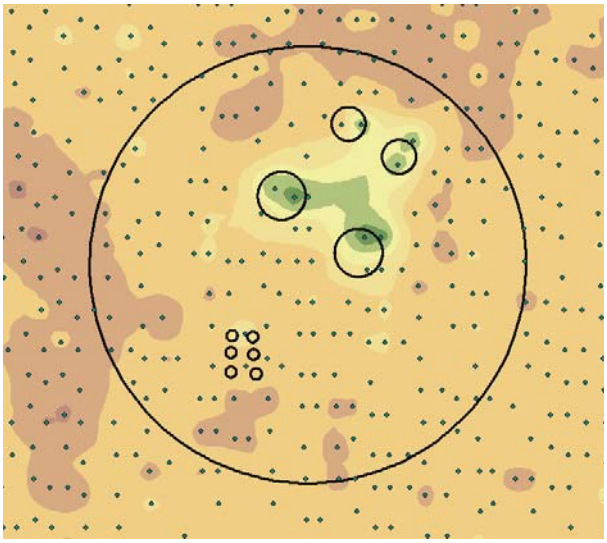

900 m lidar, ground points only. Darker green surface indicates depressions.

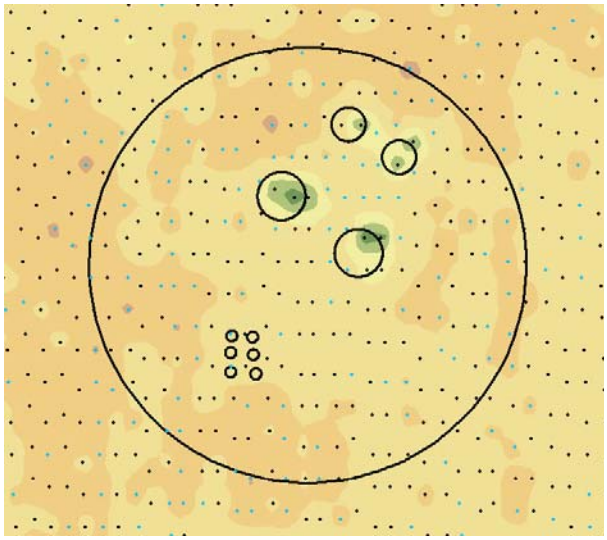

900 m lidar, ground (black) and non-ground (blue) points.

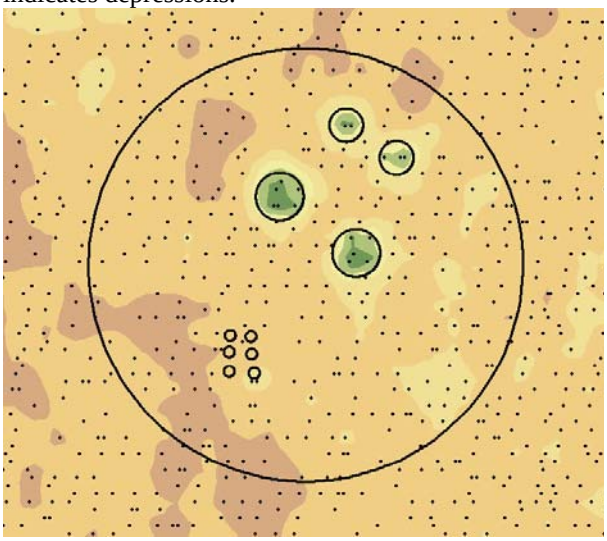

450 m lidar, ground points only.

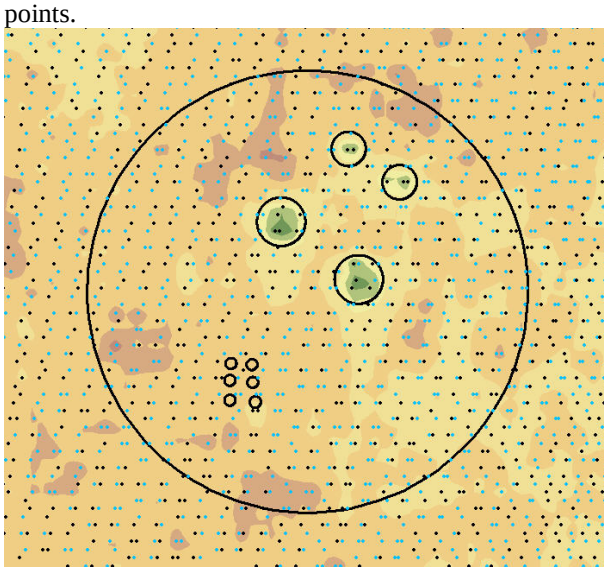

450 m lidar, ground (black) and non-ground (blue) points.

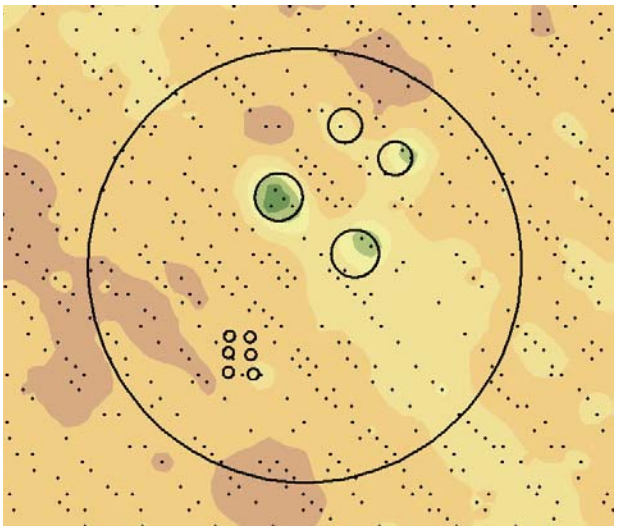

300 m lidar flight 1, ground points only.

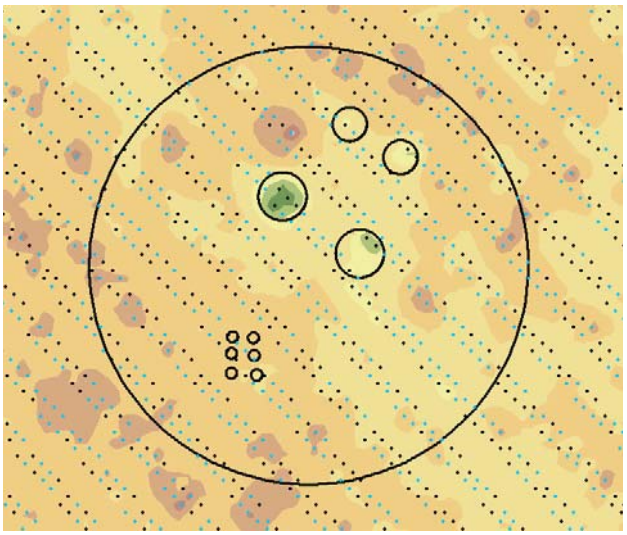

300 m lidar flight 1, ground (black) and non-ground (blue) points.

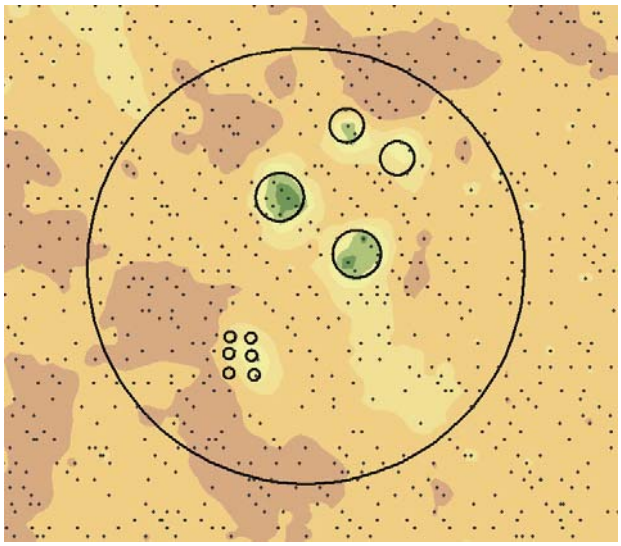

300 m lidar flight 2, ground points only.

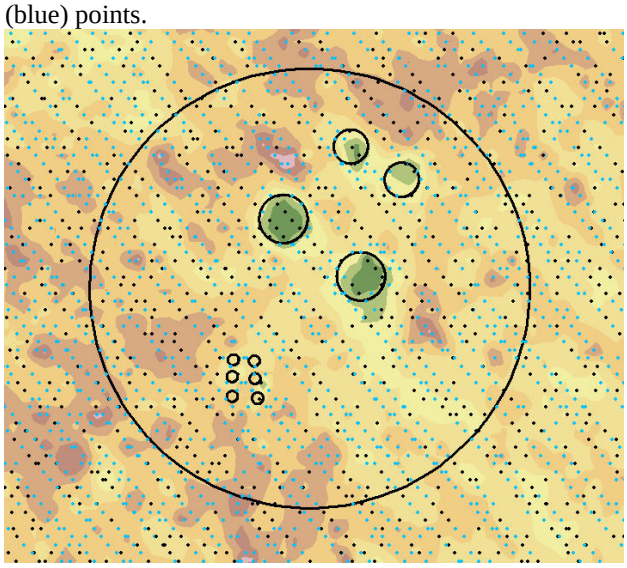

300 m lidar flight 2, ground (black) and non-ground (blue) points.

These figures illustrate several points:

- One of the 1.0 meter craters was missed completely using ground returns from both 300 m flights, despite the fact that these were the flights with the highest overall point densities.

- Data density in the test crater area was higher for the 450 m flight than for either 300 m flight, even though overall data density for the 450 m flight was lower.

- The 1.5 m craters were detected with roughly equal success, at all of the data densities tested. Nevertheless, there are areas in the 900 m and both 300 m ground point sets where a 1.5 m crater would not receive any lidar points.

CONCLUSIONS

Measures of overall lidar density such as points per square meter or average distance between points do not capture the actual variations of data density observed at the demonstration sites. Observed variation resulted primarily from flight line overlap and wind conditions, and was often a more important factor than flight altitude in affecting density for a particular area of the site.

Point classification methods had a strong effect on lidar density of the ground surface model. In effect, much of the extra point density achieved in the flight line overlap areas was removed by the point classification methods used.
Variations in lidar density did not affect the detection of the 1.5 m test craters at the Kirtland site, but three of the four lidar data sets nevertheless contained areas where a crater of this size could be missed. Detection of the 1.0 m test craters was affected by lidar density variations, and the 0.32 m craters were not detected at any of the densities tested.

APPENDIX D

GIS-Based Methods for Creating Ground Surface Models from Lidar Points

GIS-BASED METHODS FOR CREATING GROUND SURFACE MODELS FROM LIDAR POINTS

INTRODUCTION

Surface models can be created from lidar points in a variety of ways. All involve some level of interpolation from the random lidar points to a regularly-spaced array that can be analyzed using GIS methods. A limited comparison of some standard methods of creating surface models showed that the methods used to process the demonstration data gave the clearest definition of the Kirtland area test craters. However, the difference was not large, and the craters were visible using most of the methods tested.

DISCUSSION

There are two general approaches to creation of surface models, all result in a regularly-spaced grid with each cell assigned an elevation value.

The first approach is to interpolate the surface model directly from the lidar points. There are a variety of mathematical approaches to such interpolation. These include the following:

- **Inverse Distance Weighting** (IDW) interpolation determines cell values using a linearly weighted combination of a set of sample points. The weight is a function of inverse distance, and the surface being interpolated should be that of a locationally dependent variable. IDW interpolation allows the user to control the effect of known points on the interpolated values, based upon their distance from the output point. The characteristics of the interpolated surface can also be controlled by limiting the input points used to calculate each interpolated point. The input can be limited by the number of sample points to be used, or by a radius within which there are all points to be used in the calculation of the interpolated points.

- **Kriging** is an advanced geostatistical procedure that generates an estimated surface from a scattered set of points with z values. Kriging is based on a regionalized variable theory that assumes that the spatial variation in the phenomenon represented by the z values is statistically homogeneous throughout the surface (i.e., the same pattern of variation can be observed at all locations on the surface). This hypothesis of spatial homogeneity is fundamental to the regionalized variable theory.

- **Splining** performs a two-dimensional minimum curvature spline interpolation on a point data set resulting in a smooth surface that passes exactly through the input points. This basic minimum-curvature technique is also referred to as thin plate interpolation. It ensures a smooth (continuous and differentiable) surface together

with continuous first-derivative surfaces. Rapid changes in gradient or slope (the first derivative) may occur in the vicinity of the data points; hence this model is not suitable for estimating second derivative (curvature).

The second approach is to create a Triangualted Irregular Network (TIN) using every individual lidar point. The TIN is then used to create the surface model, again using one of the interpolation methods described above. Either approach can be employed using the ground points only or both the ground and vegetation points.

Both of the above approaches produce good surfaces, with each method having its own particular advantages and shortcomings. Every method uses one technique or other to interpolate (or guess at) the surface between the lidar points. However, by creating a TIN from the points before creating the grid surface model, we assure that each individual point is represented accurately in the final product, and in the TIN itself which can be examined in particular cases. Consequently, for this demonstration, the TIN method was used for all data sets.

A test of these alternative methods was conducted using the data from the Kirtland site. The points in the area surrounding the test craters was extracted and used to create a series of surfaces using the available methods.

Figure D-1
Surface Model Examples

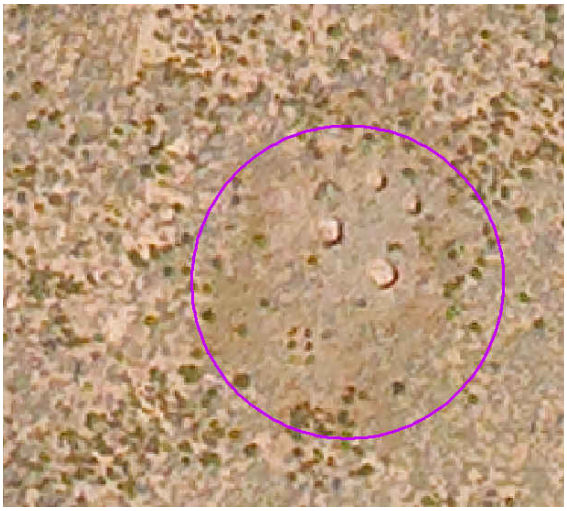

10 m pixel orthophoto.

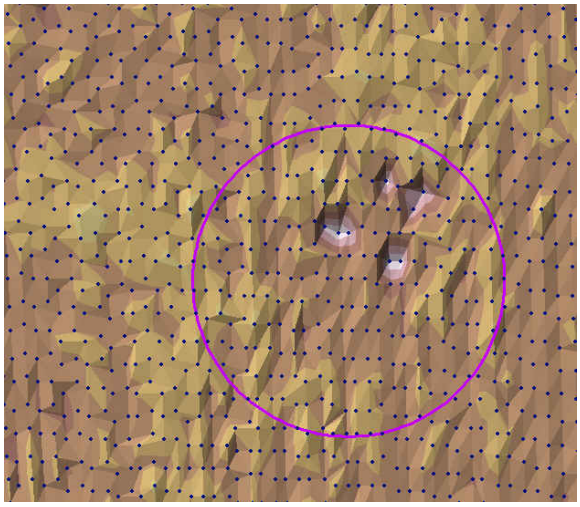

900 m TIN.

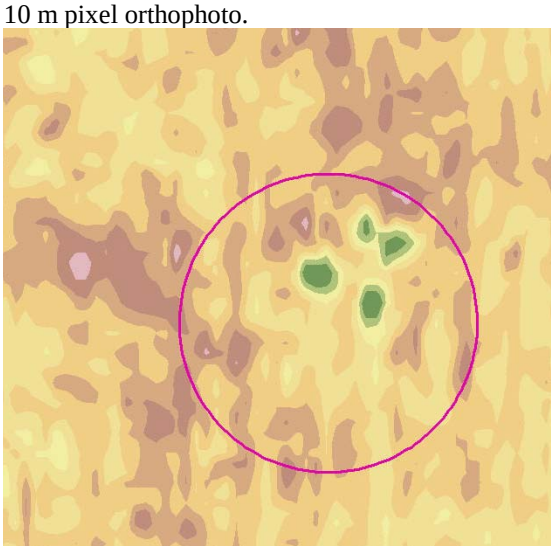

900 m TIN-derived IDW.

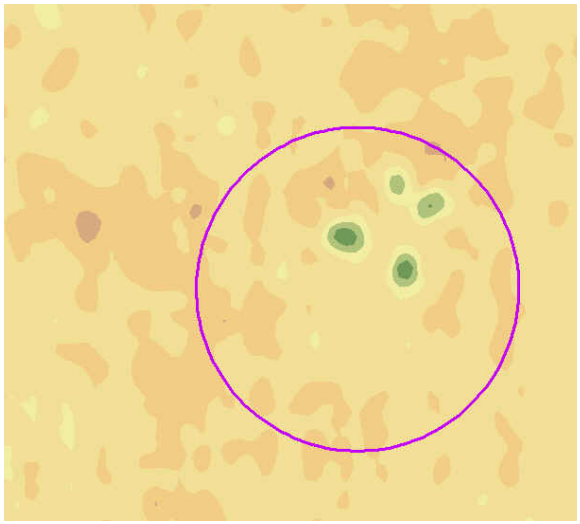

900 m spline.

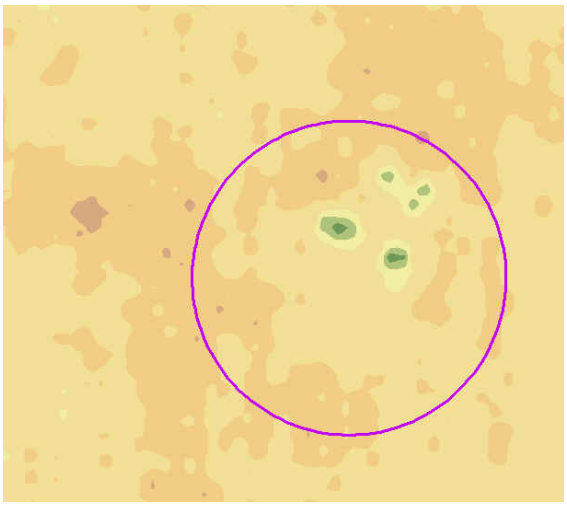

900 m IDW.

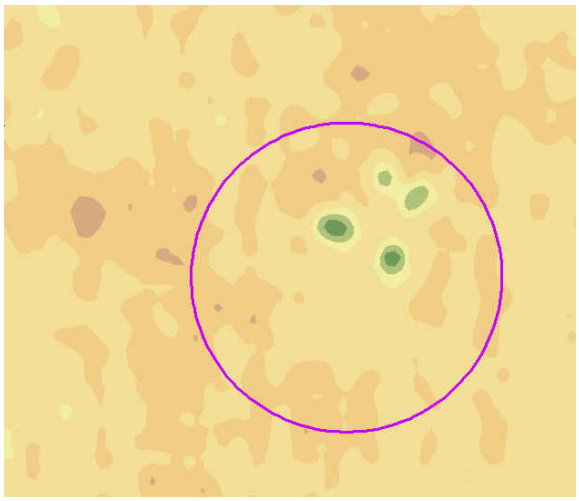

900 m kriging.

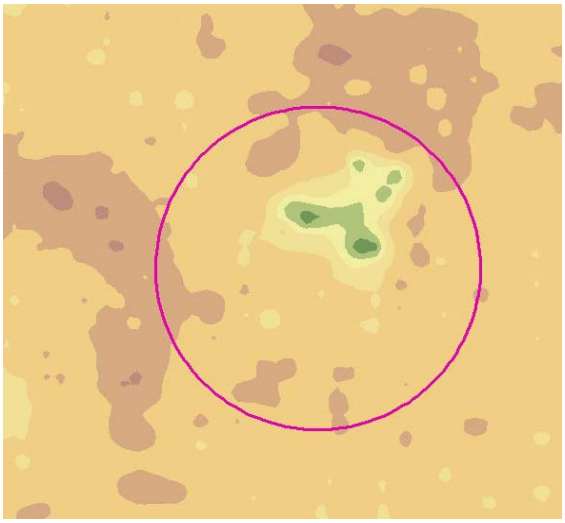

450 m TIN-derived IDW.

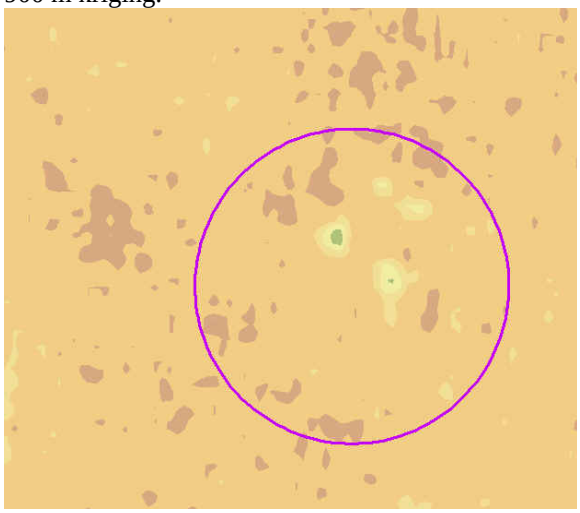

450 m spline.

450 m IDW.

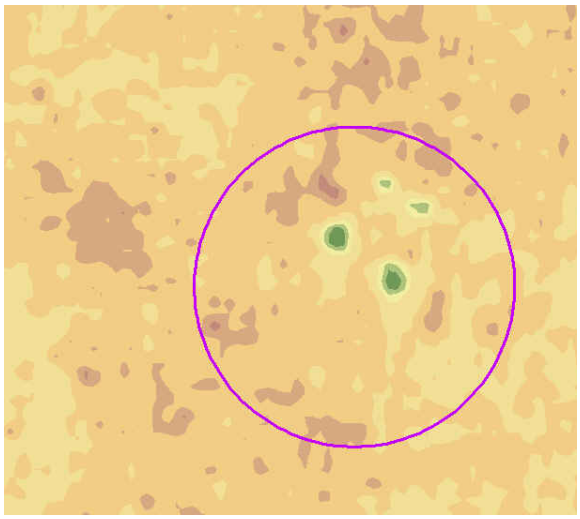

450 m kriging.

These figures illustrate that the TIN-derived surface models give a slightly more clear representation of the 1.5 and 1.0 m test craters. However, all methods showed the presence of these four test craters.

CONCLUSIONS

Lidar surface interpolation methods tested appeared to have a weak effect on feature detection, with the TIN-to-surface model method used to process the demonstration data yielding the best results. However, the difference between the methods was not pronounced.

APPENDIX E

Automation of Lidar Data Processing in the ESRI GIS Environment

AUTOMATION OF LIDAR DATA PROCESSING IN THE ESRI GIS ENVIRONMENT

INTRODUCTION

Many standard lidar data processing steps can be successfully automated. This is important since lidar data sets are very large, often involving many hundreds of data files, all of which are processed using essentially the same steps. Automation, when successful, can reduce costs and increase the reliability of the resulting products. For this demonstration, all automation was accomplished using ESRI's ArcGIS program. This software was chosen because it is in wide use by federal land managers who may use lidar data.

DISCUSSION

ArcGIS provides several avenues for process automation, including the following:

- Arc Macro Language (AML). AML is a scripting language developed for the ArcInfo Workstation environment. It is used to automate data processing and analysis tasks, the creation of complex maps, and to develop custom interfaces to aid user with various tasks such as data creation, editing and analysis. .It is a robust, full-featured programming language that can be used to automate the commands that can be used at any of the ArcInfo command line prompts (i.e., ARC:, ARCEDIT:, ARCPLOT:).Its main disadvantage is that any non 3D spatial data processing must be done using the antiquated ArcInfo coverage format. Only in some very limited situations can ArcInfo shapefiles be used, and ArcGIS feature classes and geodatabases cannot be used at all. Another disadvantage is that the very steep learning curve required to become proficient in AML. Even though it is based on standard programming concepts, AML is a proprietary language unique to ArcInfo Workstation and is not easy to learn.

- Visual Basic. ESRI has written a library of programming objects called ArcObjects that allows the programmer to develop powerful applications relatively quickly using the very popular Visual Basic for Applications (VBA) programming language that comes bundled with ArcGIS. ArcObjects can also be used with the Visual Studio .NET languages, VB.NET, C++.NET and C#.NET. Applications written in VBA must be run from an ArcGIS application like ArcMap, ArcCatalog or ArcScene while Visual Studio.NET applications can be run independently of ArcGIS though access to the ArcGIS license server is still required.

- Python. Python is an open source, object oriented, programming language developed to handle the kind of tasks normally given to scripting languages like PERL, Ruby or

Tcl but without the steep learning curve usually associated with many powerful object oriented languages. ESRI has written its Geoprocessing object specifically to be used with Python. Python is a relatively easy language to learn, and ESRI also provides some pre-designed user interfaces that custom Python scripts can be linked to. Unfortunately, ESRI has made only the Geoprocessing object, and not all of its ArcObjects collection, available to Python developers. In order to use ESRI's more extensive ArcObjects library, the developer must use VBA or one of the .NET programming languages.

For this demonstration, automation was carried out using Python. The decision to use Python was based on its ease of use, combined with the need to develop the automation scripts quickly and start the processing of the raw lidar data as soon as possible. AML scripts had already been developed to automate lidar data processing, however the conversion to Python eliminated the need to convert the lidar data sets to coverages. Python was used to create a suite of tools that handles the processing of the lidar files delivered by the vendor, starting from the creation of the initial point shapefiles and continuing through the final surface models and data analysis. The processing scripts were designed to handle batch processing of input data files, which required that a consistent naming convention be established and followed input data.

While Python was the approach taken, automation results and process steps would have been essentially the same regardless of the scripting approach chosen.

1. The first step was to create point shapefiles from the ASCII files containing the lidar points in ArcGIS.

2. The second step was to generate a continuous surface model TINs using each point shapefile as an input.

3. The third step was to create DEMs, or surface model grids, from each of the TINs. For both Victorville and Kirtland, a 1 foot cell size was used for the DEMs as the highest resolution the lidar data would support.

These three steps were run as separate scripts. There would be no barrier to combining all three processes into one script. However, running each script separately allowed for QA/QC inspection between steps. This was significant since each processing step was relatively time-consuming, and it was important to catch any errors in the data at the earliest point possible.

APPENDIX F

Analytical Methods Supporting Experimental Design

ANALYTICAL METHODS SUPPORTING THE EXPERIMENTAL DESIGN

Analytical methods appropriate to lidar and orthophoto collection include calculations of target lidar point density, orthophoto pixel size, and along-flight-line swath width. Formulas for these calculations are given below.

Lidar point density. Point density is calculated using the following formula:
Pt Density = Pulse Rate / (Forward Flying Speed * Swath Width)
= 50 000 / (20 * 204)
= 12.25 shots/m

Pixel size. Pixel size is calculated using the following formula:
Pixel size = (Altitude * CCD Grid Size) / Focal Length
= (700 (m) * 0.000008 (m)) / 0.035 (m)
= 0.16 m@

Swath width. The swath width is calculated using flying height and maximum mirror angle in the following formula:
Swath Width = Tan(MirrorAngle)* Flying Height * 2
= Tan(27) * 200 * 2
= 204 m

Units. Units for all formulas are:
Flying Height: meters
Flying Speed: meters per second
Mirror Angle: degrees

APPENDIX G

Quality Assurance Project Plan

QUALITY ASSURANCE PROJECT PLAN
LiDAR AND ORTHOPHOTOGRAPHY
DEMONSTRATION PROJECT
KIRTLAND PRECISION BOMBING RANGE, NEW MEXICO

Approvals

Name: Thomas Tomczyk, P.G., L.G., C.Q.A.
Title: Principal Investigator
URS Group, Inc.

Signature: _____ Date: _____

Name: Dale Bennett
Title: Data Evaluation and GIS Lead
URS Group, Inc.

Signature: _____ Date: _____

Name: Dave Neufeldt
Title: LiDAR / Orthophotography Technical Lead
Terra Remote Sensing, Inc.

Signature: _____ Date: _____

CONTENTS

TABLES

FIGURES

ABBREVIATIONS AND ACRONYMS

DoD	Department of Defense
DOPS	D
DQO	Data Quality Objective
ESTCP	Environmental Security Technology Certification Program
EPA	U.S. Environmental Protection Agency
GPS	Global Positioning System
HASP	Health and Safety Plan
IMU	Inertial Measurement Unit
MEC	Munitions and Explosives of Concern
MRS	Munitions Response Site
PBR	Precision Bombing Range
PI	Principal Investigator
PRF	Pulse Repetition Frequency
QA	Quality Assurance
QAO	Quality Assurance Officer
QAPP	Quality Assurance Project Plan
QC	Quality Control
SOP	Standard Operating Procedure
SOW	Statement of Work
TRSI	Terra Remote Sensing, Inc.
URS	URS Group, Inc.
URS PI	URS Principal Investigator

1.0 INTRODUCTION

This document serves as the quality assurance project plan (QAPP) for the Environmental Security Technology Certification Program (ESTCP) Demonstration Project entitled "High Density LiDAR and Orthophotography in UXO Wide Area Assessment", to be performed at the former Kirtland Precision Bombing Ranges (PBR), New Mexico (Figure 1-1). The QAPP serves as the primary guide for integrating quality assurance (QA) and quality control (QC) procedures and functions with data collection activities described in the Performance Plan to ensure that technically sound and defensible data are collected and meet project objectives. The QAPP was developed in conjunction with the Demonstration Plan, and health and safety plan (HASP).

By reference, this QAPP relies upon the management policies, objectives, principles, and general procedures presented in the URS Group, Inc. (URS) *Quality Management Plan* (URSG 1998). The quality management plan establishes the framework and general criteria for implementing the URS quality system.

Figure 1-1 Kirtland AFB PBS Vicinity Map

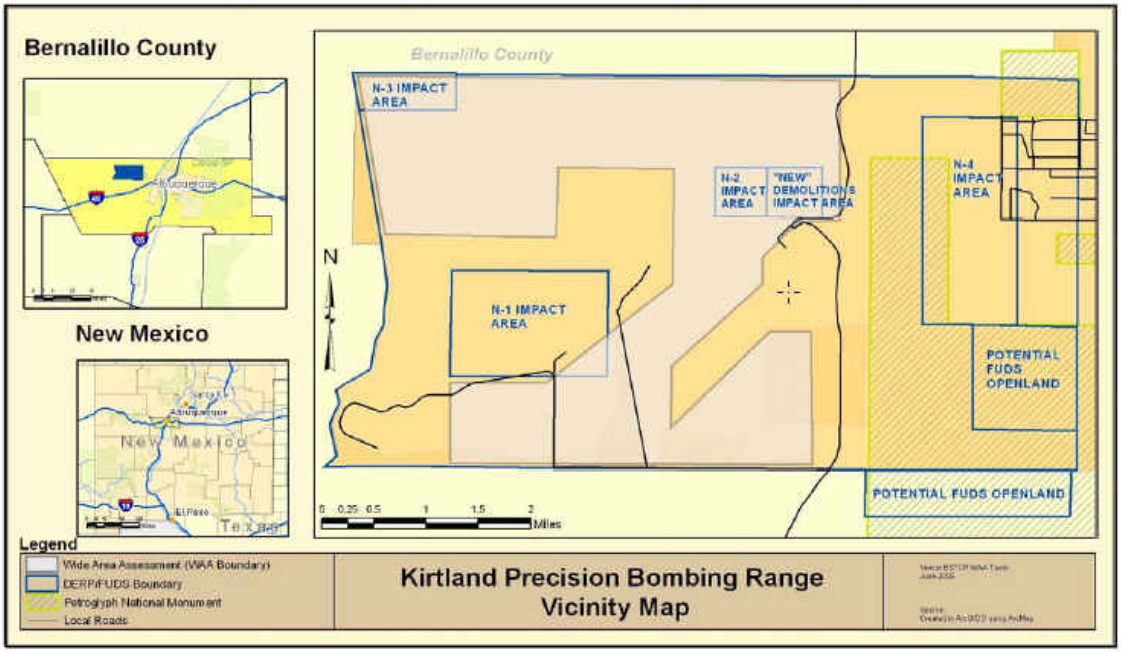

2.0 PROJECT DESCRIPTION

The WAA study area for project UX-0534 consists of 5,000 acres of the former Kirtland Precision Bombing Ranges located in the West Mesa area of Bernalillo County, New Mexico, about 10 miles west of Albuquerque. The WAA study area was selected to in accordance with WAA Pilot Program goals and includes several known WWII-era targets as well as undeveloped land surrounding the targets. Project UX-0534 explores the use of LiDAR and high-resolution orthophotography as a means to locate previously undocumented MRS, delineate the boundaries of MRS, identify site constraints on ground-based geophysical surveys, and identify munitions-related features such as craters, targets, burial pits, and ground and vegetation disturbances.

3.0 PROJECT ORGANIZATION AND QUALITY ASSURANCE RESPONSIBILITIES

3.1 PROJECT ORGANIZATION

The project-specific organization, shown in Figure 3-1, indicates key positions along with lines of authority and lines of communication and coordination. The names of individuals filling key roles on the project, along with their phone numbers, are provided in Table 3-1. The responsibilities and authorities of these key positions as they relate to project QA/QC are described in the following subsections.

It is essential that all individuals have defined responsibilities for their functional areas and that they are clearly aware of the entire project organization and the interrelationships of various roles. Because this discussion covers the project organization, those senior officials, corporate managers, and administrators whose positions are not functionally involved with data generation, data use, or decision making are not included.

QA personnel have sufficient authority, access to work areas, and organizational freedom to identify quality problems; to initiate, recommend, or provide solutions to problems through established channels; and to verify solution implementation. They ensure that all work, including any processing of information, delivery of products, and installation or use of equipment, is reviewed in accordance with the QC objectives and that all deficiencies and nonconformances are corrected. QA personnel have direct access to senior management so that the required authority is available, when needed, to carry out QA duties.

The project planning team will include the team members described below.

3.1.1 ESTCP Project Manager

The ESTCP-assigned Project Manager (ESTCP PM) is responsible for coordinating all project-related activities on behalf of ESTCP. A major component of this position involves directing the URS Principle Investigator (PI) in the execution of the work and the submission of deliverables as scheduled. Specific responsibilities of the ESTCP PM are as follows:

- Oversee all project activities.
- Provide the scope of work to the URS PI.
- Review and approve project plans and coordinate the review within ESTCP and other appropriate organizations, as necessary.
- Review and approve the QAPP and all other components of the project plan.

- Ensure that the QAPP and associated reports are transmitted to appropriate ESTCP personnel and organizations.

- Transmit to the URS PI review comments associated with the project plan from ESTCP and other organizations.

- Ensure that the URS PI addresses ESTCP and agency review comments and takes appropriate action.

3.1.2 URS Principle Investigator

The URS PI is responsible for providing senior leadership and expertise to the URS and subcontract staff and for maintaining a broad perspective of priorities. The URS PI reports to and obtains technical direction and assistance from the ESTCP PM and is responsible for monitoring and documenting the quality of all work produced by the project team, which includes the URS staff and subcontractors. The fundamental goal of this position is to produce a quality work product within the allotted schedule and budget. Duties include executing all phases of the project and efficiently applying the full resources of the project team in accordance with the project plans. Specific responsibilities of the URS PI are as follows:

- Identify the need for and expectations regarding services to be provided and, when necessary, negotiate acceptable scopes of work.

- Provide input and technical expertise to the ESTCP PM on developing or establishing project objectives, data quality objectives (DQOs), sampling rationale, and data analysis and assessment methods.

- Prepare and implement the Technology Demonstration Plan (which incorporates applicable QAPP elements) and prepare reports as required by ESTCP.

- Ensure that the QAPP and standard operating procedures (SOPs) are available and in use for activities that affect product quality and that assigned staff have been trained in the implementation of the QAPP and SOPs.

- Ensure that the best available technology is being applied to reduce potential waste and inefficiencies and that the best known processes are in use.

- Ensure that appropriate procedures for data collection, data processing, and data analysis are followed and that correct QC checks are implemented.

- Perform readiness reviews and monitor the progress of work in relation to scope, cost, and schedule.

- Monitor team and subcontractors for compliance with project and data quality requirements, records, costs, and progress of the work; replan and reschedule work tasks as appropriate.

- Review and approve calculations and data processing methods to ensure that data reduction is performed in a manner that produces quality products.

- Verify data quality, test results, equipment calibrations, and QC documentation; maintain and regularly review all QC records.

- Ensure that all key decisions and project deliverables are subjected to independent technical review by qualified personnel within the timeframe of the project schedule.

- Report QA problems to the Quality Assurance Officer (QAO) for review and/or resolution.

- Assess completion of work in accordance with ESTCP.

3.1.3 URS Quality Assurance Officer

The URS Quality Assurance Officer (QAO) communicates with the URS PI regarding the contract and additionally has direct reporting access to the URS Corporate QA Director on quality-related matters. The QAO is responsible for development, implementation, and maintenance of the comprehensive quality system. Responsibilities of this position include communicating with all levels of program and project management to ensure that a quality product is produced for delivery. Project-specific responsibilities of the QAO or designee are as follows:

- Respond to QA needs, resolve problems, and answer requests for guidance or assistance.

- Provide guidance to the URS PI in the development of project plans, including the QAPP.

- Review and approve the project plans.

- Together with the URS PI, assign competent, qualified independent reviewers to review the technical adequacy of deliverables.

- Track the progress and completion of the review and approval process.

- Ensure that ESTCP protocols and procedures, as well as SOPs, are being followed.

- Review the implementation of the Technology Demonstration Plan and the adequacy of the data or products generated based on quality objectives.

- Initiate field and office audits, if necessary.

- Review audit and nonconformance reports to determine areas of poor quality or failure to adhere to established procedures.

- Confer with the audited entity on the steps to be taken for corrective actions and track nonconformance until it has been corrected; evaluate the adequacy and completeness of the action taken; confer with the URS PI to resolve an inadequate corrective action; and confirm the adequacy and implementation of the response action.

- Upon detection and identification of an immediate adverse condition affecting the quality of results, suspend or stop work with the concurrence of the URS PI and the ESTCP PM.

3.1.4 URS Data Evaluation and GIS Lead

The URS Data Evaluation and GIS Lead is responsible for managing any project task requiring specialized technical expertise, related to the collection, assessment, analysis and reporting of LiDAR and orthophoto data. Specific responsibilities are as follows:

- Provide technical direction to URS technical staff in the specific area of LiDAR and orthophoto data collection and processing.

- Prepare a statement of work (SOW) for use in procurement of direct subcontracted services including LiDAR and orthophotography.

- Serve as a point of contact for direct subcontractors.

- Relay to the URS PI project information related to LiDAR and orthophoto data collection and processing.

- Coordinate data collection activities to be consistent with information requirements.

- Resolve problems with received data and/or analysis.

- Oversee evaluation of data received from subcontractors in accordance with the project requirements and DQOs.

- Supervise the creation of analytical products based on data provided by direct subcontractor(s).

- Ensure that data are correctly reported in appropriate data formats.

- Prepare or oversee the preparation of portions of the final report that summarize data results and present conclusions.

- Prepare and file required URS QA/QC review forms, documenting QA/QC activities related to data analysis performed by URS.

3.1.5 Subcontractor

One direct subcontractor, Terra Remote Sensing, Inc. (TRSI) will be used by URS during the demonstration. This subcontractor will collect LiDAR and photo image data in the field, and will also perform initial data processing to create LiDAR points and orthophotos. The subcontractor will be directed by the URS PI or their designee and apprised of project requirements as appropriate for their assigned tasks. In addition, the subcontractor will have the following responsibilities:

- Implement the data collection elements of the Technology Demonstration Plan and perform initial data processing elements of the Plan.

- Develop and maintain flight logs, calibration and accuracy reports, and other field activity files, forms, and logbooks as detailed in this QAPP.

- Implement technical procedures applicable to tasks, including calibration and maintenance of field equipment.

- Subcontract as necessary for specific equipment such as helicopter services, with the approval of URS.

- Provide a health and safety plan appropriate to their activities and to those of their subcontractors.

- Report any problems or deviations from project plans to URS PI.

Table 3-1
Project Contacts

Key Role	Name	Telephone
ESTCP		
ESTCP Contracting Officer	Lynn Harper	(703) 428-6551
ESTCP Project Manager (ESTCP PM)[1]	Herb Nelson	(202) 767-3686
On-Site Emergencies		
Any emergency		911
Ambulance		911
Kirtland PBR / Double Eagle Airport Manager		(505) 244-7888
Fire		911 or
University of New Mexico Hospital, Albuquerque		(505) 272-2111
URS Group, Inc.		
URS Principal Investigator	Tom Tomczyk	(206) 438-2137
URS Data Evaluation and GIS Lead	Dale Bennett	(206) 438-2026
URS Quality Assurance Officer	George Carlson	(503) 478-7661
URS Health and Safety Manager	Mark Litzinger	(206) 438-2199
TRSI.		
TRSI Technical Lead	Dave Neufeldt	(250) 656-0931

[1] In the event of an emergency, the URS PI and the ESTCP PM are to be notified immediately.

3.2 PROJECT SCHEDULE

The project schedule is provided in Table 3-2.

Table 3-2.
Project Schedule

Activity	Start Date	End Date
Mobilization	August 8, 2005	August 8, 2005
Field data collection	August 9, 2005	August 11, 2005
Complete initial data processing and deliver field data to URS	September 23, 2005	September 23, 2005
Completion of initial data deliverables and transfer to ESTCP	October 7, 2005	October 7, 2005
Data analysis. GIS-based analysis of LiDAR and image data for features; area classification.	November 30, 2005	November 30, 2006
Demonstration Report with Survey Data	February 1, 2006	February 1, 2006
Draft final report	June 1, 2006	June 1, 2006
Final report	August 1, 2006	August 1, 2006

4.0 DATA QUALITY PARAMETERS

Data Quality Objectives (DQOs) are qualitative or quantitative statements of the precision (a measure of the random error), bias (a measure of systematic error), representativeness, completeness, and comparability necessary for the data to serve the project objectives. During implementation of the demonstration, field and analytic data will be generated. These data will be evaluated to determine that DQOs have been met and that the data are usable for the project objectives.

4.1 ANALYTICAL OBJECTIVE AND RATIONALE

The objective of the demonstration is to accurately and systematically locate Munitions Response Sites (MRS) and ground features associated with the use of munitions and explosives of concern (MEC). A secondary objective is to develop realistic cost/benefit data regarding the appropriate densities of LiDAR and orthophotographs in the detection and characterization of MRS and MEC-related ground features. The primary means to achieve these objectives is through the development and analysis of detailed models of the ground surface based on several different densities of LiDAR points, and of orthophoto images at different pixel sizes. Consequently, analytical objectives are designed to ensure that LiDAR and orthophotography products created accurately reflect the capabilities of each technology, free of bias and error which will distort the experimental results.

Further, the products of the LiDAR and orthophotography demonstration will be used in subsequent phases of the overall ESTCP UXO pilot project. Consequently, a further analytic objective is to assure that the spatial coordinates of the LiDAR and orthophoto data are controlled, to the extent allowed by each technology, to on-site survey control points that will be used by other demonstrators.

4.2 QUALITY ASSURANCE MEASUREMENTS

The quality of the field data will be evaluated based on successful calibration of each instrument supplying the data based on the manufacturer's stated accuracy and precision of the instrument. The quality of data processing and data analysis steps will be evaluated based on the precision, bias, representativeness, completeness, and comparability of the data generated by each type of analysis. These data assessment parameters are described in the following subsections.

4.2.1 Precision

Precision is a measure of the scatter in the data due to random error. For airborne remote sensing technologies, the major sources of random error are the sampling rate of the sensors in relation to

the positional data provided by the Inertial Measurement Unit (IMU) and Global Positioning System (GPS). Sampling and analytical precision is expressed as the relative difference in position between the LiDAR and orthophoto data and ground-based survey control points, expressed in centimeters.

4.2.2 Bias

Bias is a measure of the difference between the analytical results for a parameter and the true value due to systematic errors. The primary source of systematic error is equipment calibration. Secondarily, systematic error can be created by improper flight line layout, which can result in uneven data collection in some types of terrain. Since the Kirtland PBR demonstration site is relatively flat, flight line layout is not expected to be a problem. Bias is expressed as positional differences in LiDAR data between one flight line and the next, or between LiDAR and orthophoto positions, that are beyond stated standards and cannot be adjusted out.

4.2.3 Representativeness

Representativeness is a qualitative parameter that expresses the degree to which sample data accurately and precisely represents a characteristic of a population, parameter variations at a sampling point, or an environmental condition. Representativeness of the environmental conditions at the time of sampling is achieved by selecting sampling locations, methods, and data collection times so that the data describe the site conditions that the project seeks to evaluate. In the context of LiDAR and orthophotography, representative sampling is influenced by proper choice of seasonal vegetative conditions (for more vegetated sites), and proper choice of sun angle to best reveal the features being sought. During data processing, representative LiDAR data is obtained by properly separating laser pulses that reflect from the ground surface from those that reflect from vegetation or buildings. Representative orthophotography data are obtained by performing appropriate color balancing on orthophoto mosaics to eliminate the effect of glare or different sun angles on images from flight lines in opposing directions, while still accurately representing the colors of the features being recorded.

4.2.4 Completeness

Completeness is a measure of the number of valid measurements obtained in relation to the total number of measurements planned. In the context of LiDAR and orthophotography, completeness is expressed in percentage of the target area for which data is successfully collected, and for which the data collected meets project specifications. For this demonstration, 100% coverage of the demonstration site is expected.

4.2.5 Comparability

Comparability is a qualitative parameter expressing the confidence with which one data set can be compared to another. During data collection the comparability goal is achieved by maintaining consistency in sampling conditions such as flight altitude, and equipment settings.

These are aimed at having data from each flight line and each flight mission be comparable to the next, and at having the LiDAR and orthophoto data positions be well controlled to ground survey control points to be used by other demonstrators.

During data processing and analysis, comparability is maintained through establishment and execution of appropriate data management and data format standards. This results in data that is organized in a consistent manner, with appropriate metadata to enable other users to understand the data processing steps used and their rationale, and in formats that have been agreed to by other demonstrators and ESTCP.

The following parameters in Table 4-1 will be subject to QA/QC review:

Table 4-1
Data Quality Parameters

Analytical Objective	Metric	Action to Achieve Metric	Sampling Frequency or Timing	Desired Result
Pre-flight Activities				
Study area boundary delineation	Site Boundary polygon characteristics agreed upon and documented to allow comparison with data collected.	Achieve stakeholder agreement to boundary parameters.	Once, start of program.	Document site boundary for measurement of future boundary metrics.
Survey control point confirmation measurement	Confirm coordinates of survey control points within at least 3rd order accuracy.	Perform and record GPS survey (static or kinematic).	Pre-flight (or during on-site acquisition).	
LiDAR Data Collection and Processing				
Sensor calibration	Resolve roll/pitch/heading for installation.	Perform opposing direction and orthogonal passes over baseline. Compare with nominal values from standard installation.	Prior to each flight day.	+/– 0.02 degrees
Sensor speed[1]	Laser pulse rate between 50-100 kHz.	Set laser pulse speed and the altitude of the low LiDAR passes depending on site conditions to achieve highest possible point density.	Prior to each flight day.	Achieve target sensor speed.
Flight altitude	Flight altitudes of 900, 450, and 200 to 300 m. The two higher altitudes are designed to achieve 10-cm and 20-cm pixel sizes; however, LiDAR will still be collected. The lowest flight altitudes will be adjusted to achieve the highest practical LiDAR point densities.	Establish and fly appropriate flight altitudes for the desired LiDAR point densities and orthophoto pixel sizes. Lay out a series of flight lines for high-density LiDAR collection to be able to respond to site conditions.	Each flight line.	+/– 50 m from planned flight altitudes[2].
Area coverage	100% coverage for each flight.	Establish and fly flight lines so as to cover the entire target area. Data from each day's flights will be examined and data gaps will be filled.	Each flight	100% coverage. 15% flightline overlap, 50m over area boundaries.

[1] Appropriate sensor speed is a site-specific determination based on site reflectivity. Higher speeds result in lower energy per laser pulse, and thus require more a reflective ground surface. Both ground material and flight altitude influence reflectivity.

[2] Flight altitudes significantly above the performance objective will fail the point density test and photo pixel size tests given below and will be repeated.

Table 4-1 (Continued)
Data Quality Parameters

Analytical Objective	Metric	Action to Achieve Metric	Sampling Frequency or Timing	Desired Result
Data collection rate	Accomplish 2 flights per day, each covering the full site. Reserve 1 additional day for QA/QC and re-flights	Establish and review flight lines and flight schedule prior to data collection.	N/A	Full data collection within planned schedule.
LiDAR point density	Achieve overall densities of: 200 m flights (2) – 8 pts/m^2 each 475 m flight (1) – 3 pts/ m^2 950 m flight (1) – 1.5pts/m^2.	Plan and accomplish appropriate sensor speed, flight altitude, and air speed. Flights more than 10% below target point densities will be repeated.	Each flight.	Data collection within 10% of target densities.
LiDAR flight line alignment	The two 200 m flights will be orthogonal.	Appropriate flight lines will be designed and flown. Planned flight lines will be submitted in advance.	Each 200 m altitude flights	Flight lines within 10^o of orthogonal.
LiDAR vertical accuracy	Vertical accuracy of +/– 15 cm compared to ground survey.	Steps: 1. Perform sensor calibration as described above 2. Obtain ground elevations on identifiable points using ground based GPS methods (static and/or kinematic) 3. Compare ground-based and airborne elevations.	Each flight	Achieve best possible match between LiDAR and ground-based elevations.
LiDAR horizontal accuracy	Horizontal accuracy of +/– 65 cm compared to ground survey.	Steps: 1. Perform sensor calibration as described above 2. Obtain ground positions on identifiable points using ground based GPS methods (static and/or kinematic) 3. Compare ground-based and airborne positions.	Each flight	Achieve best possible match between LiDAR and ground-based positions.
LiDAR data integration – flight lines	Achieve flight line to flight line edge match of +/– 12cm.	Review statistics from LiDAR processing software.	Line to line	Achieve best possible match between individual LiDAR flight lines.

Table 4-1 (Continued)
Data Quality Parameters

Analytical Objective	Metric	Action to Achieve Metric	Sampling Frequency or Timing	Desired Result
LiDAR point separation	Remove 100% of large features, (trees, buildings, vehicles) Remove small features (grass, low brush) to the level where remaining data cannot distinguish ground from non-ground features.	Operators remove non-ground laser returns through automated separation routines followed by hand cleaning and inspection.	LiDAR data set for each flight	Satisfactory visual inspection of surface model of the ground surface.
Orthophoto Data Collection and Processing				
Orthophoto area coverage	100% coverage for each flight.	Wireframes of "raw" images are compared to the project boundary to check for gaps or holes.	Each flight day as part of QA/QC checks.	100% coverage with sufficient image overlap for ortho-rectification.
Orthophoto flight altitude / pixel size	475 m (for 10 cm pixel flight) 950 m (for 20 cm pixel flight).	Orthophoto pixel size is directly related to flight altitude. Flight lines are designed for the desired pixel sizes. Flight data will be examined during and after each flight and flight lines outside of the range will be repeated.	Each flight	+/– 50m of design flying altitude.
Orthophoto image mosaicing	No obvious seams between images in the final orthophoto.	Creation of an image mosaic from individual small images is largely an operator controlled rather than an automated process.	Each orthophoto composite image (10 cm and 20 cm)	Line features are continuous with no visible discontinuity at mosaic seams.
Orthophoto image color balancing	No obvious color imbalances within data for each session.[34]	Color balancing is an operator controlled process based on viewing the mosaic to identify any areas of tonal imbalance.	Each orthophoto composite image (10 cm and 20 cm)	Continuity of tone such that individual images are not visible in mosaic.

[3] The final project area outline will determine the number of flight lines and turns necessary to cover the project area. This in turn will determine the duration of each acquisition period. In order to ensure relatively constant sun angle, if necessary, each image acquisition session will be split into two – one early in the day and one late in the day in which the sun-angle is the same with the exception of being in the opposite direction. Tonal balance between the early and late sessions may not be the same at the junction between the two collection areas.

Table 4-1 (Continued)
Data Quality Parameters

Analytical Objective	Metric	Action to Achieve Metric	Sampling Frequency or Timing	Desired Result
Orthophoto horizontal alignment to LiDAR	LiDAR and orthophotos aligned so that target features are not displaced in the two data sets.	Orthorectification is performed using the LiDAR data and fiducial locations are control data sources, followed by operator adjustment.	Each orthophoto composite image.	Orthophotos aligned to +/– 2 pixel widths.
Orthophoto horizontal alignment to fiducials	Orthophotos aligned to survey control points so that target features are not displaced.	Orthorectification is performed using the LiDAR data and fiducial locations are control data sources, followed by operator adjustment.	Each orthophoto composite image.	Orthophotos aligned to +/– 3 pixel widths.
MRS Identification and Analysis				
MRS identification[4]	Correctly identify all previously identified MRS.	Identify and document MRS from LiDAR and orthophoto data sets.	Each LiDAR and orthophoto data set and combinations.	All MRS
MRS false alarm rate	No areas incorrectly identified as MRS.	Identify and document MRS from LiDAR and orthophoto data sets.	Each LiDAR and orthophoto data set and combinations.	All MRS
MES boundary delineation	Correctly locate MRS boundaries to +/– 15% of ground-truthed area.	Identify and document MRS boundaries from LiDAR and orthophoto data sets for a selected set of test MRS.	Each LiDAR and orthophoto data set and combinations.	All MRS
MRS feature identification	Identify features presenting as human-made (anthropogenic) not including craters (e.g., walls, berms, pits, small buildings).	LiDAR and photo data sets will be examined for linear features.	Each LiDAR and orthophoto data set and combinations.	90% of features identified from selected field-identified features.
MRS feature identification	Identify craters. Count 90% of craters over 1.5 m diameter and .3 m depth.	Automated algorithms will be used to identify and count craters using LiDAR data.	Each LiDAR and orthophoto data set and combinations.	90% of craters identified outside of crater fields. 95% of craters identified inside crater fields.

[4] The analysis described will be performed for each separate LiDAR data set and for the combined LiDAR data set, and for each orthophoto data set and for the combination of LiDAR and orthophotos. The "Desired Result" metric applies to the combination of all

Table 4-1 (Continued)
Data Quality Parameters

Analytical Objective	Metric	Action to Achieve Metric	Sampling Frequency or Timing	Desired Result
MRS feature identification	Identify vegetation patterns indicating previous disturbance.	Automated algorithms will be used to map vegetation heights and patterns from LiDAR data. Results will be examined for linearity or other regular shapes. Orthophotos will be examined for regular vegetation patterns.	Each LiDAR and orthophoto data set and combinations.	[COMING]
MRS feature identification	Identify established roads	LiDAR and photo data sets will be examined for linear features.	Each LiDAR and orthophoto data set and combinations.	100% of established roads.
MRS feature identification	Identify vehicle tracks	LiDAR and photo data sets will be examined for linear features.	Each LiDAR and orthophoto data set and combinations.	90% of field-identified vehicle tracks.
MRS feature identification	Identify topography that can limit access	LiDAR data sets will be used to map areas above designated slope.	Each LiDAR data set and combinations.	100% of areas.
Data management				
Data management	Data backup and storage to achieve redundancy and security.	Data will be backed up to separate redundant hard drives or tape drives.	Daily backup during field and data processing operations.	All data products.
Data transfer	Data transfer will be in appropriate formats and file sizes for ESTCP and Kirtland AFB ongoing use.	Data will meet US Government Spatial Data Standard (SDS) and fully comply with Versar EDD specifications.	Each data transfer.	All data products.
Data collection report	Standard flight reporting includes: calibration log, flight log, QA/QC log, and site photos.	The data collection report is a standard QA/QC product.	Calibration report: each flight day. Flight log: each flight. QA/QC log: each flight. Site photos: whole project.	Full reporting is a required part of contract performance.
Data processing report	Standard data processing report includes: GPS control ties, accuracy verification report, and QA/QC report.	The data processing report is a standard QA/QC product.	Each LiDAR and orthophoto data set.	Full reporting is a required part of contract performance.

Table 4-1 (Continued)
Data Quality Parameters

Analytical Objective	Metric	Action to Achieve Metric	Sampling Frequency or Timing	Desired Result
Metadata	Metadata to accurately describe data format and processing steps.	Data will meet US Government Spatial Data Standard (SDS) and fully comply with Versar EDD specifications including metadata standards.	Each data transfer.	All data products.
QA/QC	All data and derived products will be subject to appropriate QA/QC review.	Data processing will follow the QA/QC plan described herein.	Each data transfer.	All data products.
Data delivery	All data will be delivered in a timely and easy-to-transfer manner.	Data deliverables will be made using ftp where possible, but in all cases will be followed up with delivery on physical media, primarily external hard drives.	Each data transfer.	All data products.

5.0 CALIBRATION PROCEDURES, QUALITY CONTROL CHECKS, AND CORRECTIVE ACTION

Upon arrival at the site a suitable GPS base station will be established either at one of the survey control points or near the hanger. If a location near the hanger is chosen due to security or operational reasons, a GPS control survey will be conducted to tie the base station into the control points. Targets will also be placed on the survey control points to facilitate identification in the digital images and the intensity image of the LiDAR data. Positions of the survey control points will be verified and any discrepancies immediately noted and transmitted to the URS PI and ESTCP PM.

Initial equipment calibration will be performed following equipment installation to the helicopter. Calibration will be done by means of a calibration flight, during which test data will be collected to determine optimal system operation parameters for data acquisition. This will involve collecting data at varying heights above ground between 200m and 300m with variations in the laser pulse rate (PRF).

Equipment calibration will be checked prior to each day's flight missions. GPS data will be processed and checked each day for DOPS and quality of solution. The redundant base station will be processed to verify the solution and obtain the best-fit positions.

The following QA/QC checks will be made to verify equipment calibration and data quality:

a) LiDAR
Following each day's flights, the initial calibration values will be used to process the airborne data to obtain the LiDAR points. The points will be viewed visually to inspect the coverage with respect to the overall project boundary in order to verify complete coverage. Flight lines can be displayed in different colors to allow measurement of overlap as well as checking of height variations in the overlap region. Point densities will be calculated on sample areas throughout the project to verify compliance with specifications. Visualization tools are used to manipulate the points to check for comparison of features and general alignment of the data.

b) Imagery
Following each day's flights, "raw" images will be checked individually for completeness and exposure. Images with significantly abnormal exposure such as bright spots due sun glint off ground objects will be flagged for re-flight. Using an initial ground model from the LiDAR data, the wire frame outlines of the individual images will be draped onto the ground model to determine the true coverage of each photo image. The image coverage will be reviewed for gaps within the flight lines and extents to the project perimeter. Measurements are also made on the frames to validate compliance of end-lap and side-lap with project specifications.

Following return of the data to the office, field calibration will be reviewed and fine-tuned. Following QC checks, calibration factors will be applied to laser range, GPS, and INS data to

produce x,y,z values for each LiDAR point. Points are then transformed into the delivery datum and map projection. Subsequently, the points are separated into returns from ground, vegetation and buildings. Following point separation, separate x,y,z files (in ASCII comma-delimited format) will be created for ground, vegetation and building returns for each of the four flights and delivered to URS. Calibration of orthophoto images to the LiDAR surface model and the survey control points will be performed using standard orthorectification software methods.

6.0 DEMONSTRATION PROCEDURES

6.1 FIELD ANALYTICAL PROCEDURES

Technology startup includes setting out of GPS receivers over base stations and starting. The helicopter system is started including sub-systems of GPS, INS, navigation control, and logging systems. Checks are made to ensure correct operation, flight line data is uploaded and verified. Once ground operation is verified the helicopter commences flight to the lines to be flown, during this time while aloft, the LiDAR system operation is verified (this is done aloft to prevent damage to the system firing too close to the ground). Following verification of system operation, data collection is then undertaken.

During data collection all systems are monitored to verify continuous correct operation. Should a failure occur, airborne procedures to rectify the system will be implemented including resetting various portions of the system. Should these procedures not be effective, depending on the nature of the failure, the helicopter will land in the project area or return to the base for further corrective actions.

6.2 LABORATORY ANALYTICAL PROCEDURES

Laboratory procedures include a further review of all calibration data to refine the calibration for the system installation. Following this checks are made on the fiducials and any other available control points or ground data. If the checks meet specifications, the LiDAR data is passed on to the TM (Terrain Mapping) group for processing to extract the bare earth model while the image data is passed to the Ortho group for creation of the mosaic's.

Creation of the bare-earth model through classification of the raw LiDAR points includes both automated process and manual reviews of the data. Surfaces and contours may be created to identify areas that have not been correctly classified.

7.0 CALCULATION OF DATA QUALITY INDICATORS

This section outlines the procedures for verifying the accuracy of the data reduction and analysis process and the methods used to ensure that data transfer is error free (or has an admissible error rate), that no information is lost in the transfer process, and that the output is completely recoverable from the input. To reduce the risks associated with data transfer, this process is kept to a minimum. Data are reduced either manually on calculation sheets or by computer on formatted printouts. The following responsibilities will be delegated in the data reduction process:

- Technical personnel will document and review their own work and are accountable for its correctness.

- Major calculations will receive both a method and an arithmetic check by an independent checker. The checker is accountable for the correctness of the checking process. The checker is also responsible for becoming familiar with the project requirements and criteria; and bringing to the URS PI's attention any problems uncovered.

- The URS PI is responsible for ensuring that data reduction is performed in a manner that produces quality data through review and approval of calculations.

In general, any personnel performing review or oversight shall provide resumes or equivalent documentation demonstrating their qualifications and experience needed to perform their duties. In addition, each assessor shall be independent of the process under evaluation. Independent Technical Review for this project will be performed by ESTCP or its designated subcontractors.

7.1 DATA QUALITY CALCULATIONS

The following methods will be used to calculate data quality.

Table 7-1
Data Quality Metric Calculation

Analytical Objective	Metric	Action to Achieve Metric	Desired Result	Calculation Method
Survey control point confirmation measurement	Confirm coordinates of survey control points within at least 3rd order accuracy.	Perform and record GPS survey (static or kinematic).	3rd order accuracy	(x,y,z locations of confirmation survey) – (reported x,y,z locations)
Sensor calibration	Resolve roll/pitch/heading for installation.	Perform opposing direction and orthogonal passes over baseline. Compare with nominal values from standard installation.	+/– 0.02 degrees	(x,y,z locations of control points) – (x,y,z locations from sensors)
Sensor speed	Laser pulse rate between 50–100 kHz.	Set laser pulse speed and the altitude of the low LiDAR passes depending on site conditions to achieve highest possible point density.	Achieve target sensor speed.	Examination of sensor output, calculation of point densities
Flight altitude	Flight altitudes of 900, 450, and 200 to 300 m.	Establish and fly appropriate flight altitudes for the desired LiDAR point densities and orthophoto pixel sizes. Lay out a series of flight lines for high-density LiDAR collection to be able to respond to site conditions.	+/– 50 m from planned flight altitudes.	In-flight monitoring, examination of GPS flight line data,
Area coverage	100% coverage for each flight.	Establish and fly flight lines so as to cover the entire target area. Data from each day's flights will be examined and "holes" filled.	100% coverage. 15% flightline overlap, 15% flightline length over area boundaries.	(Area flown) – (Area of demonstration site) plus visual inspection
LiDAR point density	Achieve overall densities of: 200- to 300-m flights (2) – 8 pts/m^2 each 475-m flight (1) – 3 pts/ m^2 950-m flight (1) – 2 pts/ m^2.	Plan and accomplish appropriate sensor speed, flight altitude, and air speed. Flights more than 10% below target point densities will be repeated.	Data collection within 10% of target densities.	Density = (# of points)/(area in meters)
LiDAR flight line alignment	The two 200 m flights will be orthogonal.	Appropriate flight lines will be designed and flown. Planned flight lines will be submitted in advance.	Flight lines within 10° of orthogonal.	Angle of intersection will be measured.

Table 7-1) Continued)
Data Quality Metric Calculation

Analytical Objective	Metric	Action to Achieve Metric	Desired Result	Calculation Method
LiDAR vertical accuracy	Vertical accuracy of +/– 15 cm compared to ground survey.	Steps: 1. Perform sensor calibration as described above 2. Obtain ground elevations on identifiable points using ground based GPS methods (static and/or kinematic) 3. Compare ground-based and airborne elevations.	Achieve best possible match between LiDAR and ground-based elevations.	(z locations of control points) – (z locations from sensors)
LiDAR horizontal accuracy	Horizontal accuracy of +/– 65 cm compared to ground survey.	Steps: 1. Perform sensor calibration as described above 2. Obtain ground elevations on identifiable points using ground based GPS methods (static and/or kinematic) 3. Compare ground-based and airborne elevations.	Achieve best possible match between LiDAR and ground-based elevations.	(x,y locations of control points) – (x,y locations from sensors)
LiDAR data integration – flight lines	Achieve flight line to flight line edge match of +/– 12cm.	Review statistics from LiDAR processing software.	Achieve best possible match between individual LiDAR flight lines.	(x,y,z locations from flight lines compared visually and through automated software matching
LiDAR point separation	Remove 100% of large features, (trees, buildings, vehicles) Remove small features (grass, low brush) to the level where remaining data cannot distinguish ground from non-ground features.	Operators remove non-ground laser returns through automated separation routines followed by hand cleaning and inspection.	Satisfactory visual inspection of surface model of the ground surface.	Visual inspection following automated and operator implemented separation
Orthophoto area coverage	100% coverage for each flight.	Wireframes of "raw" images are compared to the project boundary to check for gaps or holes.	100% coverage with sufficient image overlap for ortho-rectification.	(Area flown) – (Area of demonstration site) plus visual inspection

Table 7-1) Continued)
Data Quality Metric Calculation

Analytical Objective	Metric	Action to Achieve Metric	Desired Result	Calculation Method
Orthophoto flight altitude / pixel size	475 m (for 10 cm pixel flight) 950 m (for 20 cm pixel flight).	Orthophoto pixel size is directly related to flight altitude. Flight lines are designed for the desired pixel sizes. Flight data will be examined during and after each flight and flight lines outside of the range will be repeated.	+/– 50m of design flying altitude.	In-flight monitoring, examination of GPS flight line data,
Orthophoto image mosaicing	No obvious seams between images in the final orthophoto.	Creation of an image mosaic from individual small images is largely an operator controlled rather than an automated process.	Line features are continuous with no visible discontinuity at mosaic seams.	Visual inspection
Orthophoto image color balancing	No obvious color imbalances.	Color balancing is an operator controlled process based on viewing the mosaic to identify any areas of tonal imbalance.	Continuity of tone such that individual images are not visible in mosaic.	Visual inspection.
Orthophoto horizontal alignment to LiDAR	LiDAR and orthophotos aligned so that target features are not displaced in the two data sets.	Orthorectification is performed using the LiDAR data and fiducial locations are control data sources, followed by operator adjustment.	Orthophotos aligned to +/– 2 pixel widths.	(x,y locations of LiDAR points) – (x,y locations of photo pixels) at target locations
Orthophoto horizontal alignment to fiducials	Orthophotos aligned to survey control points so that target features are not displaced.	Orthorectification is performed using the LiDAR data and fiducial locations are control data sources, followed by operator adjustment.	Orthophotos aligned to +/– 3 pixel widths.	(x,y locations of photo pixels) – (x,y locations of control points) at target locations
MRS identification[5]	Correctly identify all previously identified MRS.	Identify and document MRS from LiDAR and orthophoto data sets.	All MRS	
MRS false alarm rate	No areas incorrectly identified as MRS.	Identify and document MRS from LiDAR and orthophoto data sets.	All MRS	(# of MRS previously identified) – (# of MRS identified from demonstration data)

[5] The analysis described will be performed for each separate LiDAR data set and for the combined LiDAR data set, and for each orthophoto data set and for the combination of LiDAR and orthophotos. The "Desired Result" metric applies to the combination of all available data. It is currently unknown whether the metric can be achieved for some portion of the data rather than the combined data set.

Table 7-1) Continued)
Data Quality Metric Calculation

Analytical Objective	Metric	Action to Achieve Metric	Desired Result	Calculation Method
MES boundary delineation	Correctly locate MRS boundaries to +/– 15% of ground-truthed area.	Identify and document MRS boundaries from LiDAR and orthophoto data sets for a selected set of test MRS.	All MRS	(area of MRS previously identified) – (area of MRS identified from demonstration data), plus visual inspection
MRS feature identification	Identify features presenting as human-made (anthropogenic) not including craters (e.g. walls, berms, pits, small buildings).	LiDAR and photo data sets will be examined for linear features.	90% of features identified from selected field-identified features.	(# of features previously identified) – (# of features identified from demonstration data)
MRS feature identification	Identify craters. Count 90% of craters over 1.5 m diameter and .3 m depth.	Automated algorithms will be used to identify and count craters using LiDAR data.	90% of craters identified outside of crater fields. 95% of craters identified inside crater fields.	(# of craters identified from demonstration data) – (# of craters identified through field verification)
MRS feature identification	Identify vegetation patterns indicating previous disturbance.	Automated algorithms will be used to map vegetation heights and patterns from LiDAR data. Results will be examined for linearity or other regular shapes. Orthophotos will be examined for regular vegetation patterns.	[TBD]	Visual inspection
MRS feature identification	Identify established roads	LiDAR and photo data sets will be examined for linear features.	100% of established roads.	Comparison of roads located from demonstration data to roads identified by on-site inspection.
MRS feature identification	Identify vehicle tracks	LiDAR and photo data sets will be examined for linear features.	90% of field-identified vehicle tracks.	Comparison of tracks located from demonstration data to tracks identified by on-site inspection.
MRS feature identification	Identify topography that can limit access	LiDAR data sets will be used to map areas above designated slope.	100% of areas.	Comparison of slope data derived from demonstration data with reports of on-site inspection.

7.2 HAND CALCULATIONS

Hand calculations will be legibly recorded on calculation sheets and in a logical progression, with sufficient descriptions. Major calculations will be checked by a professional at a level equal to or higher than that of the originator. After completing the check, the checker will sign and date the calculation sheet immediately below the signature of the originator. Both the originator and checker are responsible for the correctness of calculations. A calculation sheet contains the following, at a minimum:

- Project title and brief description of the task
- Task number and date performed
- Signature of person who performed the calculation
- Basis for calculation
- Assumptions made or inherent in the calculation
- Complete reference for each source of input data
- Methods used for calculations
- Results of calculations, clearly annotated

7.3 COMPUTER ANALYSIS

Computer analysis includes the use of models, programs, and data management systems. For published software with existing documentation, test case runs are periodically performed to verify that the software is performing correctly. Both systematic analysis and random error analysis are investigated and appropriate corrective action measures are taken as needed.

8.0 QUALITY ASSURANCE AUDITS AND REPORTS

8.1 STATUS REPORTS

Status reporting will occur throughout the project. Status reporting is designed to verify and record quality assurance activities in order to ensure that data quality meets project specifications. During field data collection, status reporting will be made by the Operations Manager in charge of data collection for TRSI; these reports will be delivered to the URS PI and the URS QAO. During data processing and analysis by URS, status reporting will occur during each phase of the analysis, and will consist primarily of URS QA/QC forms documenting the design of analysis methods and review of resulting products for compliance with project specifications. These reports will be signed by the Assistant Investigator and delivered to the URS PI and the URS QAO.

Status reporting for each phase of the project will take place as follows:

Pre-flight—A report will be made to URS of pre-flight activities, including the following:

- Survey control point(s) established, their locations and ties to established control
- Confirmation of locations for established control points.
- Results of calibration flights and any adjustments made.
- Selection and documentation of sensor parameters for low-level LiDAR flights, and associated planned flight lines.

Data Collection Flights—A daily QA/QC report will be made to URS, including the following items:

- GPS solution quality. Results of daily GPS check.
- Flight logs showing time, orientation, and altitude for each flight line.
- Actual flight lines from GPS records during each flight.
- Area coverage for LiDAR and images.
- LiDAR point density.

INITIAL DATA PROCESSING TO CREATE LIDAR POINTS AND ORTHOPHOTO MOSAICS—A QA/QC REPORT WILL ACCOMPANY DELIVERY OF PRIMARY DATA TO URS, INCLUDING THE FOLLOWING ITEMS:

- Calibration factors for creation of LiDAR points.
- Horizontal and vertical positional accuracies for LiDAR points and orthophoto pixels.
- Final LiDAR point densities for each LiDAR flight.

Creation of Initial GIS Products—A URS QA/QC form will be completed for each of the following steps:

- Setup of project data directories. This report will document file locations, file types, data attribute types, and compliance with EDD standards.
- Finalizing of GIS-based analysis methods. This report will document analysis methods.
- Completion of each major phase of analysis, documenting results and comparison to project specifications.

Delivery of Data and GIS Products to ESTCP—A QA/QC report will accompany all data delivered to ESTCP, documenting review of data deliverable formats and compliance with EDD specifications.

8.2 AUDITS

Systems and performance audits and surveillances are conducted as the principal means to determine compliance with the project-specific documents. Audits and surveillances are used to formally review individual projects during their course and across all levels of management. The QAO has the primary responsibility for conducting audits and surveillances, portions of which may be delegated to an auditing team of senior technical specialists. No specific audits have been planned during the field and analysis activities due to their limited duration.

Technical specialists must be familiar with the technical and procedural requirements of both field and office operations, as well as the associated QA plans. In addition, auditors may not be directly involved with the actual tasks themselves to ensure no introduction of bias into the auditing process.

An audit or surveillance may be initiated (if required) prior to the award of a subcontract to determine the capability of a potential subcontractor, when reorganization or major revision has been made to the project-specific plans, at any time a nonconformance is suspected, or to verify that corrective actions for nonconformance have been implemented.

QA audits include auditor identification, audit notification, audit reporting, identification of nonconformances, establishment of corrective actions, and audit completion notification. In circumstances where corrective actions have not been completed as planned or scheduled, the auditing process provides for management intervention to resolve problems and for issuance of stop work orders, if necessary.

Two types of audits may be performed, a performance audit or a technical system audit. Performance audits will be conducted for this project to determine the status and effectiveness of field data collection and to provide a quantitative measure of the quality of data generated. Field performance will be evaluated by URS through review of the LiDAR and orthophoto data compared to project specifications. This review will include:

- Review of LiDAR point horizontal and vertical locations compared to survey control point locations.
- Review of LiDAR point density for each flight compared to project specifications.
- Review of LiDAR point separation to create bare-earth point sets without influence of vegetation.
- Review of orthophoto image quality.
- Review of orthophoto pixel locations in comparison to LiDAR and survey control points.

Technical system audits are used to confirm the adequacy of the data collection (field operation) and data generation (laboratory or office operation) systems. The on-site audits are conducted to determine whether the project-specific plans and field and laboratory SOPs are being properly implemented. Technical audits are not planned for this project; however, if substantial nonconformances are identified or if there is concern regarding the quality of data and related documentation, then technical system audits will be employed.

8.3 INDEPENDENT TECHNICAL REVIEW AND READINESS REVIEW

An independent technical review is a documented critical review of work of a substantive nature identified as a deliverable. These reviews will be conducted by experienced and qualified personnel to ensure the quality and integrity of tasks and products by allowing the work and/or deliverable to undergo objective, critical scrutiny. For this demonstration, independent technical review will be performed by ESTCP or is designated agents.

8.4 CORRECTIVE ACTIONS

Evaluation of QC data and review of audits conducted for field and analysis operations may indicate the need for a corrective action. Problems arising with QA data will be addressed by the URS QAO through communication of the identified problem and a potential corrective action to the URS PI. The URS PI will relay this information to the project staff for implementation. Project staff will then report back to the URS PI upon successful implementation of the corrective action. All corrective actions are required to be documented. This documentation shall include at a minimum the description of the problem, when the problem was discovered, how it was communicated, and specifics of the response action.

9.0 DATA FORMAT AND STORAGE

9.1 DATA FORMAT

Project data will be collected primarily by sensors in electronic formats. Some data, however, will be collected by hand.

Hand-collected data includes GPS survey data to establish control points, calibration checklists, records of equipment settings, and flight logs. All hand data entries will be made and dated on the day of entry and signed or initialed by the person entering the data. Any change to an entry will not obscure the original entry, will indicate the reason for the change, and will be dated and initialed by the person making the change.

Electronic data will be collected by the GPS, IMU, LiDAR sensor and digital camera. The person responsible for equipment operation for each flight will be identified and recorded through initials on the field data collection sheet at the conclusion of each flight. Changes are not made to automated data entries, which are preserved in their original form. Update of automated data is accomplished only through re-flight, which creates a new data set. All electronic data contains the date and time of collection, which is automatically recorded. Repeat data sets covering the same area can be distinguished from this time stamp, however all external hard drives will be labeled with the date of collection and the project number and area name.

Following each day's flight missions, data will be reviewed as describe above to verify that data has been accurately recorded. Unforeseen circumstances that may affect the integrity of the demonstration include weather problems, equipment malfunction and failure of hard drives used for data storage. Equipment function is monitored by the operator and through automated systems throughout each data collection flight, and the impact of hard drive failure is minimized through creating a duplicate copy of all data. Weather problems will be addressed through re-scheduling of data collection activities as needed. Unanticipated problems will also be addressed through scheduling of an extra flight day past the two flight days needed in order to repeat unsatisfactory flights.

9.2 DATA STORAGE AND ARCHIVING PROCEDURES

LiDAR and orthophotography both involve collection of large quantities of data, which limits the usefulness of data storage methods such as CDs or DVDs. Large project areas can sometimes involve too much data for network backup tapes, although this is not expected to be the case for the Kirtland PBR demonstration. The principle data storage method consists of redundant external hard drives. The standard URS and TRSI procedure is as follows:

- During data collection, LiDAR and camera image data is recorded directly to the hard drive of the sensor package. At the end of each flight this data is copied to external hard

drives. Two copies are made, one of which is sent to the TRSI office for processing, and one of which is retained as a backup.

- During data processing to create and calibrate the LiDAR points orthophoto mosaics, data is backed up nightly. Backup drives are stored off-site. [CONFIRM OFF-SITE STORAGE]

When data processing has been completed, data is transferred to the URS office for analysis. Transfer is either by external hard drive or ftp transfer depending on file sizes. A copy is retained as backup.

At the URS office, data is copied to external hard drive and to the URS corporate network. During processing and analysis, files are backed up nightly; backup tapes are stored off-site. Upon completion of analysis, data will be transferred to ESTCP and a copy retained on external hard drive as backup, in addition to the corporate network backup tapes.

Data availability following changes in key personnel is accomplished through two standard procedures. First, a file naming and location protocol is established at the beginning of the project, and this information is recorded in the project files. File naming conventions, which are recorded in writing, include metadata regarding the provenance of all data files including primary data, intermediate analytic products, and final products. Second, all GIS products include metadata that will meet the specifications of the Electronic Data Deliverable (EDD) specifications.

10.0 REFERENCES

URSG (URS Greiner, Inc.). 1998. *Quality Management Plan.* June 1998.

ATTACHMENT A

TECHNICAL REVIEW QA/QC FORM

Technical Review QA/QC Form

To be completed by technical reviewers. This form is used to document technical review of methods and products.

APPENDIX H
Health and Safety Plan

HEALTH AND SAFETY PLAN
LiDAR AND ORTHOPHOTOGRAPHY
DEMONSTRATION PROJECT
KIRTLAND PRECISION BOMBING RANGE, NEW MEXICO

Approvals

Name: Thomas Tomczyk, P.G., L.G., C.Q.A.
Title: Principal Investigator
URS Group, Inc.

Signature: _____ Date: _____

Name: Dale Bennett
Title: Assistant Investigator
URS Group, Inc.

Signature: _____ Date: _____

Name: Dave Neufeldt
Title: LiDAR / Orthophotography Technical Lead
Terra Remote Sensing, Inc.

Signature: _____ Date: _____

CONTENTS

TABLES

FIGURES

ABBREVIATIONS AND ACRONYMS

ESTCP	Environmental Security Technology Certification Program
EPA	U.S. Environmental Protection Agency
HASP	Health and Safety Plan
MEC	Munitions and Explosives of Concern
PBR	Precision Bombing Range
PI	Principal Investigator
SSR	Site Safety Representative
TRSI	Terra Remote Sensing, Inc.
URS	URS Group, Inc.
URS PI	URS Principal Investigator

1.0 INTRODUCTION

This document serves as the health and safety plan (HASP) for the Environmental Security Technology Certification Program (ESTCP) Demonstration Project entitled "High Density LiDAR and Orthophotography in UXO Wide Area Assessment", to be performed at the former Kirtland Precision Bombing Range (PBR), New Mexico (Figure 1-1). This HASP has been prepared to describe the procedures that will be implemented to manage the health and safety aspects of the demonstration. This HASP complies with, but does not replace, applicable Federal, State and local regulations. This HASP is to be used by URS and subcontract personnel as a supplement to these rules, regulations, and guidance. For URS employees, this HASP is to be augmented by applicable provisions of the Demonstration Plan, along with the URS Health and Safety Program and Management System; relevant standards from that program and system are required to be available on site during all activities.

Figure 1-1 Kirtland AFB PBS Vicinity Map

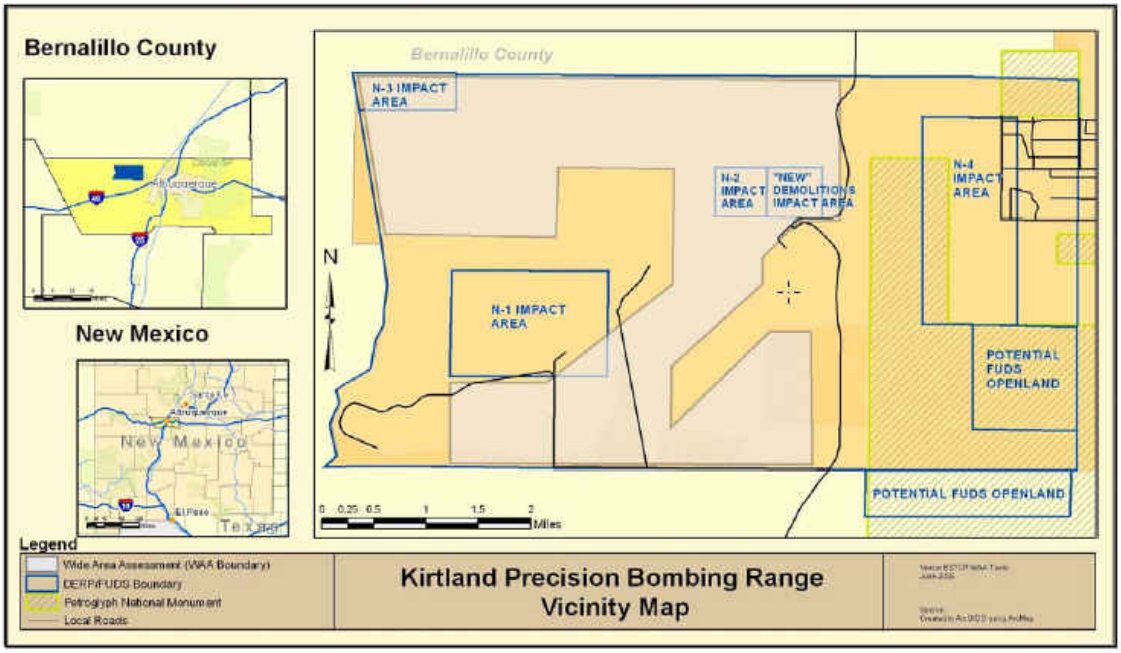

2.0 ORGANIZATION SAFETY RESPONSIBILITIES

2.1 RESPONSIBILITIES

The following subsections describe personnel with safety-related duties and their specific responsibilities.

2.1.1 URS Principle Investigator (PI)

The URS PI is responsible for all site operations and project implementation. In addition, the PI performs the following duties:

- Ensures adequate resources are available to implement and carry out all site safety activities
- Ensures that all personnel assigned to the site have received the necessary health and safety training
- Familiarizes all on-site personnel with the site safety requirements
- Assigns key safety duties and responsibilities to team members
- Ensures that all necessary personal protective equipment (PPE) is available and on site.

2.1.2 Subcontractor Safety Representative

Each subcontractor is requested to designate a Subcontractor's Safety Representative (SSR) who is the subcontractor supervisor. URS will consider the SSRs responsible for the safe and healthful performance of work by their work force and subcontractors. During subcontractor activities on site, the SSR will perform continuing work area inspections, and conduct safety meetings and safety orientations for all his subcontractor employees. The SSR will attend all safety meetings and will also investigate accidents and overexposures involving subcontractor personnel.

2.1.3 TRSI

Safety is an integral part of Terra Remote Sensing Inc.'s (TRSI) day-to-day activities. It is our first priority in the performance of our work. The protection of people, equipment, property and the public is an attitude that is emphasized and rewarded in all of our operations.

The economic benefits of working safely far outweigh the costs of non-compliance. The greatest cost is the human cost. By protecting our employees, TRSI is also protecting their friends, families, fellow workers, management, the public and the environment.

Protection of one's livelihood is first and foremost with our safety program. This program will also contribute to employee morale and pride because of their involvement in identifying safety needs and developing safe work procedures.

TRSI will ensure that recognized health and safety standards and legal requirements are met through the provision of adequate facilities, equipment, procedures, training and management systems.

Everyone employed by TRSI is responsible for maintaining our safety program. Supervisors and managers are responsible for identifying safety needs, communicating safety hazards, investigating hazardous conditions and accidents, providing training, supplying or wearing appropriate safety and personal protective equipment, and ensuring all equipment is properly maintained and meets legislated safety standards. Their role is supported by input from all employees.

All company employees, contractors and subcontractors on company worksites are responsible for obeying all safety rules, following recommended safe work procedures, wearing and using personal protective equipment when required, participating in safety training programs and informing party chiefs of any unsafe work conditions. Everyone has the right and responsibility to refuse to do work when unsafe conditions exist.

TRSI takes the approach that safety, and all of the implications of a health and safety program are part of an overall attitude expressed by all of its employees, supervisors and managers. An open and ongoing dialogue on all aspects of loss prevention is paramount to the well being of all concerned. By fulfilling our safety responsibilities, everyone who works for our company will share the benefits of a safe workplace.

2.1.4 AeroWest Helicopters

AeroWest Helicopters, Inc. is a full-service helicopter company based at the Double Eagle airport on the demonstration site. AeroWest is regulated under FAR 135, Operating Requirements: Commuter and On-Demand Operations and Rules Governing Persons On Board Such Aircraft, promulgated by the Federal Aviation Administration. AeroWest is certified under these regulations; a copy of the certification is attached and further information is available upon request. Additional material submitted by AeroWest includes that the company flies an average of 2500 hours per year and has never had a passenger hurt since operations were initiated in 1984.

Table 2-1.
Project Safety Contacts

Key Role	Name	Telephone
On-Site Emergencies		
Any emergency		911
Ambulance		911
Kirtland PBR / Double Eagle Airport Manager		(505) 244-7888
Fire		911 or
University of New Mexico Hospital, Albuquerque		(505) 272-2111
URS		
URS Principal Investigator	Tom Tomczyk	(206) 438-2137
URS Health and Safety Manager	Mark Litzinger	(206) 438-2199
TRSI		
TRSI Site Safety Officer		(xxx) xxx-xxxx

[1] In the event of an emergency, the URS PI and the ESTCP PM are to be notified immediately.

3.0 PERSONNEL MEDICAL QUALIFICATIONS AND TRAINING REQUIREMENTS

Team members performing critical functions, such as pilot, must have a physical examination prior to participation in field activities to verify that the worker is capable of performing those duties, and is free of medical conditions that may be aggravated while performing those duties. All site personnel will participate in an initial safety briefing, followed by daily briefings to discuss the effectiveness of controls and overall project safety. All necessary certifications and licenses will be produced prior to mobilization and a copy of the documentation will be kept on site.

4.0 SITE HAZARD ANALYSIS

This section describes the physical hazards that may be encountered during site operations.

4.1 LASER

TRSI uses a class 4 laser in their aerial survey equipment MPE (Maximum Permissible Exposure) and NHZ (Nominal Hazard Zone) have been calculated and demonstrate that the current laser is a potential hazard during indoor scenarios only. Indoor control measures have been implemented to reduce the possibility of exposure to the beam.

During the intended operation (outdoors) of the survey laser, the laser beam is fully enclosed except at the scanning mirror that disperses the laser down onto the earth's surface. The remote sensing pod is located on the underside of the aircraft where access is not possible during data collection. Therefore, immediately at the output aperture, the NHZ computation is not applicable. For distal outdoor targets, NHZ is not applicable as the beam is collimated at high altitude. Plus, the likelihood is very small that a subject on the ground will be exposed to more than one pulse of the laser because the laser is reflected in multiple directions at a high rate combined with the velocity of the aircraft. As standard safety precautions, the scanner is always running prior to laser initiation and the laser is not energized until the aircraft carrying the unit is 100m above ground.

4.2 AIRCRAFT

TRSI's aerial survey process requires the use of a helicopter or fixed wing aircraft. These aircrafts are chartered and the responsibility of flying the aircraft is with the subcontractor. Hazards associated with these transportation vehicles ranges from Class I to III and are: crash resulting in injury or fatality, struck by rotor or propeller, noise, stranded in remote location, hot exhaust, improper storage of equipment. TRSI employees working around aircraft follow general helicopter and fixed wing safety rules and guidelines, and follow instructions from the contracted pilot.

4.3 OTHER POTENTIAL HAZARDS

MEC. MEC may be present in the study area. Survey personnel are not expected to be on the ground outside of the airport for extended periods. If personnel do encounter MEC, avoid the item and contact the Site Safety Officer.

Heat Stress. Heat stress is considered an issue when the ambient temperature exceeds 70°F. Personnel are expected to keep hydrated by consistent intake of fluids, especially water. If

5.0 EMERGENCY RESPONSE

Injuries that occur at job sites must be handled quickly and competently. When serious injuries, breathing difficulties, intense pain, or unconsciousness occur, site personnel will immediately seek help from professional paramedics using a building phone or cellular phone and dialing **911**. For non-life-threatening injuries that do not impair driving ability, site personnel will drive to the hospital. If driving ability is affected by the injury, site personnel will use the designated phone to call **911** for assistance.

A first aid kit will be available at the site to treat minor injuries. First aid responders should protect themselves from contact with blood and other human body fluids by wearing latex gloves or establishing an equivalent barrier. Antiseptic wipes and latex gloves should be carried in the first aid kit. First aid responder's hands should be washed with hot, soapy water as soon as possible after first aid treatment is administered. All injuries will be reported to the PI as soon as possible.

After making initial contact with PI, and within 24 hours of a serious injury of fatality, a Contractor Significant Incident Report (CSIR) must be submitted. If the mishap is a lost-time or a recordable incident, submit the CSIR within 5 days of the incident.

symptoms of heat stress are observed, immediate rest and monitoring of the individual is imperative.

Traffic. Air and vehicle traffic at the site is expected to be moderate to heavy and personnel should exercise caution at the airport and on or near roadways. Communication with air traffic controllers and ground crews is vitally important and will be constantly monitored.

Noise. High noise levels may be encountered during flight operations. Noise and hearing conservation practices will be in effect.

Slip-Trip-Fall Hazards. Care will be taken to ensure proper footing and handholds, particularly if wet conditions make the ground surface or hand/sampling tools slippery. The sampling area will be kept uncluttered. Good housekeeping around equipment will be enforced.

Back Injuries. Workers will use proper lifting techniques, lifting with the legs and not the back. Lifting loads over 50 pounds require a second person or mechanical device. Whenever possible, mechanical devices should be used to lift or move heavy loads.

Hand Tools. Eye injuries, puncture wounds, cuts, or lacerations could result from use of hand tools while collecting samples or repairing equipment. Tools should be in good condition and the right tool should be selected for the job. Safety glasses with side shields or safety goggles should be worn whenever projectiles are a potential problem. Loose clothes or jewelry will not be worn because they could get caught in moving equipment. Steel-toed shoes should be worn when there is any risk that something could fall on the foot. Tools should be stored safely, with sharp edges protected.

Screwdrivers should not be used as chisels, because their tips could break or fly off. The head could fly off a hammer with a loose or cracked wooden handle. Impact tools such as chisels or wedges with mushroomed heads might shatter on impact, sending sharp fragments flying. Knives, saw blades, and scissors must be sharp.

APPENDIX I

Points of Contact

POINTS OF CONTACT

Name	Organization and Address	Phone/Fax/email	Role in Project
Jeffrey Marqusee	ESTCP 901 North Stuart St. Suite 303 Arlington, VA 22203	703-696-2120 703-696-2114	Director, ESTCP
Anne Andrews	ESTCP 901 North Stuart St. Suite 303 Arlington, VA 22203	703-696-3826 703-696-2114	Program Manager, Munitions Management
Herb Nelson	Naval Research Lab 1155 Herndon Parkway Suite 900 Herndon, WA 20170	202-767-3686 202-404-8119 Herb.nelson@nrl.navy.mil	Project Manager, ESTCP Wide Area Assessment Pilot Program
Dale Bennett	URS 1501 4th Ave Suite 1400 Seattle WA 98101-1616	206-438-2026 206-438-2699 dale_bennett@urscorp.com	Data Evaluation and GIS Lead
Rick Quinn	TRSI 1962 Mills Road Sidney BC Canada V8L 5Y3	250-656-0931 250-656-4604 rick.quinn@terraremote.com	Terra Remote Sensing Principle in Charge
Jim Vosberg	TRSI 1962 Mills Road Sidney BC Canada V8L 5Y3	250-656-0931 250-656-4604 jim.vosberg@terraremote.com	Terra Remote Sensing Operations Manager
Bill Rohrer	URS 1501 4th Ave Suite 1400 Seattle WA 98101-1616	206-438-2296 206-438-2699 bill_rohrer@urscorp.com	Senior QA/QC